Journal of Chemistry

Chemical EOR

Guest Editors: Ibnelwaleed A. Hussein, Yujun Feng, and Baojun Bai

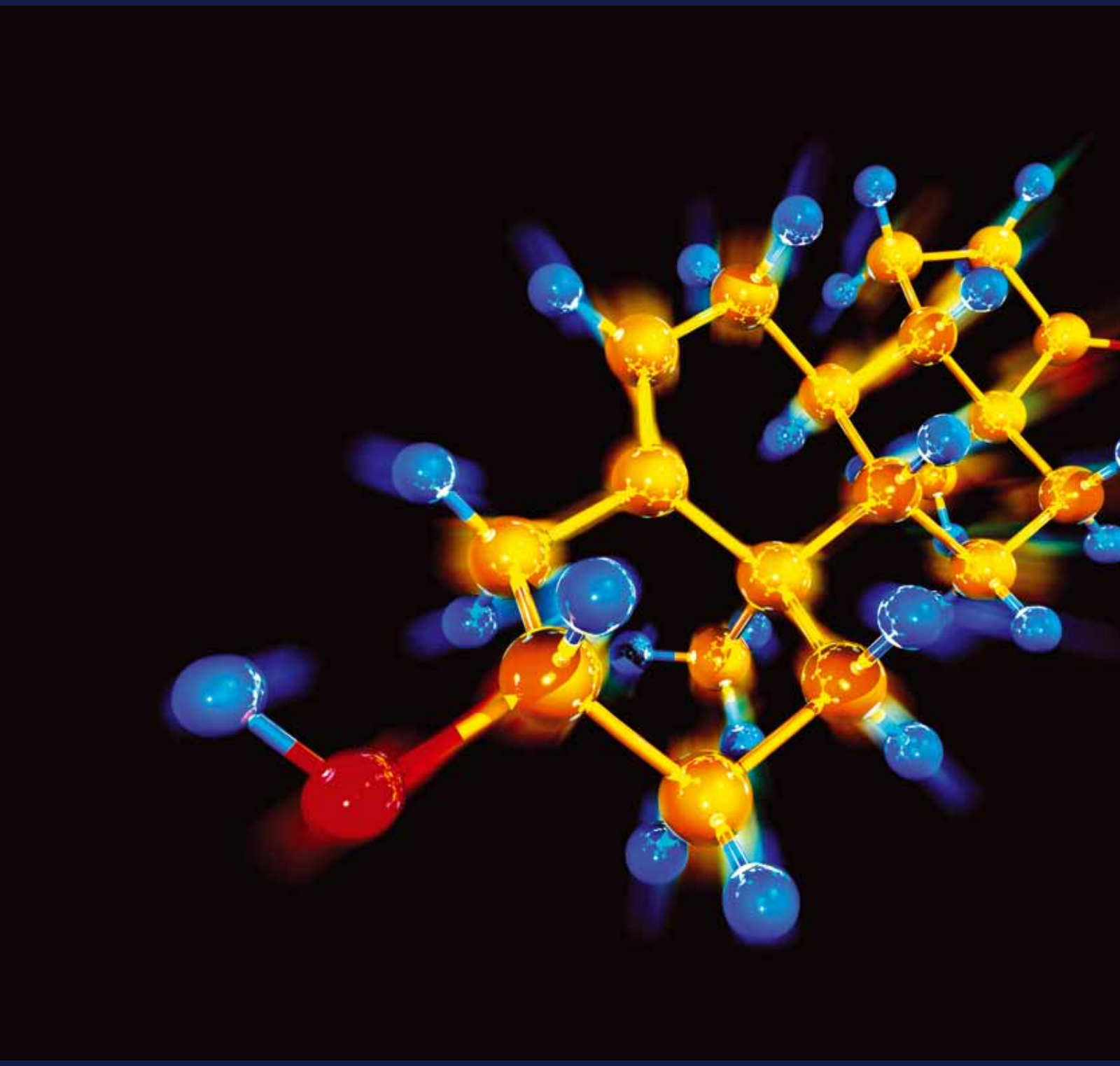

Chemical EOR

Journal of Chemistry

Chemical EOR

Guest Editors: Ibnelwaleed A. Hussein, Yujun Feng, and Baojun Bai

Contents

Hindawi Publishing Corporation
Journal of Chemistry
Volume 2013, Article ID 871542, 1 page
http://dx.doi.org/10.1155/2013/871542

Editorial

Chemical EOR

Ibnelwaleed A. Hussein,[1] Yujun Feng,[2] and Baojun Bai[3]

[1] *Polymers & Rheology Research Laboratory, Department of Chemical Engineering, King Fahd University of Petroleum & Minerals, Dhahran 31261, Saudi Arabia*
[2] *Polymer Research Institute, State Key Laboratory of Polymer Materials Engineering, Sichuan University, Chengdu 610065, China*
[3] *Petroleum Engineering, Missouri University of Science and Technology, Rolla, MO 65409, USA*

Correspondence should be addressed to Ibnelwaleed A. Hussein; ihussein@kfupm.edu.sa

Received 15 December 2013; Accepted 15 December 2013

Enhanced oil recovery (EOR) has become more and more important due to the growing energy demand and depleting oil reserves. Among the various EOR methods, chemical EOR was considered to be expensive and not economic when oil price was below $40 and field applications have almost completely stopped during that time except in China, where around 13 million tons of oil is produced additionally per year by these chemical flooding techniques. However, chemical EOR has recently drawn increasing interest due to the continuous high oil prices within the last 7 years and the scarcity of cheap oil reserves. Therefore, the chemical EOR research has shown major growth in the recent years.

This special issue is on chemical EOR systems. It reports some results of research, pilot tests, and field applications related to chemical EOR. The focus is on synthesis and laboratory testing as well as field applications of new chemical EOR materials used in flooding processes. These manuscripts covered a broad spectrum of topics ranging from synthesis of new polymers for EOR applications to both onshore and offshore field applications of commercially available polymers and foams systems. The subject of designing new systems for high-temperature, high-salinity reservoir environment is also investigated. The chemical systems reported in these papers can be used to reduce interfacial tension, increase injection fluid viscosity, and reduce the permeability of high-permeability streaks. They can increase microscomic displacement efficiency and/or sweep efficiency, thus improving the oil recovery.

Acknowledgments

Finally, we would like to thank the authors who contributed to this special issue. Special thanks are due to the reviewers for their help in evaluating the submitted papers. We hope that this special issue on chemical EOR will help the readers in advancing their knowledge in such an important field.

Ibnelwaleed A. Hussein
Yujun Feng
Baojun Bai

Hindawi Publishing Corporation
Journal of Chemistry
Volume 2013, Article ID 956027, 6 pages
http://dx.doi.org/10.1155/2013/956027

Research Article

Experimental Study on the Properties and Displacement Effects of Polymer Surfactant Solution

Ke-Liang Wang, Lei-Lei Zhang, Xue Li, and Yang-Yang Ming

The Key Lab of Enhanced Oil and Gas Recovery of the Ministry of Education, Northeast Petroleum University, Daqing 163318, China

Correspondence should be addressed to Ke-Liang Wang; wangkl0608@126.com

Received 7 April 2013; Revised 29 September 2013; Accepted 14 October 2013

Academic Editor: Ibnelwaleed Ali Hussien

Based on the characteristics of oil reservoirs and the requirements of further enhancing oil recovery at high water cut stage of Pubei Oilfield, the displacement performance of polymer surfactant is evaluated. Reasonable injection parameters and oil displacement effects after water flooding are also researched. Compared with conventional polymer with intermediate molecular weight, polymer surfactant has the properties of higher viscosity at low concentration condition and lower interfacial tension. Laboratory experiments indicate that the displacement effect of polymer surfactant is much better than that of conventional polymer at a slug size of 0.57 PV. The oil recovery of polymer surfactant increases by more than 10% after water flooding. Considering the actual situation of low-permeability of Pubei Oilfield reservoirs, the system viscosity of 30 mPa·s is chosen. The corresponding concentration of Type III polymer surfactant is 600 mg/L and the injected slug is 0.57 PV and the oil recovery can be increased by 11.69%.

1. Introduction

Polymer flooding has already entered the industrial application period in major reservoirs of Daqing Oilfield, and pilot trial has also been conducted in Pubei Oilfield, one of the many oilfields of Daqing Oilfield. Both laboratory and field data have shown that polymer flooding could improve oil recovery by nearly 10%, but this value was not perfect [1]. It was indicated that the oil recovery of ASP flooding was 20% higher than that of water flooding in Daqing Oilfield pilot tests [2, 3]. However, some problems such as formation damage due to alkali scale, production well pollution, and effluent treatment difficulties appeared in ASP development process [4, 5]. Experimental results showed that the oil recovery of binary combination flooding in major reservoirs increased by more than 15% [6]. However, the adsorption, diffusion, and migration properties of different chemical agents in porous media are quite different. This difference may result in the phenomenon of chromatographic separation and negative synergistic effect during the mixture system simultaneous flow [7]. In recent years, some functional groups have been grafted to hydrocarbon main chains to form a multivariate graft copolymer which is called functional polymer surfactant (also referred to as polymer surfactant) [8, 9]. As a new type of polymer, polymer surfactant is a single component oil displacement agent. In addition to the general nature of polymer, polymer surfactant can improve solubilization and emulsification capacity of crude oil in the absence of alkali. At present, many main blocks in Daqing Oilfield have entered high water cut stage and the conventional polymer have already couldn't meet the requirements of tertiary oil recovery. Thus, the use of polymer surfactant is an attractive option in further enhancing oil recovery for high water cut or low-permeability oilfields.

The performance of Type I and Type III polymer surfactant produced by Shanghai Haibo Company was investigated in this paper. According to the reservoir characteristics of Pubei Oilfield, core flooding experiments were conducted to study the oil displacement effects. Besides, optimized system slug concentration and final oil recovery were achieved on the basis of experiment results.

Table 1: The composition of fresh water and produced water.

Name	PH	Cl^- (mg/L)	SO_4^{2-} (mg/L)	HCO_3^- (mg/L)	CO_3^{2-} (mg/L)	$K^+ + Na^+$ (mg/L)	Ca^{2+} (mg/L)	Mg^{2+} (mg/L)	Salinity (mg/L)
Fresh water	8.5	53.77	33.71	137.62	110.86	196.00	4.37	5.30	541.63
Produced water	7.8	877.00	10.47	694.53	862.07	1481.29	6.55	3.97	3935.88

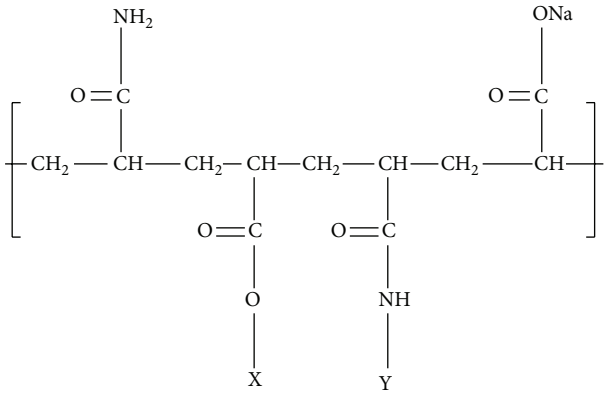

Figure 1: Molecular structure of polymer surfactant.

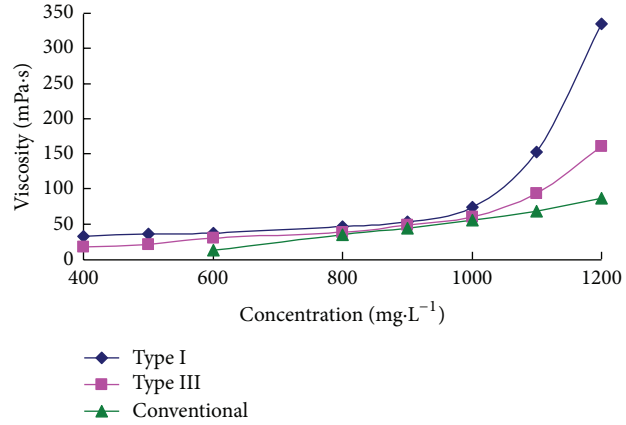

Figure 2: Viscosities versus concentrations of different polymer solutions prepared by fresh water.

2. Properties of Polymer Surfactant

2.1. Molecular Structure. Figure 1 shows the diagram of polymer surfactant molecular structure, where X, Y represents one of the following functional groups, respectively: –OR, –NHR, $-RSO_3Na$, quaternary ammonium surfactant unit, cationic Gemini unit, –RSH, and so forth.

Polymer surfactant has superior properties to conventional polymer because of the various functional groups in the molecular structure. For instance, quaternary ammonium surfactant unit, as one of the groups, is a kind of viscoelastic surfactant that has been identified; it can reduce the technical disadvantages of lacking solubilization, emulsification, the ability of altering rock wettability, and reducing oil-water interfacial tension when polymer is used alone as oil displacement agent.

2.2. Property of Increasing Viscosity. The sweep efficiency and displacement effect can be improved as the viscosity of polymer solution increases. Therefore, the polymer surfactant solution viscosity is an important parameter which reflects the performance of polymer.

The viscosity of Type I (solid content of 88.5%) and Type III polymer surfactant (solid content of 90.2%) was estimated at 45°C. The results were compared with that of the conventional intermediate-molecular-weight polymer (relative molecular mass of 1570×10^4, solid content of 89.3%) produced by Daqing Refining and Chemical Company under the same conditions. Brookfield viscometer was used in this study. The viscosity was measured at 6 r/min rotor speed (7.34 s^{-1} shear rate).

Viscosity measurements were performed on the three polymer solutions with fresh water and produced water and the composition of the two waters is listed in Table 1.

Figures 2 and 3 show that both of Type I and Type III polymer surfactant solutions possess higher viscosity than conventional at the same concentration. As shown in Figure 2, there is a critical concentration in the range of 1000 mg/L–1100 mg/L, and viscosity increasement is particularly evident when system concentration is above this critical concentration. The viscosity of Type I is better than that of Type III in Figure 2. Similarly, the critical concentration in produced water is lower and within the range of 600 mg/L–800 mg/L in Figure 3, the viscosity of Type III is high and with great salt tolerance as well.

There is a self-crosslinking unit in Type I polymer surfactant, and the poor salt tolerance of this unit results in solution viscosity reduction as the salinity increases. While the quaternary ammonium surfactant unit in Type III polymer surfactant has great salt tolerance, thus, the solution viscosity is slightly influenced by water salinity. Therefore, the different salt tolerance leads to the different phenomena in fresh water and produced water.

2.3. Interfacial Tension. One mechanism of enhancing oil recovery for surfactant and polymer compound system is the ultralow interfacial tension produced by surfactant. Ultralow interfacial tension contributes to mobilizing trapped oil and displacing oil out of formation. Laboratory evaluation shows that polymer surfactant solution has a certain ability to reduce interfacial tension and exhibits some characteristics

Table 2: Interfacial tensions (mN/m) of Type I and Type III polymer surfactant prepared with fresh and produced water, respectively.

Polymer concentration ($mg \cdot L^{-1}$)	Type I prepared by fresh water	Type I prepared by produced water	Type III prepared by fresh water	Type III prepared by produced water
200	30.82	29.12	22.15	20.26
400	31.21	28.69	23.14	22.32
600	29.23	28.63	21.85	20.36
800	29.01	28.12	22.18	21.26
1000	29.51	27.65	22.75	19.85

Table 3: Wetting angles of the cores treated before and after by Type I polymer surfactant.

Core number	Wetting angles before (°)	Wetting angles after (°)
Berea 200-1	99	95
Berea 200-2	96	93
Natural 200-1	120	123
Natural 200-2	126	118

Table 4: Wetting angles of the cores treated before and after by Type III polymer surfactant.

Core number	Wetting angles before (°)	Wetting angles after (°)
Berea 200-3	93	73
Berea 200-4	96	87
Natural 200-3	125	105
Natural 200-4	130	102

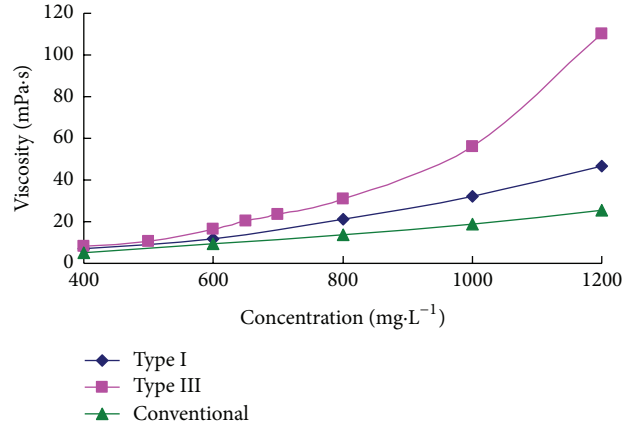

Figure 3: Viscosities versus concentrations of different polymer solutions prepared by produced water.

of surfactant. This property is due to the special structure of polymer surfactant. The hydrophilic and hydrophobic parts in the molecular structure have orientation on interface or surface and hence cause interfacial tension reduction. Experiment results are listed in Table 2. It is obvious that the interfacial tension of polymer surfactant solutions prepared by produced water is slightly lower than fresh water, and the ability of reducing interfacial tension of Type III is a little better than Type I. In addition, the interfacial tension of Type III is less than 24 mN/m either by fresh water or produced water.

2.4. Ability to Change Rock Wettability. In the process of water injection, oil phase and water phase coexist within the pores of rock. Whether the water attaches to the pore surface and displaces the oil or only squeezes out the oil in central pore mainly depends on the wettability of rock. Generally speaking, oil displacement efficiency of oil-wet reservoir is lower, while the water-wet reservoir is higher. Therefore, a suitable displacing agent is required to reduce the adhesion power of crude oil on the rock surface and hence improve oil displacement efficiency.

In this paper, Germany Dataphysics OCA20 video optical contact angle measuring device is used to evaluate the influence on the wettability of solid surface through measuring wetting angles. Type I and Type III polymer surfactant solutions and columnar natural cores and Berea cores are also used. Experimental procedure consists of the following sequence: (1) make the 10 cm length columnar core sample into three sections, each section is a new short core with a length of 3 cm; (2) the short cores were vacuumed for several hours and then saturated with formation water. Put the three short cores into core holders and saturate with crude oil; (3) after water flooding, take one of the short cores out of core holder. Dry the core and determine its wettability; (4) displace the other two cores, respectively, with 10 PV Type I and 10 PV Type III polymer surfactant solutions, dry the cores after sufficient follow-up water flooding, and then determine the wettability again. The results are listed in Tables 3 and 4.

It is shown that the wetting angles of both kinds of cores changed significantly after treatment with Type III solution, and the wettability exhibits a tendency to water-wet. In contrast, the variation in wetting angles is not obvious after treatment with Type I solution, and the wettability is basically unchanged. Overall, Type III polymer surfactant solution has a certain ability to change rock wettability, it is because that the special surfactant unit in molecular structure is easily adsorbed onto the rock surface which result in hydrophobic ability weakened and hydrophilic ability enhanced.

3. Core Flooding Experiments

The oil displacement effect of Type I and Type III polymer surfactant solutions in different injection concentrations is concerned. Polymer surfactant solutions of different viscosity 30 mPa·s, 40 mPa·s, and 60 mPa·s are prepared, respectively.

Table 5: Experimental results of Type I polymer surfactant flooding.

Experimental project	Absolute permeability (10^{-3} μm^2)	Porosity (%)	Oil saturation (%)	Water flooding recovery (%)	Polymer flooding recovery (%)	Overall recovery (%)
Polymer surfactant (400 mg/L, 31.83 mPa·s) + water flooding	309	23.83	73.16	37.60	10.38	47.98
Polymer surfactant (650 mg/L, 39.7 mPa·s) + water flooding	298	24.09	72.36	37.50	13.48	50.98
Polymer surfactant (925 mg/L, 61.35 mPa·s) + water flooding	307	24.90	69.88	37.88	16.29	54.17

Table 6: Experimental results of Type III polymer surfactant flooding.

Experimental project	Absolute permeability (10^{-3} μm^2)	Porosity (%)	Oil saturation (%)	Water flooding recovery (%)	Polymer flooding recovery (%)	Overall recovery (%)
Polymer surfactant (600 mg/L, 30.5 mPa·s) + water flooding	336	24.78	72.43	39.49	11.69	51.18
Polymer surfactant (850 mg/L, 40.2 mPa·s) + water flooding	310	24.33	72.51	40.12	16.30	56.42
Polymer surfactant (1000 mg/L, 60.53 mPa·s) + water flooding	321	24.91	69.83	39.47	18.21	57.68

The experiments were carried out to research the influence of polymer surfactant viscosity on oil displacement efficiency when slug size is 0.57 PV and the optimal injection concentration is also determined.

3.1. Experimental Materials. Cores: the artificial heterogeneous core is selected, the core size is 4.5 cm × 4.5 cm × 30 cm, and the Dykstra-Persons permeability variation factor is 0.68. The core sample includes three layers with the same thickness and different permeability. The permeability of three layers is 100×10^{-3} μm^2, 220×10^{-3} μm^2, and 580×10^{-3} μm^2, respectively, and the average permeability is about 300×10^{-3} μm^2; water: fresh water and produced water from no. 7 Oil Plant of Daqing Oilfield; oil: simulated oil which is prepared with dehydrated crude oil and kerosene, the viscosity is 5.1 mPa·s at 45°C; solutions: according to the requirement of viscosity, polymer solutions of different concentrations with fresh water are prepared, including Type I solutions of 400 mg/L, 650 mg/L, and 925 mg/L, Type III solutions of 600 mg/L, 850 mg/L, and 1000 mg/L, and conventional polymer solutions of 785 mg/L.

3.2. Experimental Procedure. The core was first vacuumed for several hours at ambient temperature and then the core was 100% saturated with formation water and pore volume was determined. After the first step, the core was saturated with simulated oil to establish irreducible water and the residual water saturation and initial oil saturation were determined during this period. Water flooding was continued until 98% water cut (oilfield economic limit of water cut) and oil recovery was calculated at the end of water flooding. After water flooding, a predetermined volume of polymer solution was injected according to different projects. Then follow-up water flooding was contained until 98% water cut, and the additional oil recovery of polymer flooding was calculated.

3.3. Results and Discussion

3.3.1. Oil Displacement Efficiency. Type I and Type III polymer surfactant solutions of three viscosities 30 mPa · s, 40 mPa·s, and 60 mPa·s were selected for coreflooding experiment. The oil displacement efficiency results were compared with that of the conventional polymer with a viscosity of 30 mPa·s. The injected polymer slug size is always maintained 0.57 PV at each experiment. Experimental results are listed in Tables 5, 6, and 7.

It is shown that both of the two polymer surfactant flooding can improve oil recovery by more than 10% after water flooding, and the oil displacement efficiency increases with the increase of solution concentration. At the same viscosity, the oil displacement efficiency of Type III polymer surfactant is better than that of Type I, and the efficiency of Type I and conventional polymer is almost the same.

It is indicated that the follow-up water flooding after polymer surfactant is significantly longer than conventional polymer, and corresponding water injection volume is larger (Figure 4). For example, the follow-up water flooding after Type III is the longest and this process needs about 1.17 PV injection water. While Type I requires only about 0.78 PV injection water, the difference is 0.39 PV. This is due to the ability of Type III polymer to change rock wettability and reduce interfacial tension. This ability leads to residual oil saturation further reducing and thus improves microscopic oil displacement efficiency.

3.3.2. Injection Pressure. As shown in Figure 4, polymer surfactant injection pressure is higher than conventional polymer in coreflooding experiment. At the same viscosity, the polymer surfactant thread molecule is larger than the conventional polymer and then results in the higher injection pressure.

Table 7: Experimental results of conventional intermediate-molecular-weight polymer flooding.

Experimental project	Absolute permeability (10^{-3} μm^2)	Porosity (%)	Oil saturation (%)	Water flooding recovery (%)	Polymer flooding recovery (%)	Overall recovery (%)
Polymer (785 mg/L, 29.7 mPa·s) + water flooding	305	24.22	70.75	39.75	10.25	50.00

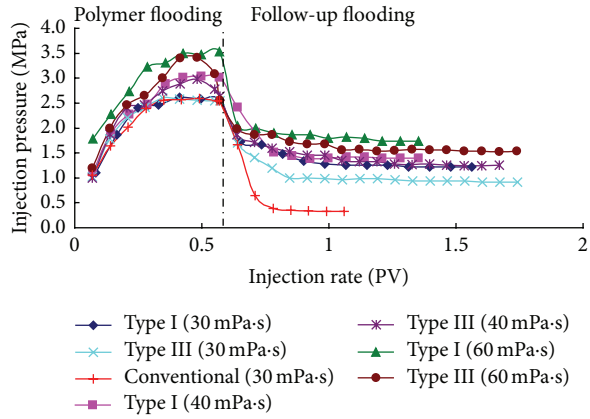

Figure 4: Injection rates versus pressures of different kinds of polymer.

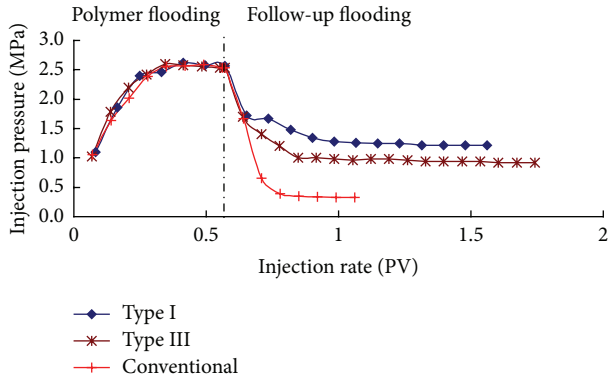

Figure 5: Injection rates versus pressures of different kinds of polymer at 30 mPa·s.

It can be seen that the injection pressure is relatively high for Type I and Type III polymer surfactant at 40 mPa·s and 60 mPa·s from Figures 4 and 5. High injection pressure may result in some injection problems when applied in low permeability oilfield. But both Type I and Type III polymer surfactant have a lower injection pressure at 30 mPa·s. In follow-up water flooding, the strong adsorption of polymer surfactant can maintain high injection pressure and obtain larger swept volume so that oil recovery can be improved. In addition, polymer surfactant can reach or even exceed the conventional polymer displacement efficiency at a lower concentration under the same conditions. Overall, it is suggested that Type III polymer surfactant solution of 30 mPa·s is the most reasonable choice as injection agent.

4. Conclusions

(1) The property of increasing viscosity of polymer surfactant is better than that of conventional polymer. In fresh water, the property of Type I is better than Type III. However, the situation is just the reverse in produced water.

(2) Compared with the conventional intermediate-molecular-weight polymer produced by Daqing Refining and Chemical Company, polymer surfactants possess a certain ability to reduce the interfacial tension and change the wettability of rock.

(3) Oil displacement efficiency increases with the increase of solution viscosity. At the same viscosity, the oil displacement efficiency of Type III polymer surfactant is better than that of Type I, and the efficiency of Type I and conventional polymer is almost the same.

(4) Type III polymer surfactant has great injection capacity when viscosity is 30 mPa·s, which is suited for the application in Pubei low-permeability reservoirs. So, Type III polymer surfactant solution prepared with fresh water is recommended.

References

[1] M. F. Fakoya and S. N. Shah, "Rheological properties of surfactant-based and polymeric nano-fluids," in *SPE/ICoTA Coiled Tubing & Well Intervention Conference & Exhibition*, The Woodlands, Tex, USA, 2013, SPE 163921.

[2] L. Eoff, D. Dalrymple, and B. R. Reddy, "Development of associative polymer technology for acid diversion in sandstone and carbonate lithology," *SPE Production & Facilities*, vol. 20, no. 3, pp. 250–256, 2005.

[3] X. Guo, A. A. Abdala, B. L. May, S. F. Lincoln, S. A. Khan, and R. K. Prud'homme, "Rheology control by modulating hydrophobic and inclusion associations in modified poly(acrylic acid) solutions," *Polymer*, vol. 47, no. 9, pp. 2976–2983, 2006.

[4] S. Barhoum and A. Yethiraj, "An NMR study of macromolecular aggregation in a model polymer-surfactant solution," *The Journal of Chemical Physics*, vol. 132, no. 2, Article ID 024909, 2010.

[5] K. Holmberg, B. Jonsson, and B. Kronberg, *Surfactats and Polymers in Aqueous Solution*, Wiley, New York, NY, USA, 2003.

[6] S. Wu, R. A. Shanks, and G. Bryant, "Properties of hydrophobically modified polyacrylamide with low molecular weight and interaction with surfactant in aqueous solution," *Journal of Applied Polymer Science*, vol. 100, no. 6, pp. 4348–4360, 2006.

[7] Q. Niuyabin et al., "Research on hydrophobically associating water-soluble polymer used for EOR," in *SPE International Symposium on Oilfield Chemistry*, Houston, Tex, USA, 2001, SPE 65378.

[8] J. Lu, P. J. Liyanage, S. Solairaj et al., "Recent technology developments in chemical enhanced oil recovery," in *International Petroleum Technology Conference (IPTC '13)*, March 2013, IPTC 16425.

[9] M. Roshanfekr, R. T. Johns, G. Pope et al., "Effect of pressure, temperature, and solution gas on oil recovery from surfactant polymer floods," in *SPE Annual Technical Conference and Exhibition (ATCE '09)*, pp. 4398–4412, October 2009, SPE 125095.

Hindawi Publishing Corporation
Journal of Chemistry
Volume 2013, Article ID 845031, 8 pages
http://dx.doi.org/10.1155/2013/845031

Research Article

Wettability Alteration of Sandstone by Chemical Treatments

Yan-ling Wang,[1] Li Ma,[1] Bao-jun Bai,[2] Guan-cheng Jiang,[3] Jia-feng Jin,[1] and Zeng-bao Wang[1]

[1] *Petroleum Engineering College, Petroleum University of China, Qingdao Shandong 266555, China*
[2] *Petroleum Engineering, Missouri University of Science and Technology, Rolla, MO 65409-0410, USA*
[3] *Key Laboratory of Petroleum Engineering of Education Ministry in China University of Petroleum, Beijing 102249, China*

Correspondence should be addressed to Yan-ling Wang; wangyl_hdpu@hotmail.com and Bao-jun Bai; baib@mst.edu

Received 25 June 2013; Accepted 13 August 2013

Academic Editor: Yujun Feng

Liquid condensation in the reservoir near a wellbore may kill gas production in gas-condensate reservoirs when pressure drops lower than the dew point. It is clear from investigations reported in the literature that gas production could be improved by altering the rock wettability from liquid-wetness to gas-wetness. In this paper, three different fluorosurfactants FG1105, FC911, and FG40 were evaluated for altering the wettability of sandstone rocks from liquid-wetting to gas-wetting using contact angle measurement. The results showed that FG40 provided the best wettability alteration effect with a concentration of 0.3% and FC911 at the concentration of 0.3%.

1. Introduction

The wettability of the reservoir is not only a key factor for controlling the flow of reservoir fluids into the porous media, but it also had a great effect on both the relative permeability values of the liquid and gas phases and recovery [1, 2]. The wettability of the reservoir would be altered adversely if the liquid for drilling and production were not adequate. This would damage the reservoir and reduce production [2, 3]. Therefore, it has become a very important task in the field of petroleum and surface chemistry, at home and abroad, to improve the recovery and protection of oil and gas. Recently, with the development of gas reservoirs and gas-condensation reservoirs, a study of "gas wetness" was proposed by Li and Firoozabadi in 2000 [4]. A new method was introduced for recovering productivity in gas wells by altering wettability in gas-condensation reservoirs from liquid-wetting to intermediate gas-wetting. A substantial increase in gas well delivery and oil recovery would show when the wettability of a reservoir was altered from strong liquid wetness to the preferred gas wetness [4–7].

In Li and Firoozabadi's work, the alteration of wettability was achieved by treating the rocks with the chemical solutions FC754 and FC722 [5]. Significant changes in the wettability were demonstrated by imbibition tests and capillary tube tests. The contact angle of the gas-water systems increased to about 90° from 50°, and the contact angle of the gas-oil systems increased to about 60° from 0°, at a concentration of approximately 0.1%, showing that the gas-wetting was not as strong as expected. FC722 was more effective than FC754 in altering wettability in the gas-liquid-Berea systems, but it was difficult to use because FC722 is neither soluble in water nor in oil.

Tang and Firoozabadi [7] altered the wettability of Berea and Chalk from liquid-wetting to intermediate gas-wetting using two polymers, FC722 and FC759. All the results showed clearly that the application of wettability alteration to intermediate gas-wetting may significantly increase deliverability in gas condensation reservoirs.

Yao et al. [8] studied the ability and characteristics of sodium dodecyl sulfate, CTAB, OP-15, Dimethyl silicone oil, and dimethyldichlorosilane in altering the wettability of synthetic sandstone from liquid-wetting to intermediate gas-wetting. Dimethyl silicone oil and dimethyldichlorosilane were found to be very effective for altering the wettability of gas-liquid-sandstone systems.

Liu et al. [9] changed the wettability of the rock from water-wetness to gas-wetness effectively by using a new and

Table 1: Contact angle of the sandstone after treated with FG1105.

Concentration of FG1105 (%)	0.05	0.1	0.2	0.3	0.5
Contact angle (°)					
Brine	50	45	46	42	36
Normal decane	10	10	0	0	0

Table 2: Contact angle of the sandstone after treated with FC911.

Concentration of FC911 (%)	0	0.1	0.2	0.3	0.5	1
Contact angle (°)						
Brine	43	65	72	80	40	40
Normal decane	12	64	68	74	52	76

Table 3: Contact angle of the sandstone after treatment with FG40.

Concentration of FG40 (%)	0	0.05	0.1	0.2	0.3	0.5
Contact angle (°)						
Brine	40	93	142	134	140	130
Normal decane	10	75	88	89	93	84

cheaper chemical, WA12. Aspontaneous water imbibition test and a flooding test were run to show the effect of wettability alteration on recovery.

However, in the above studies, the contact angle of the gas-water systems increased to only about 90° and the contact angle of the gas-oil systems increased to only about 60°. Hydrocarbon surfactants, cationic fluorosurfactants, organic silicon, and polymers were evaluated for their ability to alter the wettability of rocks from liquid wetness to gas wetness.

In this paper, three fluorosurfactants, FG1105, FC911, and FG40 were used to alter the wettability of the sandstone from liquid-wetting to gas-wetting for the first time. FG1105 and FG40 are nonionic fluorosurfactants. FC911 is a cationic fluorosurfactant. In order to evaluate their ability to alter the wettability of sandstone to gas wetness, the contact angle for gas-water-sandstone systems and gas-oil-sandstone systems were measured by a contact angle meter using the sessile drop method. In addition, the effects of a concentration of chemicals on gas wetness are discussed in this work.

2. Experimental

2.1. Apparatus. The contact angles were measured using the sessile drop method by a Powereach JY-82 Contact Angle Meter provided by Shanghai Zhongchen Digital Technology Apparatus Co. Ltd.

2.2. Fluids and Rocks. Normal decane was used as oil phase with specific gravity and viscosity of 0.73 and 0.92×10^{-3} Pa·s at 25°C, respectively. The surface tension of air-normal decane was 0.0234 N/m (25°C). Brine of 0.2% (wt) NaCl was used as water phase with specific gravity and viscosity 1.012 and 1.0×10^{-3} Pa·s (25°C), respectively. The surface tension of air-brine was 0.0728 N/m (25°C). Sandstone cores from Shengli reservoir were used as the rock samples.

2.3. Chemicals. CTAB, OP-10, and dodecyl sulfate were provided by Sinopharm Chemical Reagent Co. Ltd. FG1105, FC911, and FG40 were provided by Shanghai Institute of Organic Chemistry, Chinese Academy of Sciences. FG1105 and FG40 were nonionic surfactants and FC911 [10] was cationic surfactant.

2.4. Procedure. The cores were cut to slices of approximately 2.5 cm in diameter and 1 cm in length. The sandstone chips were washed with tap water and rinsed with distilled water after cutting, placed in an oven at 120°C for 4 days to dry, and then soaked in the solution of fluorosurfactants (FC911, FG40, or FG1105) for 10 hours at 25°C. The core slices were pulled from the solution and dried at 25°C. This procedure produced core surfaces of altered wettability [11].

Sessile drop contact angle measurements were performed using a JY-82 Contact Angle Meter. Each core after treatment was put on the meter. In actual experiments, a drop of liquid approximately 0.3 cm radius was carefully deposited on the surface of each core using a gas-tight Hamilton syringe with a stainless steel needle. A picture of the drop was then typically recorded by the computer. Normally, at least three contact angle measurements were performed on a new solid surface each time. Then the contact angle could be calculated by a computer according to the pictures. All readings were then averaged to give an average contact angle [12].

3. Results

The mean contact angles of the gas-water systems and those of the gas-oil systems of the sandstones after treatment with FG1105 are shown in Table 1. It can be seen that FG1105 did not alter the wettability of rock to gas-wetting.

The mean contact angles of the gas-water systems and the contact angles of the gas-oil systems of the sandstone, after treatment with FC911 are shown in Table 2. It can be seen that, with the increasing of FC911 concentration, the contact angle of the gas-water systems increased from 0° to 80°, while the contact angle of the gas-oil systems increased to 74° at a concentration of 0.3%. This implies that wettability of the sandstone was altered to intermediate gas-wetting by FC911 at a concentration of 0.3%. And then, as the concentration continued to increase, the contact angle of the gas-water systems suddenly decreased to 40°, and the contact angle of the gas-oil systems decreased to 52° at a concentration of 0.5%. Pictures of liquid droplets on the surface of the sandstone cores, before and after treatment with FC911 at different concentrations, are shown in Figures 1 and 2. It can be seen that liquid droplets were not spread on the surface of the gas-wetting sandstone cores.

Table 3 shows the mean contact angle of the gas-water systems and the contact angle of the gas-oil systems of the sandstone after treatment with FG40. It can be seen that the wettability of the cores treated with FG40 were effectively altered to gas-wetting. It should be noted that the observed trends in the contact angle of the sandstone treated with FG40 were similar to those of sandstone treated with FC911, which was different from results in Li's work [5]. The contact

(a) Water (without chemical treatment)

(b) Water (treated with 0.1% FC911, $\theta = 65^{\circ}$)

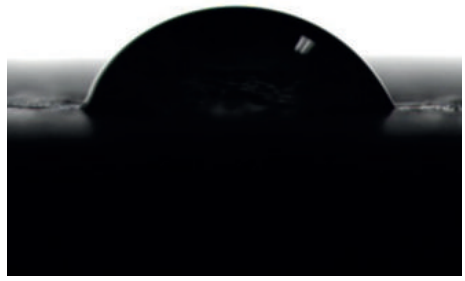

(c) Water (treated with 0.2% FC911, $\theta = 72^{\circ}$)

(d) Water (treated with 0.3% FC911, $\theta = 80^{\circ}$)

(e) Water (treated with 0.5% FC911, $\theta = 40^{\circ}$)

(f) Water (treated with 1.0% FC911, $\theta = 40^{\circ}$)

Figure 1: Water droplets on the surface of the sandstone cores before and after treatment with FC911.

angle increased with the increase of the concentration and then decreased when the concentration reached 0.3%. The contact angle of the gas-water systems increased to 140° and the contact angle of the gas-oil systems increased to 93° at a concentration of about 0.3%. This implies that the strongest gas-wetting can be obtained using FG40 at a concentration of 0.3%. Liquid droplets on the surface of the sandstone cores, before and after treatment with FG40 at different concentrations, are shown in Figures 3 and 4. It can be seen that liquid droplets were not spread on the surfaces of all of the sandstone cores that had been treated with FG40.

As the concentration of FG40 increased from 0 to 0.5%, the contact angle of the gas-water systems increased from 40° to 93°, and the contact angle of the gas-oil systems increased from 10° to 75°. This implies that wettability of the sandstone was altered to intermediate gas-wetting by FG40. With the increase of surfactant concentration, the contact angle continued to increase as well. At the concentration of 0.3%, the contact angle with the gas-water systems reached up to 140° and the gas-oil systems up to 93°. After that, the contact angle decreased with the increase of concentration.

4. Discussion

All of the three chemicals used in our study are fluorosurfactants with fluorocarbon groups. The fluorosurfactants have the highest surface activity of all of the surfactants identified so far [13]. The fluorochemical group provided

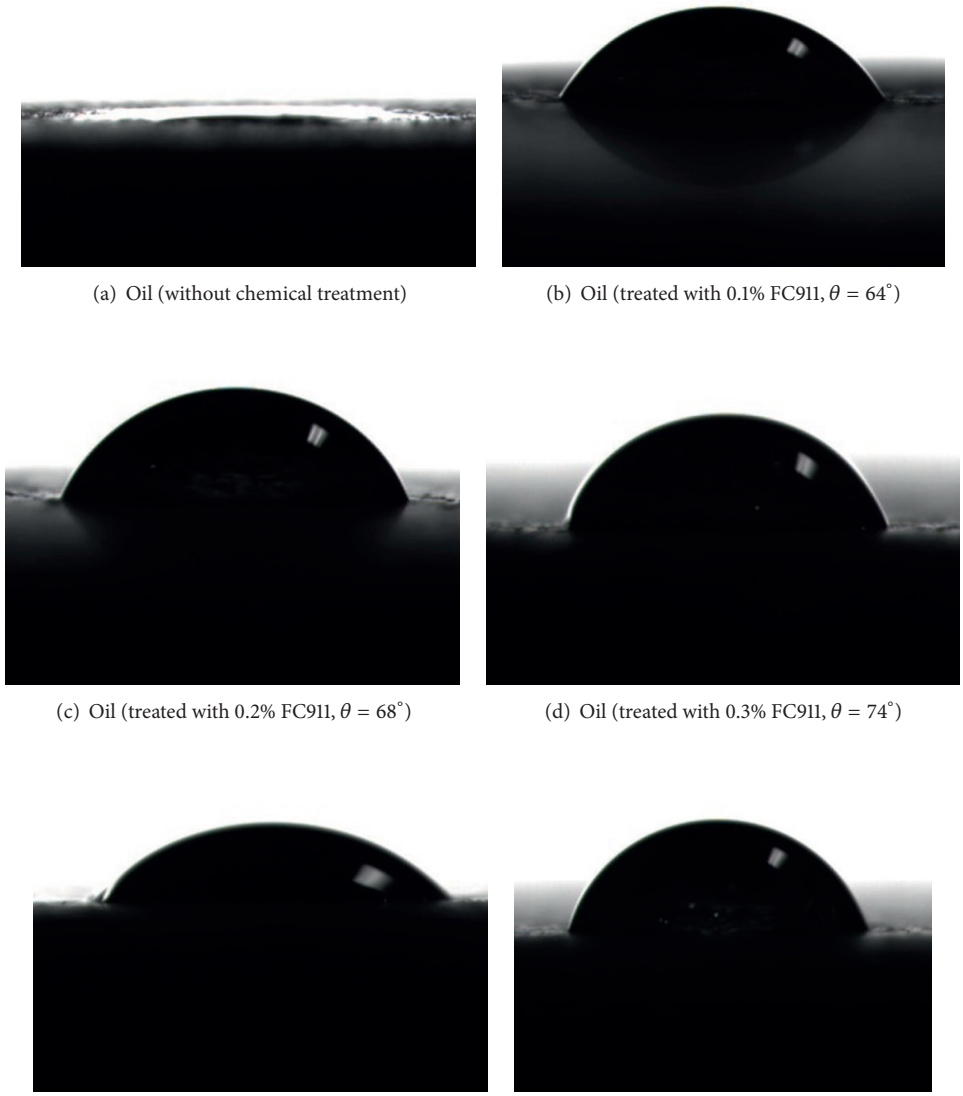

(a) Oil (without chemical treatment)

(b) Oil (treated with 0.1% FC911, $\theta = 64^{\circ}$)

(c) Oil (treated with 0.2% FC911, $\theta = 68^{\circ}$)

(d) Oil (treated with 0.3% FC911, $\theta = 74^{\circ}$)

(e) Oil (treated with 0.5% FC911, $\theta = 52^{\circ}$)

(f) Oil (treated with 1.0% FC911, $\theta = 76^{\circ}$)

Figure 2: Oil droplets on the surface of the sandstone cores before and after treatment with FC911.

the water and oil repellency; the cationic and nonionic groups chemically bonded onto the rock surfaces providing a surfacial treatment; the cationic and nonionic groups made the surfactant hydrophilically soluble [14].

The fluorocarbon group provided the water and oil repellency because it had a small van der Waals force between the fluorine and the carbon [15]. Fluorine atoms had a very strong electronegativity of 4.0. On the contrary, fluorocarbon molecules were extremely resistant to oxidation because fluorine atoms, with an electronegativity of 4.0, were attached to their carbon atoms, thereby bringing the carbon atoms into a more oxidized state than that of those bound to the oxygen atoms of an electronegativity of 3.6. Halogens were generally strongly electronegative with high bond energy between carbon and fluorine (in particular) which had the strongest bond energy at 484 kJ/mol. Moreover, fluorine atoms were small in size (next to the smallest hydrogen atoms) and their van der Waals and covalent bond radii were larger than those of the hydrogen atoms by only 10%, or so. This rather small difference in size caused the hydrocarbon chains to have a zigzag structure and the fluorocarbon chains to have a rigid rod-like shape with a period of twist with 13 carbon atoms. In addition, the carbon skeleton (within this rigid structure) was covered by densely packed fluorine atoms that were attached to the carbon atoms, much like a rod with a fluorine sheath on it [16]. The protective action of the fluorine atoms is shown in Figure 5.

The nature of fluorine atom leads to the water and oil repellency characteristic of the fluorosurfactants. Fluorine atom has the strongest electronegativity and the smallest

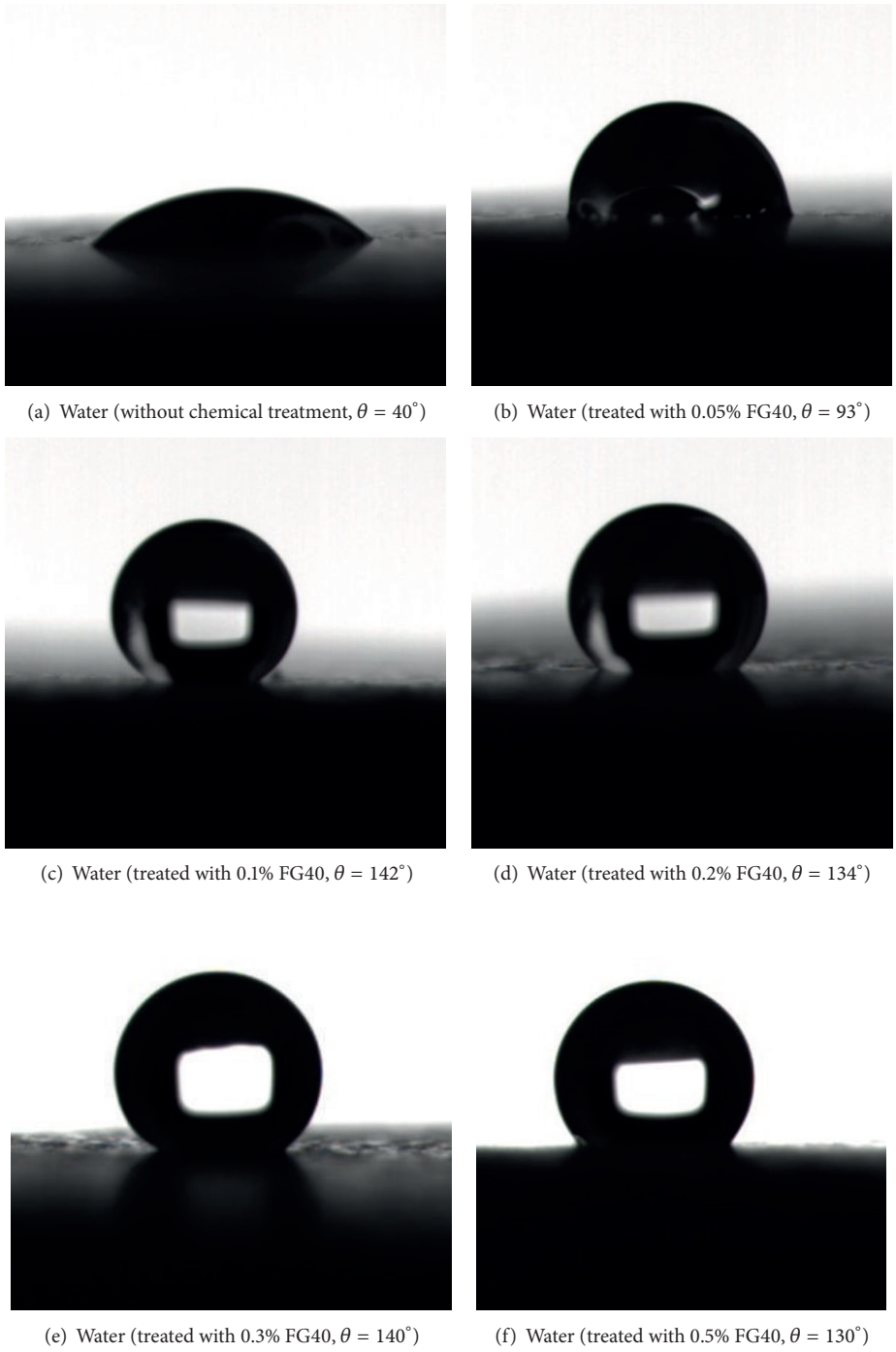

(a) Water (without chemical treatment, $\theta = 40^{\circ}$)

(b) Water (treated with 0.05% FG40, $\theta = 93^{\circ}$)

(c) Water (treated with 0.1% FG40, $\theta = 142^{\circ}$)

(d) Water (treated with 0.2% FG40, $\theta = 134^{\circ}$)

(e) Water (treated with 0.3% FG40, $\theta = 140^{\circ}$)

(f) Water (treated with 0.5% FG40, $\theta = 130^{\circ}$)

Figure 3: Water droplets on the surface of the sandstone cores before and after treatment with FG40.

atomic polarizability among the elements. Its atom radius is also smaller than other elements except for hydrogen. This enables the formation of a strong carbon-fluorine bond thereby forming the perfluoroalkyl group having weak intermolecular Van der Waals force and small interaction with other substances such as water and hydrocarbons. Then, the surfaces of the cores were altered to gas-wetting because of the water and oil repellency characteristic of the fluorosurfactants.

In Li's study [5], the contact angle was measured by a capillary tube test. Li found that the contact angle increased when the concentration of chemicals increased and then remained constant when the concentration increased to a certain value. After that, the gas-wetting remained the same with an increase in concentration. However, our findings are different from Li's results. Our results illustrate that the strongest gas-wetting of the surface of cores will appear at optimistic concentration of surfactants as shown in

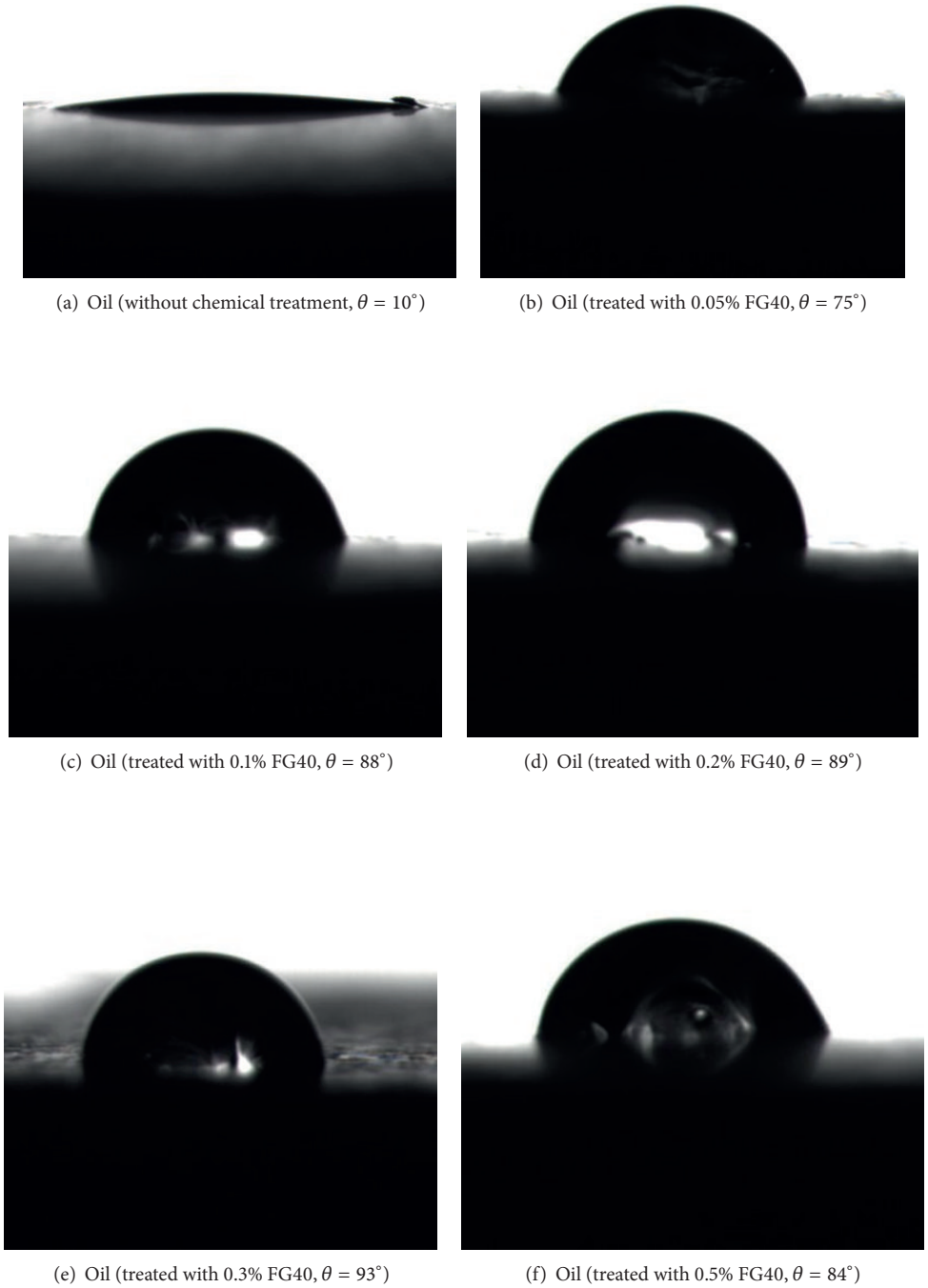

(a) Oil (without chemical treatment, $\theta = 10^{\circ}$)

(b) Oil (treated with 0.05% FG40, $\theta = 75^{\circ}$)

(c) Oil (treated with 0.1% FG40, $\theta = 88^{\circ}$)

(d) Oil (treated with 0.2% FG40, $\theta = 89^{\circ}$)

(e) Oil (treated with 0.3% FG40, $\theta = 93^{\circ}$)

(f) Oil (treated with 0.5% FG40, $\theta = 84^{\circ}$)

Figure 4: Oil droplets on the surface of the sandstone cores before and after treatment with FG40.

Table 3. The reduction in the gas-wetting may be due to the double-layer adsorption of the chemical [17, 18]. As shown in Figure 6, after the surface of the core is saturated by the adsorption of surfactant molecules, moleculars will adsorb and spread on the surfactants film through hydrophobic interactions with hydrophilic groups outward. Thus, the gas-wetting of the surface decreased, the water-wetting became stronger, and the contact angles decreased as the concentration increased.

5. Conclusions

The effectiveness of three fluorosurfactant treatments in altering reservoir core wettability from liquid-wetting to

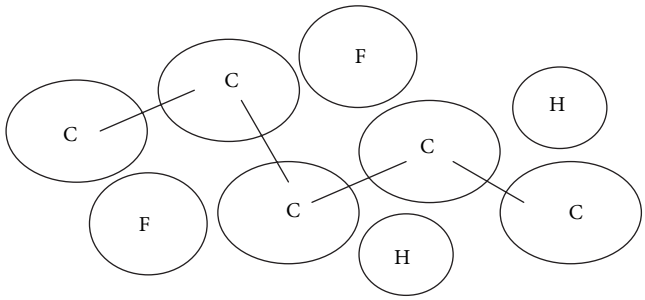

Figure 5: Protective action of fluorine atoms.

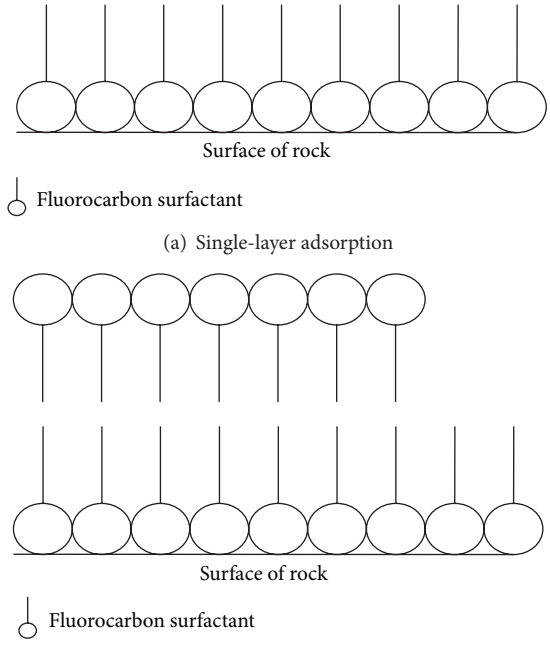

Figure 6: Adsorption of the Fluorocarbon Surfactant on the Surface of Rock.

intermediate gas-wetting was assessed. No significant improvement was observed after treating sandstone cores with FG1105. A 0.3% FC119 solution was found to effectively change the wettability of the sandstone rocks from preferential liquid-wetness to gas-wetness. FG40 had a better effect in altering reservoir core wettability from liquid wetting to intermediate gas wetting, with a very low concentration ranging from 0.05% to 0.5%. The contact angle increased with the increase of the concentration and then decreased when the concentration reached 0.3%. This was because of the adsorption of chemical changes from single-layer to double-layer with the increase in concentration.

Acknowledgments

We gratefully acknowledge the financial support from the Natural Foundation for Outstanding Youth of China (50925414), the Project of Science and Technology Development of Shandong Province (2010GSF10601), the Research Award Fund for Young Scientist of Shandong Province (BS2009CL019), the National Oil & Gas Key Special Project of China (2011ZX05005-006-007HZ), and the Fundamental Research Funds for the Central Universities.

References

[1] J. Yan, "Effect of rock wettability on oil recovery by waterflooding," *Journal of the University of Petroleum*, vol. 22, no. 3, pp. 43–46, 1998.

[2] H. Chun, T. Zhiqiang, and J. Guancheng, "Effect of wettability on water injection recovery factor of heavy oil reservoir of Kendong Block 29," *Oil Drilling & Production Technology*, vol. 21, no. 3, pp. 92–94, 1999.

[3] R. S. Barnum, F. P. Brinkman, T. W. Richardson, and A. G. Spillette, "Gas condensate reservoir behaviour: productivity and recovery reduction due to condensation," in *Proceedings of the SPE Annual Technical Conference and Exhibition*, vol. 30767, pp. 677–687, Dallas, Tex, USA, October 1995.

[4] K. Li and A. Firoozabadi, "Phenomenological modeling of critical condensate saturation and relative permeabilities in gas/condensate systems," *SPE Journal*, vol. 5, no. 2, pp. 138–147, 2000.

[5] K. Li and A. Firoozabadi, "Experimental study of wettability alteration to preferential gas-wetting in porous media and its effects," *SPE Reservoir Evaluation and Engineering*, vol. 3, no. 2, pp. 139–149, 2000.

[6] A. Delavarmoghaddam, S. A. Mirhaj, and P. L. J. Zitha, "Gas condensate productivity improvement by chemical wettability alteration," in *Proceedings of the 8th European Formation Damage Conference*, vol. 122225, pp. 27–29, Scheveningen, The Netherlands, May 2009.

[7] G.-Q. Tang and A. Firoozabadi, "Relative permeability modification in gas/liquid systems through wettability alteration to intermediate gas wetting," *SPE Reservoir Evaluation and Engineering*, vol. 5, no. 6, pp. 427–436, 2002.

[8] T.-Y. Yao, J.-S. Li, and F.-Y. Yao, "Effects of gas-wetting on porous flow behavior in gas-condensate reservoirs," *Oilfield Chemistry*, vol. 25, no. 2, pp. 101–104, 2008.

[9] Y. Liu, H. Zheng, G. Huang, G. Li, and K. Li, "Production enhancement in gas-condensate reservoirs by altering wettability to gas wetness: field application," in *Proceedings of the 16th SPE/DOE Improved Oil Recovery Symposium (IOR '08)*, vol. 99739, pp. 175–181, Tulsa, Okla, USA, April 2008.

[10] X. Wang and Z. Shi, "Fluoro surfactant," *Fine and Specialty Chemicals*, no. 24, pp. 14–15, 1999.

[11] D. Y. Kwok and A. W. Neumann, "Contact angle measurement and contact angle interpretation," *Advances in Colloid and Interface Science*, vol. 81, no. 3, pp. 167–249, 1999.

[12] D. Y. Kwok, R. Lin, M. Mui, and A. W. Neumann, "Low-rate dynamic and static contact angles and the determination of solid surface tensions," *Colloids and Surfaces A*, vol. 116, no. 1-2, pp. 63–77, 1996.

[13] A. H. Ahlbrecht and B. T. White, "Fluorocarbon sulfonamide alkanols and Sulfates Thereof," USP, 2803656, 1957.

[14] J. G. Linert, "A new water-soluble fluoropolymer silanol and its application in stone and concrete protection," in *Proceedings of the Waterborne, High-Solids, and Powder Coating Symposium*, 1997.

[15] W. Jiang, *Special surfactants*, Beijing Light Industrial Press, Beijing, China, 1995.

[16] M. Abe, "Synthesis and applications of surfactants containing fluorine," *Current Opinion in Colloid and Interface Science*, vol. 4, no. 5, pp. 354–356, 1999.

[17] Z. Bi, Y. Shi, W. Yan, and J. Yu, "Adsorption of cetyl trimethylamm on ium bromide on surface of silicon dioxide," *Huaxue Shiji*, vol. 19, no. 6, pp. 331–333, 1997.

[18] W. A. Ducker and E. J. Wanless, "Adsorption of hexadecyltrimethylammonium bromide to mica: nanometer-scale study of binding-site competition effects," *Langmuir*, vol. 15, no. 1, pp. 160–168, 1999.

Hindawi Publishing Corporation
Journal of Chemistry
Volume 2013, Article ID 675826, 5 pages
http://dx.doi.org/10.1155/2013/675826

Research Article

Study on Properties of Branched Hydrophobically Modified Polyacrylamide for Polymer Flooding

Lei-Ting Shi,[1] Cheng Li,[2] Shan-Shan Zhu,[1] Jie Xu,[2] Bao-Zong Sun,[3] and Zhong-Bin Ye[1]

[1] *State Key Laboratory of Oil & Gas Reservoir and Exploitation Engineering, Southwest Petroleum Institute, Chengdu 610500, China*
[2] *College of Chemistry & Chemical Engineering, Southwest Petroleum University, Chengdu 610500, China*
[3] *Institute of Xinjiang Oilfield Company, Karamayi, Xinjiang 834000, China*

Correspondence should be addressed to Cheng Li; 343317905@qq.com

Received 4 April 2013; Accepted 19 August 2013

Academic Editor: Ibnelwaleed Ali Hussien

The effect of partially hydrolyzed polyacrylamides (HPAMs) used for polymer flooding is unsatisfactory under the conditions of high temperature and high salinity. In order to improve the viscosifying ability of HPAM, branched macromolecular skeleton monomer is used to change the linear backbone structure. A new branched hydrophobically modified polyacrylamide (BHMPAM) was synthesized by the free radical copolymerization of functionalized branched macromolecular skeleton monomer, acrylamide (AM), acrylic acid (AA), and hydrophobic monomer hexadecyl-allyl-dimethyl ammonium chloride (C_{16}DMAAC). The properties of polymer solution were characterized; the results of the experiments showed that BHMPAM exhibited the properties of pseudoplastic fluid, and the viscosity of BHMPAM was 345.9 mPa·s (polymer concentration was 1750 mg/L) under the condition of 75°C and 9374 mg/L of salinity. Moreover, BHMPAM also performed well in viscoelasticity which can meet the property requirements for EOR polymer.

1. Introduction

Currently, the common used oil displacement agent is partially hydrolyzed polyacrylamide (HPAM), the viscosity of which, however, descends drastically with the increase of temperature and salinity [1]. Hence, along with the continuous development of oilfield and with the increasing severity of reservoir conditions, polyacrylamide should be improved in molecular weight or by increasing polymer concentration to satisfy the necessary viscosity. The former way makes its antishearing capacity decrease, while the latter makes its production costs increase dramatically. Hydrophobically associating water-soluble polymers (HAWSP), which contain a small amount of hydrophobic groups on the macromolecular chains, are developed to solve the problem of PAM as an oil displacement agent [2–4]; the viscosifying ability of HAWSP is improved, but HAWSP performs poorly in shear tolerance due to its linear molecular chain [5].

Compared with the traditional linear polymer, branched macromolecule, as a new highly branched polymer whose structure is similar to three-dimensional sphere, owns its unique features, including shear tolerance, rheology, and thermal stability [6, 7]. Moreover, combining branched macromolecule with linear hydrophobically associating polymer can improve the anti-shearing performance, temperature tolerance, and salt tolerance of the polymer aqueous solution, because there are more combination points producing hydrophobic intramolecular interaction, leading to stronger network structure in solution. In order to improve traditional polyacrylamide's properties and its applications in high temperature and salinity reservoirs, HPAM should be modified to change the viscosifying way. In this paper, we synthesized a new branched hydrophobically modified polyacrylamide (BHMPAM) and evaluated the properties of the polymer solution.

2. Experiments Involved

2.1. Materials. Ethylene diamine (≥99.0%), methyl acrylate (≥99.0%), methanol (≥99.0%), sulfuric acid (95–98%), maleic anhydride (≥99.0%), acrylic acid (≥99.0%), dimethyl

sulfoxide, acrylamide (≥99.0%), sodium hydrogen sulfite (≥58.5%), and ammonium persulfate (≥98.0%) were purchased from Chengdu Kelong Chemical Reagent Factory. C_{16}DMAAC is laboratory homemade. HPAMs (viscosity average molecular weight is 1.72×10^7, and degree of hydrolysis is 15%) were purchased from French SNF Company. The experiment water was prepared with doubly distilled water, and the ionic composition was shown in Table 1.

2.2. Synthesis

2.2.1. Synthesis and Functionalization of Branched Polyamidoamine. The methods of synthesis and modification of branched polyamidoamine macromolecular skeleton monomer refer to the literature [8]. The processes can be described as follows. At first, certain amounts of ethylene diamine and methyl acrylate were added into a three-necked flask with methanol as solvent under nitrogen at room temperature for 48 h. Then, the mixture was put on the rotary evaporator to react several hours under different temperatures, and the branched polyamidoamine was prepared. A certain quantity of branched polyamidoamine was dissolved with dimethyl sulfoxide as solvent in the wide-necked bottle. A certain quantity of maleic anhydride was added slowly when branched polyamidoamine was dissolved completely in order to obtain modified branched polyamidoamine macromolecule.

2.2.2. Synthesis of BHMPAM. The mechanical stirrer and N_2-inlet/outlet installation were equipped in a 250 mL, three-neck round-bottomed flask, in which acrylamide and acrylic acid were added at the mass ratio of 4 : 1 with distilled water as solvent, and then a certain quantity of hydrophobic monomer and functionalized branched macromolecular skeleton monomer was added. The initiators (sodium bisulfite and ammonium persulfate) were added at 45°C, and then solution reacted for 12 h. After reaction, the products were purified by methanol several times and then dried for several days under vacuum at 50°C, so BHMPAM were obtained. The result of measuring BHMPAM's viscosity average molecular weight was 7×10^6. The structure of BHMPAM compared to HPAM was shown in Figure 1.

2.3. Polymer Dissolving Time Test. Referring to China's National Standards about determination of the dissolution rate of powdered polyacrylamide (GB12005.8-1989), dissolving time was conducted on a DDS-11A conductivity meter at (30± 0.1)°C. The solvents used were distilled water and synthetic formation water.

2.4. Polymer Dissolution Preparation. For the dissolution of the polymers, a stock solution of 5000 mg/L was prepared by stirring the synthetic formation water (or distilled water) with a mechanical stirrer until a vortex was established. The polymer powder was poured slowly into the vortex and stirred for at least 3 h. This stock solution was subsequently diluted to obtain the desired concentration.

2.5. Viscosity Measurements. All viscosities were measured at a shearing rate of 7.34 s^{-1} with Brookfield DV-III at 65°C.

2.6. Rheological Property Test. Rheological measurements were conducted on a HAAKE RS600 Rotational Rheometer (Germany) at 65°C. Shear viscosity range was 0.01–200 s^{-1}.

2.7. Viscoelasticity Test. Storage modulus (G') and loss modulus (G'') measurements were conducted on a HAAKE RS600 Rotational Rheometer (Germany) at 65°C. Immobilization stress is 0.1 Pa, and vibration frequency range is 0.1–1.0 Hz.

3. Results and Discussion

3.1. Polymer Solubility. The results of dissolving time are shown in Table 2.

As shown in Table 2, BHMPAM exhibits good solubility in distilled water and in synthetic formation water. Normally, in the laboratory study, a dissolving time of polymer of less than 6 hours can be applied in the engineering field, and the time changes with the dissolving process conditions in engineering field. Although BHMPAM's solubility was poorer than HPAM's, the dissolving time of BHMPAM could still meet the solubility requirements in engineering application. The hydrophobic groups contained in BHMPAM were difficult to dissolve in the polar aqueous solution, and the strong molecular structure slowed down the diffusion rate between the polymer molecules and the solvent molecules, so that the BHMPAM's dissolving time was longer.

3.2. Effect of Polymer Solution Concentration on Apparent Viscosity. The viscosity of BHMPAM increased swiftly with the increasing polymer concentration when the polymer concentration was between 1000 and 1500 mg/L, as shown in Figure 2. BHMPAM exhibited the unique viscosifying ability, which meant that BHMPAM could substantially improve the mobility control capacity of aqueous phase in lower polymer concentrations.

The viscosity of polymer was constituted by the structural viscosity and bulk viscosity [9]. The structural viscosity was influenced by the structural strength of aggregates which was formed by polymer molecular chain in solution, and the key factor of affecting bulk viscosity was molecular weight. Due to intermolecular association and high degree of branching increasing the intermolecular entanglement, the structural viscosity was enhanced, so that the viscosity of BHMPAM is rather high while the molecular weight of BHMPAM was less than HPAM.

3.3. Effect of Temperature on Apparent Viscosity. In general, the viscosity of polymer solutions shows a temperature dependent behavior. As shown in Figure 3, the viscosity of BHMPAM changed little with the temperature below 55°C and then decreased with the increasing temperature. The viscosity of BHMPAM decreased by 43.4%. For HPAM, the viscosity was plummeting quickly at the elevated temperature, and the viscosity decreased by 63.5%. Hence, it could be shown that the BHMPAM performed better at temperature

Table 1: The ionic composition of synthetic formation water.

Synthetic formation water	Composition	Na^+ and K^+	Ca^{2+}	Mg^{2+}	CO_3^{2-}	HCO_3^-	SO_4^{2-}	Cl^-	TDS
	Content (mg/L)	3091.96	276.17	158.68	14.21	311.48	85.29	5436.34	9374.12

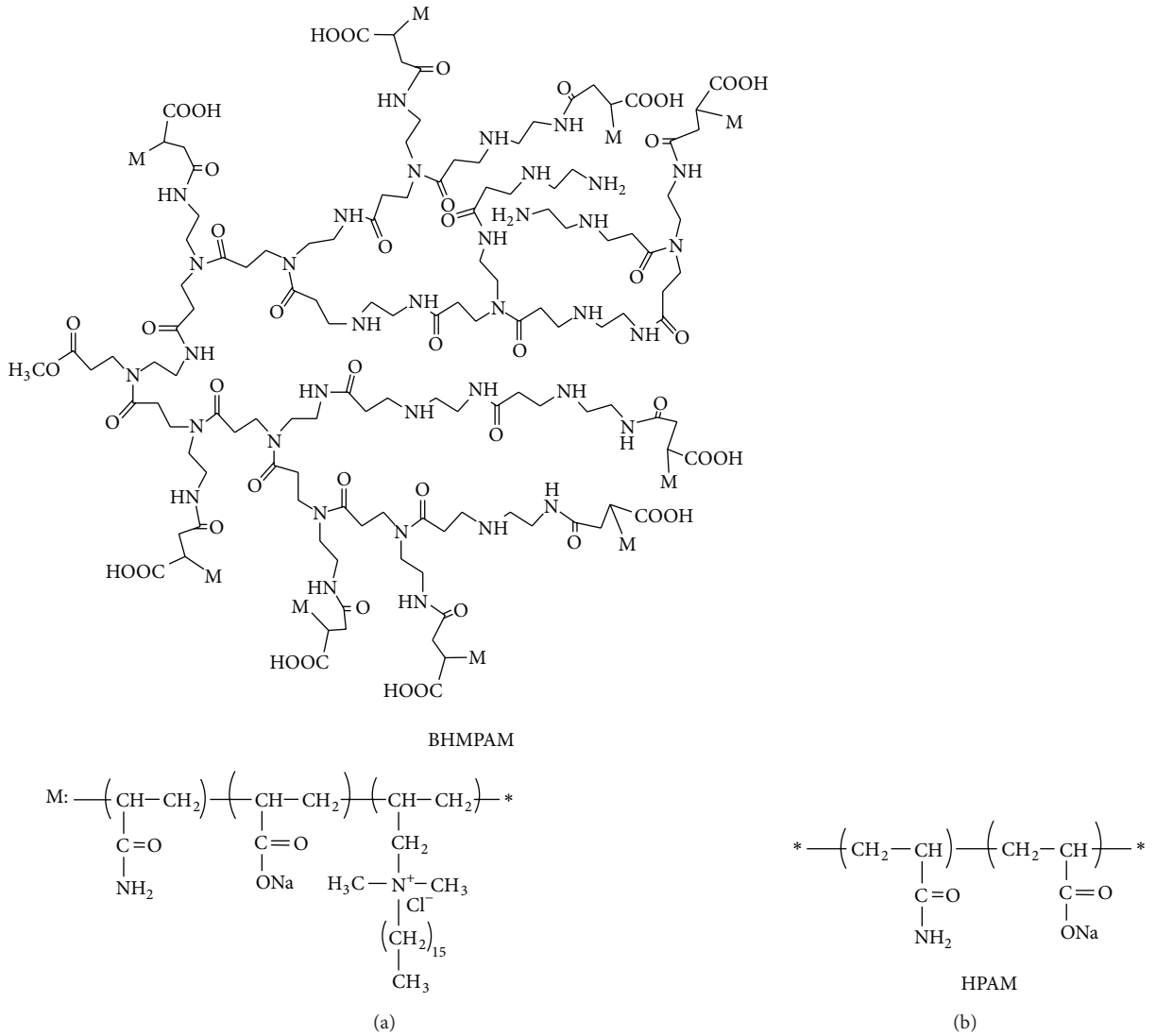

Figure 1: The structure of BHMPAM compared to HPAM.

tolerance. When BHMPAM was used in high temperature reservoirs, it could also meet the viscosifying requirement.

The influence of temperature on the viscosity of BHMPAM appeared in two aspects [10, 11]. On one hand, the increasing temperature intensified the thermal motion of the hydrophobic groups and water molecules, which changed the hydration around the hydrophobic group and weakened the hydrophobic interaction, so the viscosity decreased. On the other hand, the intermolecular association increased with the rising temperature, because the hydrophobic association was an endothermic entropy-driven process. As a result of the two aspects, the viscosity of BHMPAM decreased by 12.6% below 55°C and decreased by 47.6% when temperature reached 75°C. But for HPAM, the hydrogen bond interactions among molecules decreased with the rise of temperature, which curled the molecular chains, so the viscosity decreased quickly over the whole temperature range.

3.4. Effect of Shearing Rate on Apparent Viscosity. As shown in Figure 4, BHMPAM exhibited good shearing thinning under the high shearing rate; when the shearing rate is low, BHMPAM solution presented high viscosity. In polymer flooding, the shearing rate was higher in near borehole zones, BHMPAM's shearing thinning under high shearing rate is beneficial for its injection, the shear rate decreased after solution was injected into formation, and the viscosity of BHMPAM was high under low shearing rate which made it perform well in the mobility control capacity.

Table 2: The solubility of BHMPAM and HPAM.

Sample	Granularity (μm)	Stirring rate (r/min)	Temperature (°C)	Concentration (mg/L)	Time (h)
BHMPAM[1]	350~833	90	30	5000	2.5
BHMPAM[2]	350~833	90	30	5000	4.3
HPAM[1]	350~833	90	30	5000	1.6
HPAM[2]	350~833	90	30	5000	2.4

(1: the solvent is distilled water; 2: the solvent is synthetic formation water.)

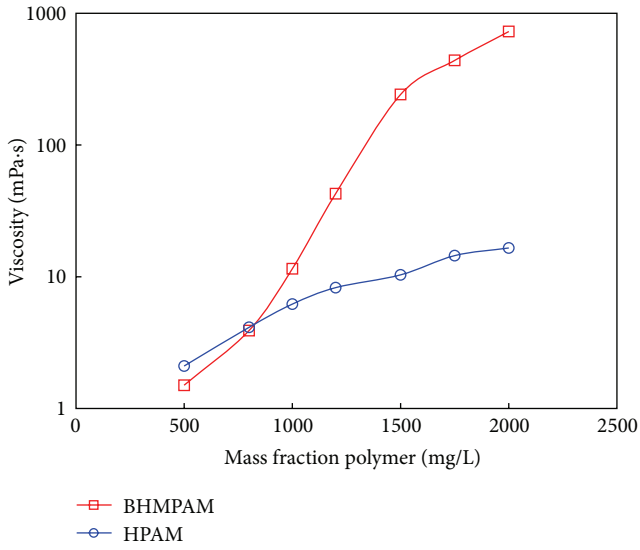

Figure 2: Viscosity versus polymer concentration of BHMPAM compared to HPAM in synthetic formation water.

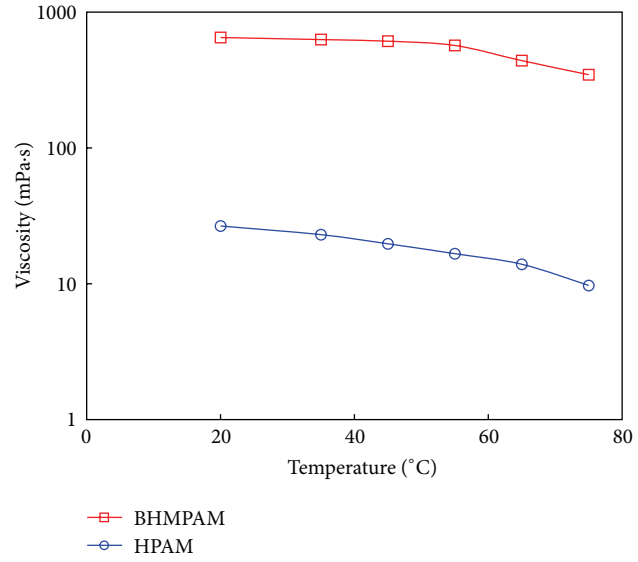

Figure 3: Viscosity versus temperature of BHMPAM compared to HPAM in synthetic formation water (concentration of both polymers: 1750 mg/L).

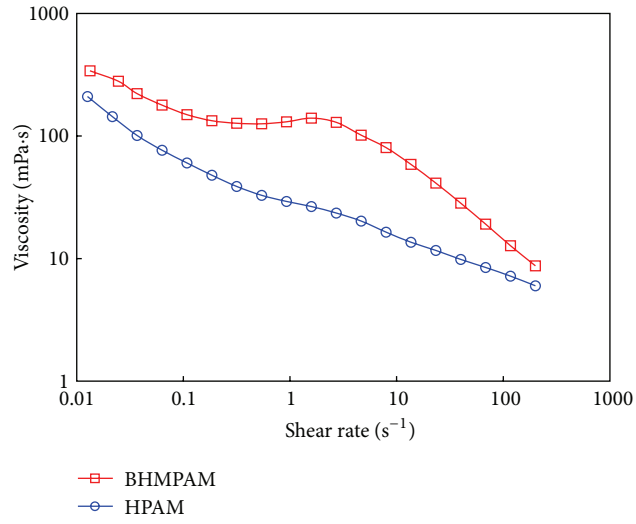

Figure 4: Viscosity versus shearing rate of BHMPAM compared to HPAM in synthetic formation water (concentration of both polymers: 1750 mg/L).

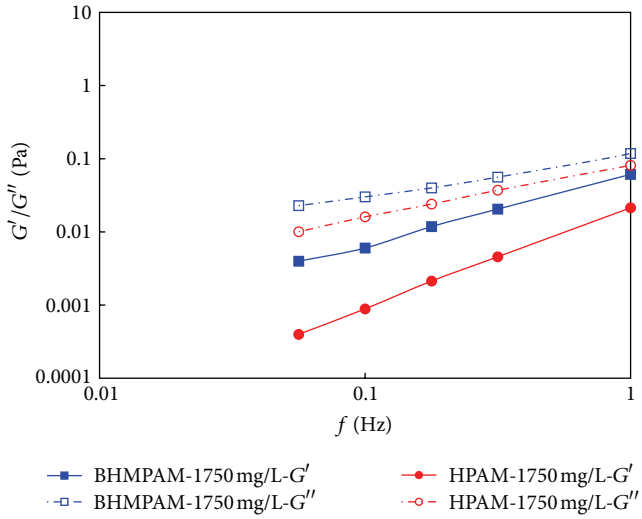

Figure 5: Viscoelasticity versus vibrational frequency of BHMPAM compared to HPAM in synthetic formation water (concentration of both polymers: 1750 mg/L).

When the BHMPAM solution concentration exceeded associating concentration, the hydrophobic association formed mainly between different polymer chains, which generated supramolecular aggregates. The hydrophobic association may present a reversible equilibrium state with both formation and destruction under shearing. With the increasing of shearing rate, the destruction rate of the association of aggregates was greater than the rate of formation, so that the size of the aggregates in the solution decreased, and the viscosity decreased with the increasing

of shear rate and the polymer solution performed shear thinning [12].

BHMPAM's viscosifying is superior to HPAM under shearing. On one hand, the hydrophobic association formed network structure in solution; on the other hand, BHMPAM's degree of branching was so high that the hydrodynamic radius was relatively small, while compared to the same molecular weight of straight chain HPAM. The results were absolutely obvious; that is, the entanglement of molecular chains increased and the chain was hard to cut.

3.5. Viscoelasticity. The G', G'' of BHMPAM and HPAM were unceasingly going up along with the increasing of vibrational frequency which was shown in Figure 5. Because G'' was larger than G', the viscosity of polymer solution was greater than elasticity, and the viscoelasticity of BHMPAM increased dramatically compared with HPAM which was beneficial for BHMPAM as oil displacement agent.

Solution structure was formed by entanglement or intermolecular interaction. The deformation of solution structure would consume energy under imposed stress; at this time, the polymer solution would present viscosity. Also, the deformation of solution structure was a relaxation process, and the elasticity of polymer would be triggered when the deformation lagged behind imposed stress [13]. The viscoelasticity of BHMPAM increased, because the hydrophobic association formed network structure in solution and the high degree of branching increased the entanglement of molecular chains in BHMPAM solution which enhanced the solution structure and extended the relaxation time of deformation.

4. Conclusion

(1) A new branched hydrophobically modified polyacrylamid (BHMPAM) was synthesized by the free radical copolymerization; this method is simple and convenient and can be easily implemented into industrial production.

(2) The structure of main chain of BHMPAM is highly branched, which enhances the temperature tolerance and the salinity tolerance of polymer aqueous solution, and BHMPAM shows the property of shearing thinning which is beneficial for injection.

(3) BHMPAM shows higher viscosifying ability, and the viscoelasticity, especially elasticity of BHMPAM, increases dramatically compared with HPAM, which makes BHMPAM able to meet the requirements for oil displacement agent used in high temperature and high salinity reservoir.

Acknowledgment

This financial support by the special fund of China's central government for the development of local colleges and universities—the project of National First-Level Discipline in Oil and Gas Engineering is gratefully acknowledged.

References

[1] L. D. Chen, "Polyacrylamides for enhanced oil recoveries," *Oilfield Chemistry*, vol. 10, no. 3, pp. 283–290, 1993.

[2] D. G. Peiffer, "Hydrophobically associating polymers and their interactions with rod-like micelles," *Polymer*, vol. 31, no. 12, pp. 2353–2360, 1990.

[3] S. Biggs, A. Hill, J. Selb, and F. Candau, "Copolymerization of acrylamide and a hydrophobic monomer in an aqueous micellar medium: effect of the surfactant on the copolymer microstructure," *The Journal of Physical Chemistry*, vol. 96, no. 3, pp. 1505–1511, 1992.

[4] S. Zou, W. Zhang, X. Zhang, and B. Jiang, "Study on polymer micelles of hydrophobically modified ethyl hydroxyethyl cellulose using single-molecule force spectroscopy," *Langmuir*, vol. 17, no. 16, pp. 4799–4808, 2001.

[5] Y. J. Feng, C. Q. Luo, P. Y. Luo et al., "Study on characterization of microstructure of hydrophobically associating water-soluble polymer in aqueous media by scanning electron microscopy and environmental scanning electron microscopy," *Acta Petroleli Sinica*, vol. 17, no. 6, pp. 39–44, 2001.

[6] C. Gao and D. Yan, "Hyperbranched polymers: from synthesis to applications," *Progress in Polymer Science*, vol. 29, no. 3, pp. 183–275, 2004.

[7] K. Ishizu, D. Takahashi, and H. Takeda, "Novel synthesis and characterization of hyperbranched polymers," *Polymer*, vol. 41, no. 16, pp. 6081–6086, 2000.

[8] L. T. Shi, Z. B. Ye, H. Liji, S. X. Wang, and K. L. Zhou, "Preparation method and application of one anti-shearing polymer," China, CN201210117149.9[P], August 15 2012.

[9] J. Wang, Y. Zheng, Y. J. Feng, and P. Y. Luo, "A novel associative polymer for EOR: performance properties," *Oilfield Chemistry*, vol. 16, no. 2, pp. 149–152, 1999.

[10] F. S. Hwang and T. E. Hogen-Esch, "Effects of water-soluble spacers on the hydrophobic association of fluorocarbon-modified poly(acrylamide)," *Macromolecules*, vol. 28, no. 9, pp. 3328–3335, 1995.

[11] X. H. Huang and G. Q. Xu, "Study on solution properties of poly(acrylamide/tetrad-ecyl acrylate) hydrophobically associating copolymer," *Fine Chemicals*, vol. 17, no. 3, pp. 152–155, 2000.

[12] B. G. Cao, *The experiment study on the rheological properties and viscoelastic of hydrophobic associating polymer solution used to displace crude oil [Ph.D. thesis]*, Southwest Petroleum University, Chengdu, China, 2006.

[13] Y. X. Sun, *The research on the mechanism of oil displacement efficiency by polymer flooding with viscoelasticity [Ph.D. thesis]*, Daqing Petroleum Institute, Daqing, China, 2009.

Hindawi Publishing Corporation
Journal of Chemistry
Volume 2013, Article ID 437309, 10 pages
http://dx.doi.org/10.1155/2013/437309

Research Article

Synthesis and Performance of an Acrylamide Copolymer Containing Nano-SiO_2 as Enhanced Oil Recovery Chemical

Zhongbin Ye,[1,2] Xiaoping Qin,[1,2] Nanjun Lai,[1,2] Qin Peng,[2] Xi Li,[2] and Cuixia Li[3]

[1] *State Key Laboratory of Oil and Gas Reservoir Geology and Exploitation, Southwest Petroleum University, Chengdu 610500, China*
[2] *College of Chemistry and Chemical Engineering, Southwest Petroleum University, Chengdu 610500, China*
[3] *Department of Petroleum Chemical Engineering, Karamay Vocational & Technical College, Karamay 833600, China*

Correspondence should be addressed to Xiaoping Qin; 948801727@qq.com and Nanjun Lai; 29511393@qq.com

Received 4 April 2013; Revised 9 July 2013; Accepted 12 August 2013

Academic Editor: Ibnelwaleed Ali Hussien

A novel copolymer containing nano-SiO_2 was synthesized by free radical polymerization using acrylamide (AM), acrylic acid (AA), and nano-SiO_2 functional monomer (NSFM) as raw materials under mild conditions. The AM/AA/NSFM copolymer was characterized by infrared (IR) spectroscopy, ^{1}H NMR spectroscopy, elemental analysis, and scanning electron microscope (SEM). It was found that the AM/AA/NSFM copolymer exhibited higher viscosity than the AM/AA copolymer at 500 s^{-1} shear rate (18.6 mPa·s versus 8.7 mPa·s). It was also found that AM/AA/NSFM could achieve up to 43.7% viscosity retention rate at 95°C. Mobility control results indicated that AM/AA/NSFM could establish much higher resistance factor (RF) and residual resistance factor (RRF) than AM/AA under the same conditions (RF: 16.52 versus 12.17, RRF: 3.63 versus 2.59). At last, the enhanced oil recovery (EOR) of AM/AA/NSFM was up to 20.10% by core flooding experiments at 65°C.

1. Introduction

Polymer flooding plays an important role in the field of enhanced oil recovery (EOR) [1, 2]. However, the current widely used polymers, polyacrylamide (PAM) and partially hydrolyzed polyacrylamide (HPAM), cannot completely meet the requirements due to the hydrolysis, degradation, and others under high temperature or high salinity [3–6]. Furthermore, PAM and HPAM have poor shear resistance [2–7]. Polymer molecular chains will be cut off when polymer solution passes through the pump, pipeline, perforation, and porous medium at high speed, so the viscosity of polymer solution will be greatly reduced [1, 7, 8].

Recently, many studies have demonstrated that performance of composite material could be significantly improved by combination or copolymerization with a functional monomer containing nano-SiO_2. The composite material containing Nano-SiO_2, such as polyethylene terephthalate [9], styrene butadiene rubber [10], polyaniline [11], polyimide [12], and nylon 6 [13], may exhibit more satisfactory thermal stability, toughness, and strength owing to the effect of physical adsorption, hydrogen bond, Si–O bond, and C–Si bond [10, 12, 14–16]. However, there are no papers about the application of nano-SiO_2 in polymer for flooding to develop temperature tolerance, salt tolerance, and shear resistance of copolymer.

Keeping in mind these fundamental conditions, herein, a novel nano-SiO_2 functional monomer (NSFM; see Scheme 1) was introduced into AM/AA copolymer aiming to obtain satisfying temperature tolerance, salt tolerance, and shear resistance [17–20].

2. Experimental

2.1. Chemicals and Reagents. Ethanol (C_2H_5OH, ≥99.7%), ammonia (NH_4OH, 28.0%), vinyltriethoxysilane (VTES, ≥98.0%), acrylic acid (AA, ≥99.5%), acrylamide (AM, ≥99.0%), sodium hydrogen sulfite ($NaHSO_3$, ≥58.5%), ammonium persulfate ($(NH_4)_2S_2O_8$, ≥98.0%), sodium hydroxide (NaOH, ≥96.0%), sodium chloride (NaCl, ≥99.5%), magnesium chloride hexahydrate ($MgCl_2{\cdot}6H_2O$, ≥98.0%), calcium chloride anhydrous ($CaCl_2$, ≥96.0%), potassium chloride (KCl, ≥99.5%), sodium sulfate (Na_2SO_4, ≥99.0%),

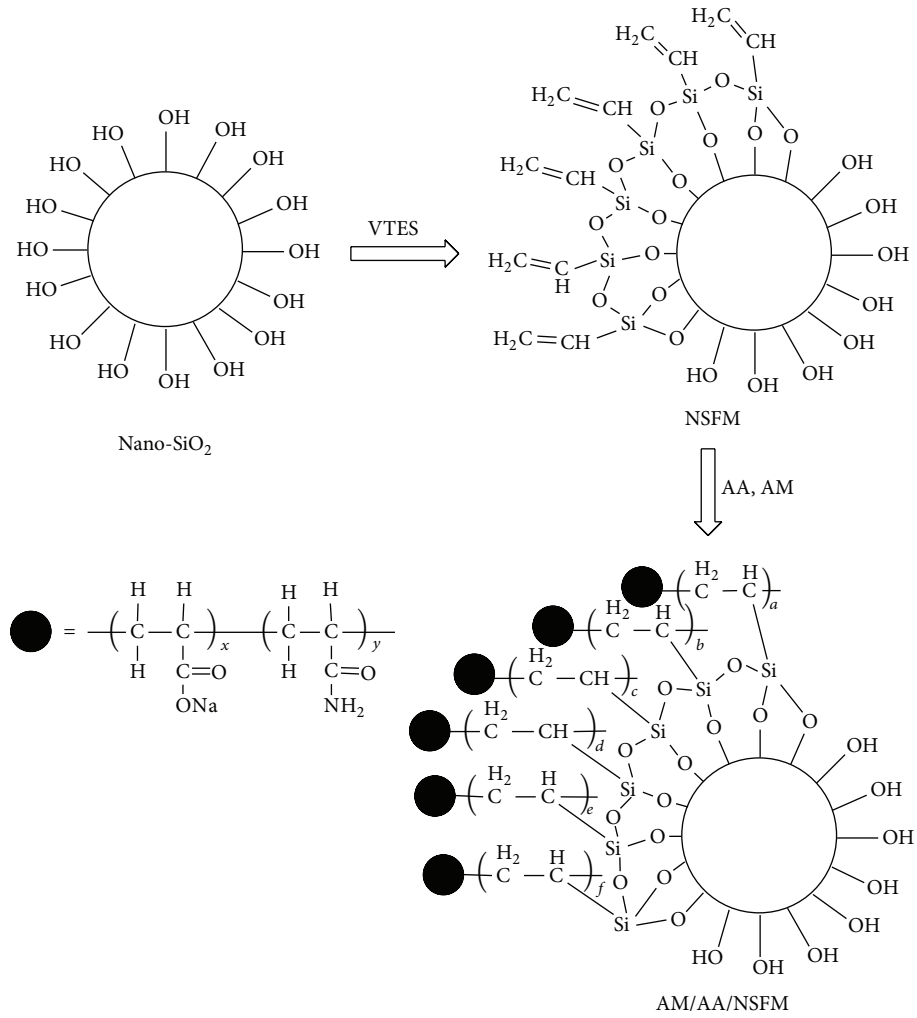

Scheme 1: The synthesis of AM/AA/NSFM.

and sodium bicarbonate ($NaHCO_3$, ≥99.5%) were purchased from Chengdu Kelong Chemical Reagent Factory (Sichuan, China). Nano-SiO_2 (10–20 nm) was obtained from Aladdin chemistry (Shanghai, China) Co., Ltd. All chemicals and reagents were used as received without any further purification. Water was deionized by passing through an ion-exchange column and doubly distilled.

2.2. Preparation of Nano-SiO_2 Functional Monomer. Firstly, 83.6 mL ethanol, 1.5 g nano-SiO_2, 13.6 mL distilled water, and 1.3 mL ammonia were added into a 250 mL round-bottom flask, and the mixture was dispersed with supersonic wave for 30 min. Then 2.0 mL VTES was added into the stirred solution in the round-bottom flask, and the reaction time was 18 h at 30°C. After reaction, the product was NSFM which was separated by centrifugation and washed with distilled water [21–23].

2.3. Synthesis of AM/AA/NSFM. 0.05 g NSFM, 6.50 g AM, 3.45 g AA, and a certain amount of distilled water were added into a 100 mL three-necked flask, respectively, and the pH value of the mixture was regulated to 7.0 using sodium hydroxide solution; then the solution with 20% total monomer mass concentration was prepared. 0.05 g $NaHSO_3$-$(NH_4)_2S_2O_8$ initiator (mol ratio = 1 : 1) was taken along with distilled water in the three-necked flask assembled with a nitrogen (N_2) inlet. Then the copolymerization was carried out at 45°C under N_2 atmosphere for 6 h. Finally, the AM/AA/NSFM copolymer was obtained after ethanol washing, drying, and pulverizing. The synthesis of AM/AA/NSFM is shown in Scheme 1 [20]. The AM/AA copolymer was synthesized by using the same method.

2.4. Characterization. Infrared (IR) spectra of AM/AA and AM/AA/NSFM were measured with KBr pellets using a Perkin Elemer RX-1 spectrophotometer. ^{1}H NMR spectrum of AM/AA/NSFM was recorded on a Bruker AC-E 200 spectrometer by dissolving the copolymer in D_2O and operating at 400 MHz. The elementary analysis of AM/AA/NSFM was carried out with a Vario EL-III elemental analyzer. The microstructures of AM/AA and AM/AA/NSFM were observed by a scanning electron microscope (SEM). The

Table 1: Composition and TDS of brine.

Composition	NaCl	KCl	$CaCl_2$	$MgCl_2{\cdot}6H_2O$	Na_2SO_4	$NaHCO_3$	TDS
Content (wt%)	0.8495	0.0149	0.0764	0.2154	0.0125	0.0428	1.0951

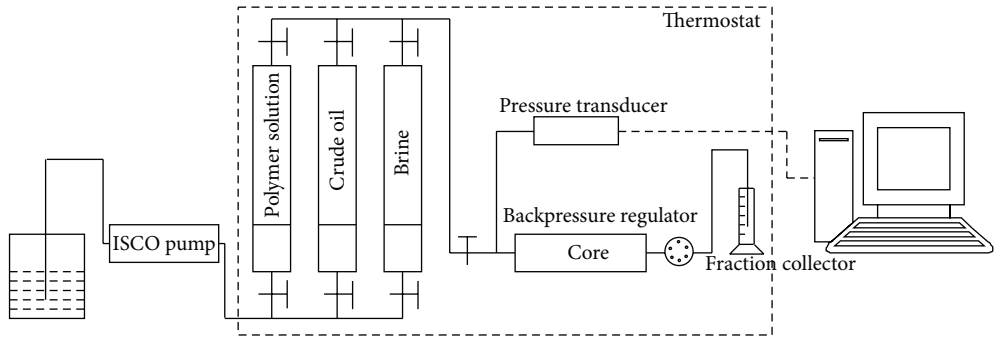

Figure 1: Flow chart of the core flooding experiments.

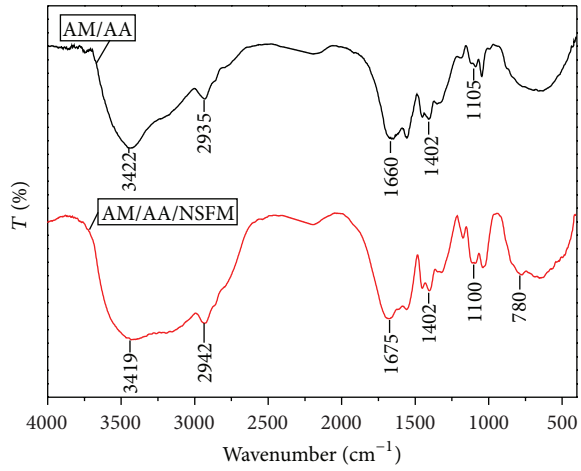

Figure 2: IR spectra of AM/AA and AM/AA/NSFM.

weight-average molecular weight (M_w) of the copolymers was obtained by using a BI-200SM wide angle dynamic/static laser light scattering apparatus.

2.5. Intrinsic Viscosity. The intrinsic viscosity of copolymer was measured with an Ubbelohde viscometer at 25°C. The test temperature was controlled using a constant temperature bath. The flux time was reproducible to 0.05 s using a stopwatch. The copolymer solutions, at five different concentrations (0.1000, 0.0667, 0.0500, 0.0333, and 0.0250 wt%), were prepared with distilled water. The specific viscosity is calculated via the following equation [6, 24, 25]:

$$\eta_{sp} = \frac{t - t_0}{t_0}, \tag{1}$$

where η_{sp} is the specific viscosity of copolymer; t_0 is flux time of distilled water, s; and t is flux time of copolymer solution, s.

Then the intrinsic viscosity is calculated with the Huggins equation [6, 26]:

$$\frac{\eta_{sp}}{C} = [\eta] + K'[\eta]^2 C, \tag{2}$$

where $[\eta]$ is intrinsic viscosity, mL/g; C is concentration of copolymer solution, wt%; and K' is the Huggins constant.

2.6. Rheological Property and Viscoelasticity. Rheological property and viscoelasticity measurements of the copolymers were conducted on a HAAKE RS 600 Rotational Rheometer (Germany). The shear rate was from 0.007 s^{-1} to 500 s^{-1}, and the temperature was 65°C with a heating rate of 1.5°C/min, while the test system was binocular tube and the rotor was DG41Ti in rheological measurements. The scanning range of frequency (f) was 0.01–10 Hz, and the stress was 0.1 Pa by using the same test system and rotor in viscoelasticity measurements.

2.7. Mobility Control Ability. The mobility control ability of the copolymer solutions is characterized by the resistance factor (RF) and the residual resistance factor (RRF) [27–29]. The RF is calculated with the following equation:

$$\mathrm{RF} = \frac{K_w/\mu_w}{K_p/\mu_p}, \tag{3}$$

where K_w is aqueous phase permeability, mD; K_p is polymer phase permeability, mD; μ_w is the viscosity of aqueous phase, mPa·s; and μ_p is the viscosity of polymer phase, mPa·s.

The RRF is calculated with the following equation:

$$\mathrm{RRF} = \frac{K_{wb}}{K_{wa}}, \tag{4}$$

where K_{wb} is aqueous phase permeability before polymer flooding, mD; K_{wa} is aqueous phase permeability after polymer flooding, mD.

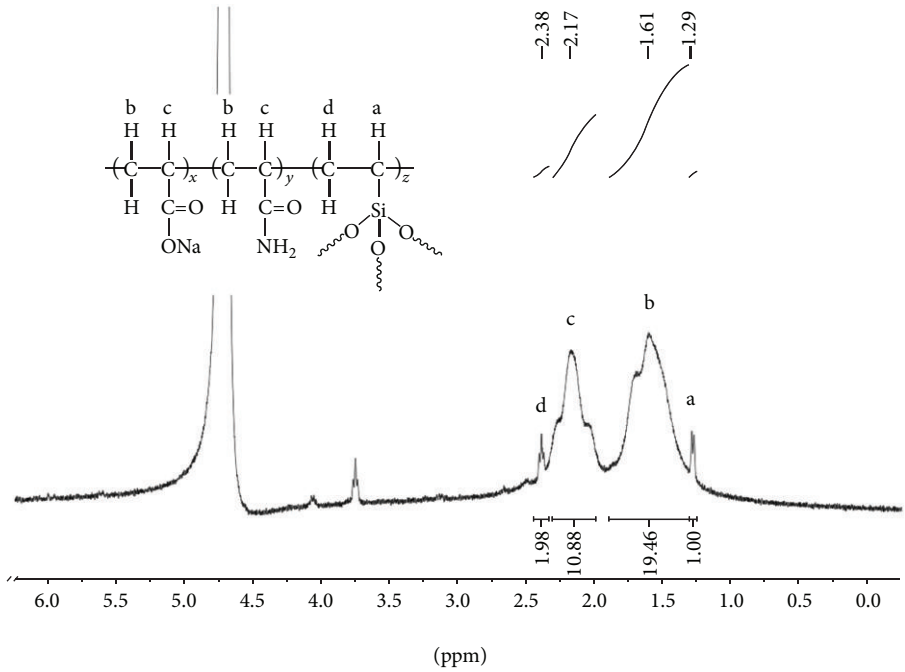

Figure 3: ^{1}H NMR spectrum of AM/AA/NSFM in D_2O.

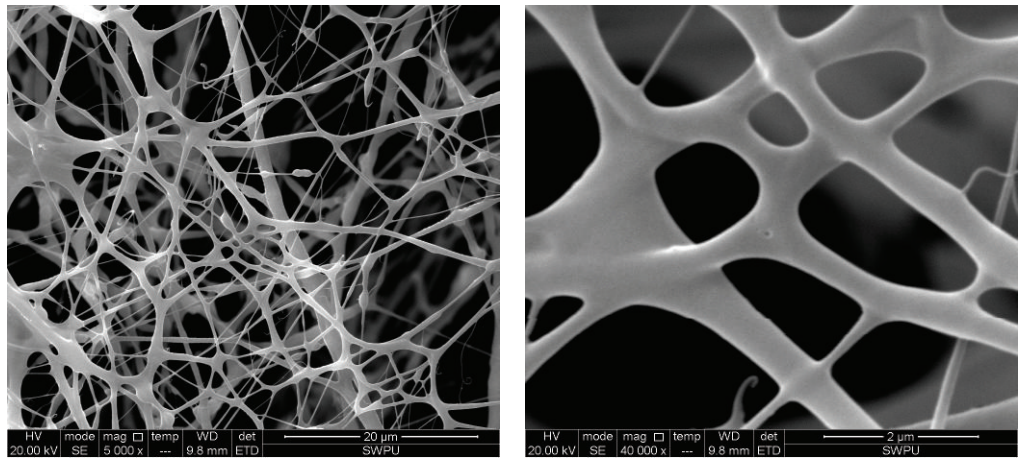

(a) (b)

Figure 4: SEM images of AM/AA.

2.8. Core Flooding Tests. Two Berea sandstone cores were used for core flooding experiments. The cores were dried at 65°C, and then their length, diameter, porosity, and gas permeability were measured by using a SCMS-B2 core multiparameter measurement system. A Hassler core holder was used with 3.5 MPa confining pressure and 1.5 MPa backpressure. The core, after being saturated with brine, was saturated with crude oil (52.5 mPa·s at 65°C) at 0.1-0.2 mL/min until irreducible water saturation (S_{wi}) was obtained. After 72 h of aging, the core was flooded by the brine at 0.2 mL/min until water cut was up to 95%, and then the copolymer solution (0.2 wt%) was injected at 0.2 mL/min until water cut reached 95% once more [6, 29]. All the core flooding procedures were conducted at 65°C. Chemical composition and total dissolved solids (TDS) of the brine are listed in Table 1. The maximum work pressure of the ISCO 260D syringe pump is 50 MPa, and its minimum and maximum displacement velocity is 0.001 and 50.000 mL/min, respectively. The EOR is calculated with the following equation:

$$\text{EOR} = E - E_w, \tag{5}$$

where EOR is enhanced oil recovery, %; E is the oil recovery of the whole displacement process, %; and E_w is the oil recovery of water flooding, %.

Flow chart of the core flooding experiments is shown in Figure 1.

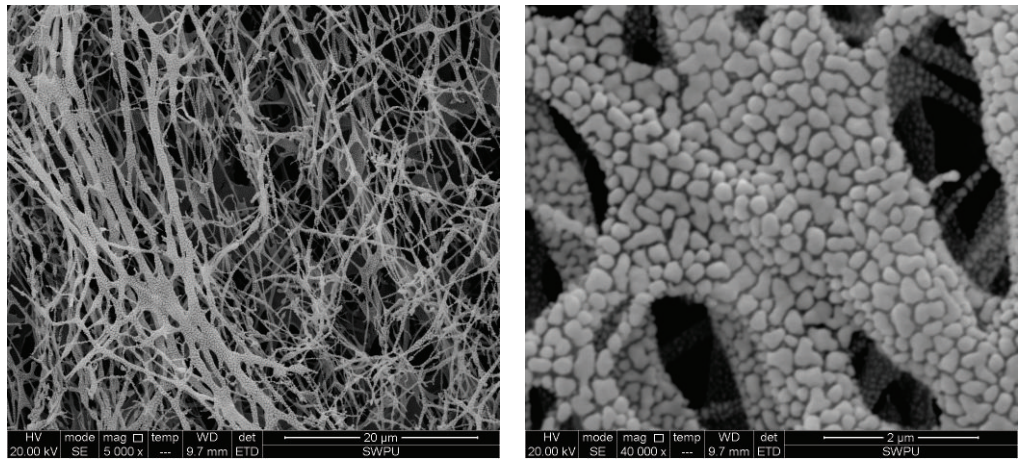

(a) (b)

Figure 5: SEM images of AM/AA/NSFM.

Table 2: The relevant core properties and the results of core flooding experiments.

Copolymer	Cores	Length (cm)	Diameter (cm)	Porosity (%)	Permeability (mD)	S_{wi} (%)	E (%)	E_w (%)	EOR (%)
AM/AA	1#	8.84	3.77	23.11	937.03	19.18	45.73	31.51	14.22
AM/AA/NSFM	2#	8.92	3.78	23.05	926.28	19.37	52.85	31.75	20.10

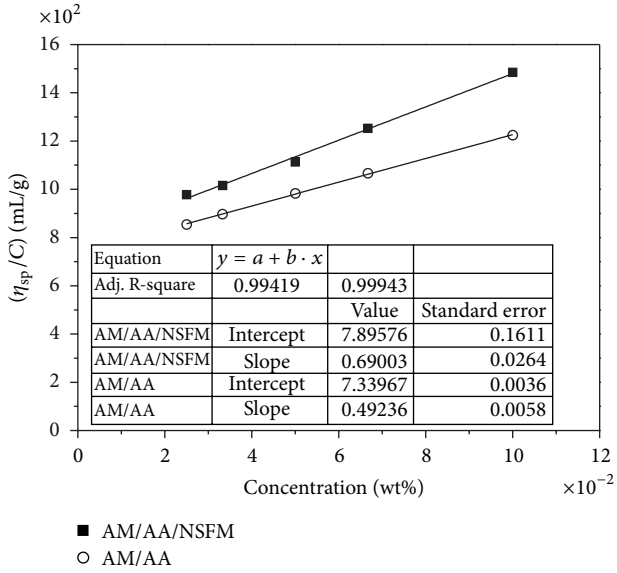

Figure 6: The η_{sp}/C versus C relationships of AM/AA and AM/AA/NSFM.

3. Results and Discussion

3.1. IR Spectra Analysis. The structures of AM/AA and AM/AA/NSFM were confirmed by IR spectra as illustrated in Figure 2. The AM/AA/NSFM which was prepared using acrylic acid, acrylamide, and NSFM by free radical polymerization was confirmed by strong absorptions at 3419 cm^{-1} (–NH stretching vibration and –OH stretching vibration), 2942 cm^{-1} (–CH_2 stretching vibration), 1675 cm^{-1} (C=O stretching vibration), 1402 cm^{-1} (C–N stretching vibration), 1100 cm^{-1} (Si–O–Si asymmetric stretching vibration), and 780 cm^{-1} (Si–O–Si symmetric stretching vibration) in the spectrum of AM/AA/NSFM [18, 20]. The peak at 3419 cm^{-1} was broad in the IR spectrum of AM/AA/NSFM partly due to the hydroxyl on nano-SiO_2 surface [20]. As expected, the IR spectra confirmed the presence of different monomers in AM/AA/NSFM.

3.2. ^1H NMR Analysis. The ^{1}H NMR spectrum of AM/AA/NSFM is shown in Figure 3. The chemical shift value at 1.29 ppm is due to the protons of [–CH_2–C**H** ($Si(O–)_3$)–]. The chemical shift value at 1.61 ppm is assigned to the protons of [–C**H**$_2$–CH ($CONH_2$)–] and [–C**H**$_2$–CH (COONa)–]. The protons of [–CH_2–C**H** ($CONH_2$)–] and [–CH_2–C**H** (COONa)–] appear at 2.17 ppm. The characteristic peak due to the protons of [–C**H**$_2$–CH ($Si(O–)_3$)–] is observed at 2.38 ppm.

3.3. Elementary Analysis of AM/AA/NSFM. The elementary analysis of the AM/AA/NSFM copolymer was carried out using a Vario EL-III elemental analyzer. The content of different element in the copolymer can be obtained by detecting the gases, which are the decomposition products of the copolymer at high temperature. Theoretical value: 0.21% (Si %), 45.4% (C %), and 5.4% (H %); found value: 0.17% (Si %), 40.1% (C %), and 4.8% (H %).

3.4. Microscopic Structure. The microscopic structures of AM/AA and AM/AA/NSFM were observed through SEM at room temperature. The copolymers solution samples

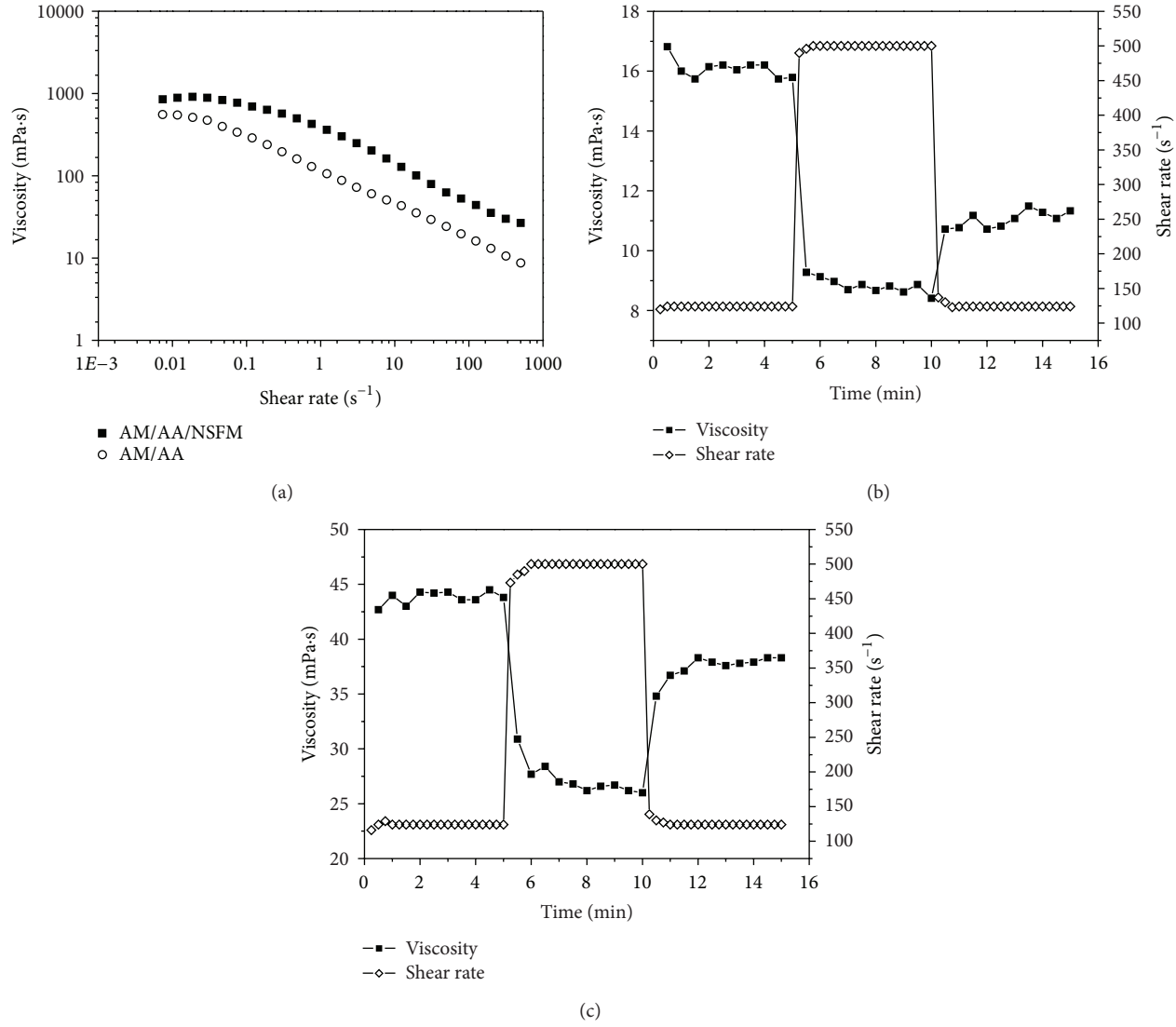

FIGURE 7: (a) Effect of shear rate on viscosity; (b) shear resistance of AM/AA; (c) shear resistance of AM/AA/NSFM. The copolymers solutions (0.2 wt%) were prepared with distilled water.

(0.05 wt%) were prepared with distilled water and cooled with liquid nitrogen, and then these samples were evacuated in order to keep original appearance of the copolymers as far as possible. As shown in Figures 4 and 5, the molecular chains of copolymer were obviously changed when NSFM was introduced into the AM/AA copolymer. Compared with the images of AM/AA, the molecular coils of AM/AA/NSFM were composed of many micro-nano structure units, and the force between these units could be heightened due to Si–O and C–Si bonds. In addition, this structure may increase retention of AM/AA/NSFM on the rock face which is favorable to mobility control and EOR.

3.5. Weight-Average Molecular Weight. Five different concentrations (0.001, 0.002, 0.004, 0.006, and 0.008 wt%) copolymer solutions were prepared with distilled water and filtered using a 0.5 μm Millipore Millex-LCR filter before static laser light scattering (SLLS) experiments. The M_w of AM/AA and AM/AA/NSFM can be calculated with the following equation [30]:

$$\frac{KC}{R_{vv}(q)} \cong \frac{1}{M_w}\left(1 + \frac{1}{3}\left\langle R_g\right\rangle^2 q^2\right), \tag{6}$$

where K is a constant; C is the concentration of copolymer solution, g/mL; $R_{vv}(q)$ is the Rayleigh ratio; $\langle R_g\rangle$ is the average radius of gyration, nm; and $q = (4\pi n/\lambda_o)\sin(\theta/2)$ with θ, λ_o, and n being the scattering angle, the wavelength of light in vacuo, and the solvent refractive index, respectively.

The M_w of AM/AA and AM/AA/NSFM is (1.33 ± 0.30) × 10^7 g/mol and (1.32 ± 0.45) × 10^7 g/mol, respectively (for details, see Supporting Material available online at http://dx.doi.org/10.1155/2013/437309).

3.6. Intrinsic Viscosity. The η_{sp}/C versus C relationship is shown in Figure 6. The fitted line of η_{sp}/C versus C was

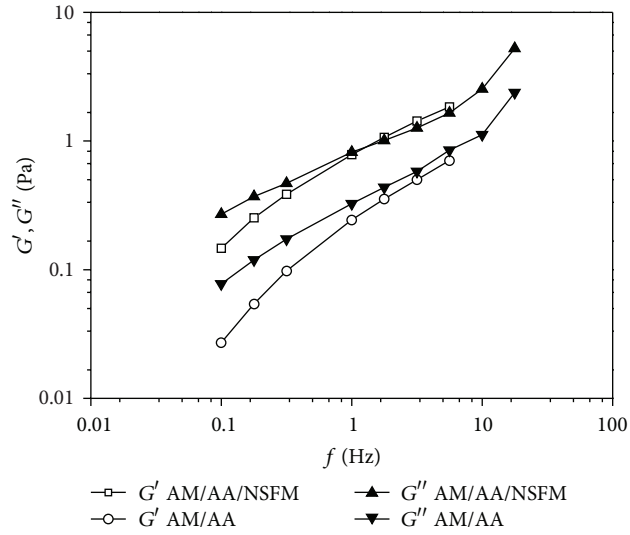

Figure 8: Viscoelasticity of AM/AA and AM/AA/NSFM at 65°C. The copolymers solutions (0.2 wt%) were prepared with distilled water.

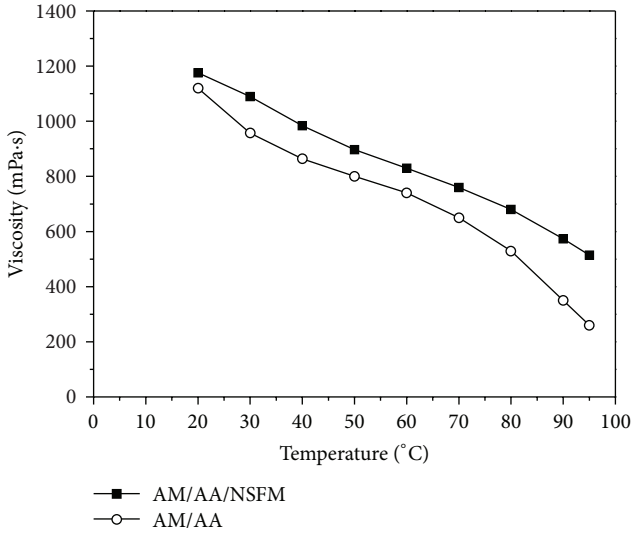

Figure 9: Viscosity versus temperature for AM/AA and AM/AA/NSFM solution. The viscosity of copolymer solution (0.5 wt%) was measured by Brookfiled DV-3 viscometer at 7.34 s^{-1} using number 62 rotor (rotation speed: 18.8 r/min).

extrapolated to zero concentration. According to the Huggins equation, the y-intercept is the intrinsic viscosity of the copolymers. The results revealed that the intrinsic viscosity of AM/AA and AM/AA/NSFM was 733.9 and 789.5 mL/g, respectively.

3.7. Shear Resistance. The viscosity versus shear rate curves of AM/AA and AM/AA/NSFM (0.2 wt%) are shown in Figure 7(a). It was clearly found that AM/AA and AM/AA/NSFM revealed non-Newtonian shear-thinning behavior. Hence, with the increase of the shear rate (from 0.007 to 500 s^{-1}), the viscosity of copolymer solutions dropped obviously. The results indicated that AM/AA/NSFM had better viscosifying property than AM/AA, and the viscosity of AM/AA/NSFM was higher than that of AM/AA at 500 s^{-1} shear rate (18.6 mPa·s versus 8.7 mPa·s). Furthermore, AM/AA and AM/AA/NSFM were investigated by changing the shear rate from 124 s^{-1} to 500 s^{-1} and from 500 s^{-1} to 124 s^{-1} around (Figures 7(b) and 7(c)). Compared with AM/AA, AM/AA/NSFM had higher retention rate of viscosity (85% versus 68%) when one cycle was completed. This phenomenon may support the Si–O and C–Si bonds in AM/AA/ NSFM which can improve the shear tolerance of the copolymer. The structures of AM/AA/NSFM may be restored after being sheared.

3.8. Viscoelasticity Measurements. The viscoelasticity curves of AM/AA and AM/AA/NSFM solutions (0.2 wt%) are shown in Figure 8. When the frequency was lower than 1 Hz, the viscous modulus (G'') of AM/AA/NSFM was higher than the elastic modulus (G'); when the frequency was higher than 1 Hz, the situation was just the opposite. However, the G'' of AM/AA was higher than G' in the entire frequency scan range. Compared with AM/AA, AM/AA/NSFM exhibited higher G' and G'' under the same conditions. This phenomenon may support the micro-nano structure units in AM/AA/NSFM can enhance the acting force of polymer molecular coils.

3.9. Temperature Tolerance. AM/AA and AM/AA/NSFM solutions were prepared with distilled water. And the viscosity of copolymer solutions was measured by the Brookfiled DV-3 viscometer at different temperatures. The viscosity versus temperature curves of AM/AA and AM/AA/NSFM solutions are shown in Figure 9. The test results showed that the AM/AA/NSFM solution had higher viscosity at the same temperature. Additionally, the viscosity of AM/AA/NSFM solution decreased less than that of AM/AA when temperature was above 80°C. This may support the stable Si–O and C–Si bonds which can obviously improve temperature tolerance of AM/AA/NSFM.

3.10. Salt Tolerance. As shown in Figures 10(a), 10(b), and 10(c), with the increase of salt concentration (NaCl, $CaCl_2$, and $MgCl_2{\cdot}6H_2O$), the viscosity of copolymers decreases rapidly and then kept at a low value. It was found that AM/AA and AM/AA/NSFM had less satisfactory salt tolerance to Na^+ or Ca^{2+} than to Mg^{2+} under the same conditions. Compared with AM/AA, AM/AA/NSFM exhibited no obvious advantage in salt tolerance due to the shrinking of copolymer chain with the increase of salt concentration.

3.11. Mobility Control Ability. The core barrel was packed with quartz sand which was washed by hydrochloric acid and distilled water for several times. The injection rate of brine (sodium chloride concentration was 0.5 wt%) and polymer solution prepared with the brine was 2.0 mL/min with the ISCO 260D syringe pump. Experiments were carried out at 65°C in an incubator with precision of 0.1°C. The injection

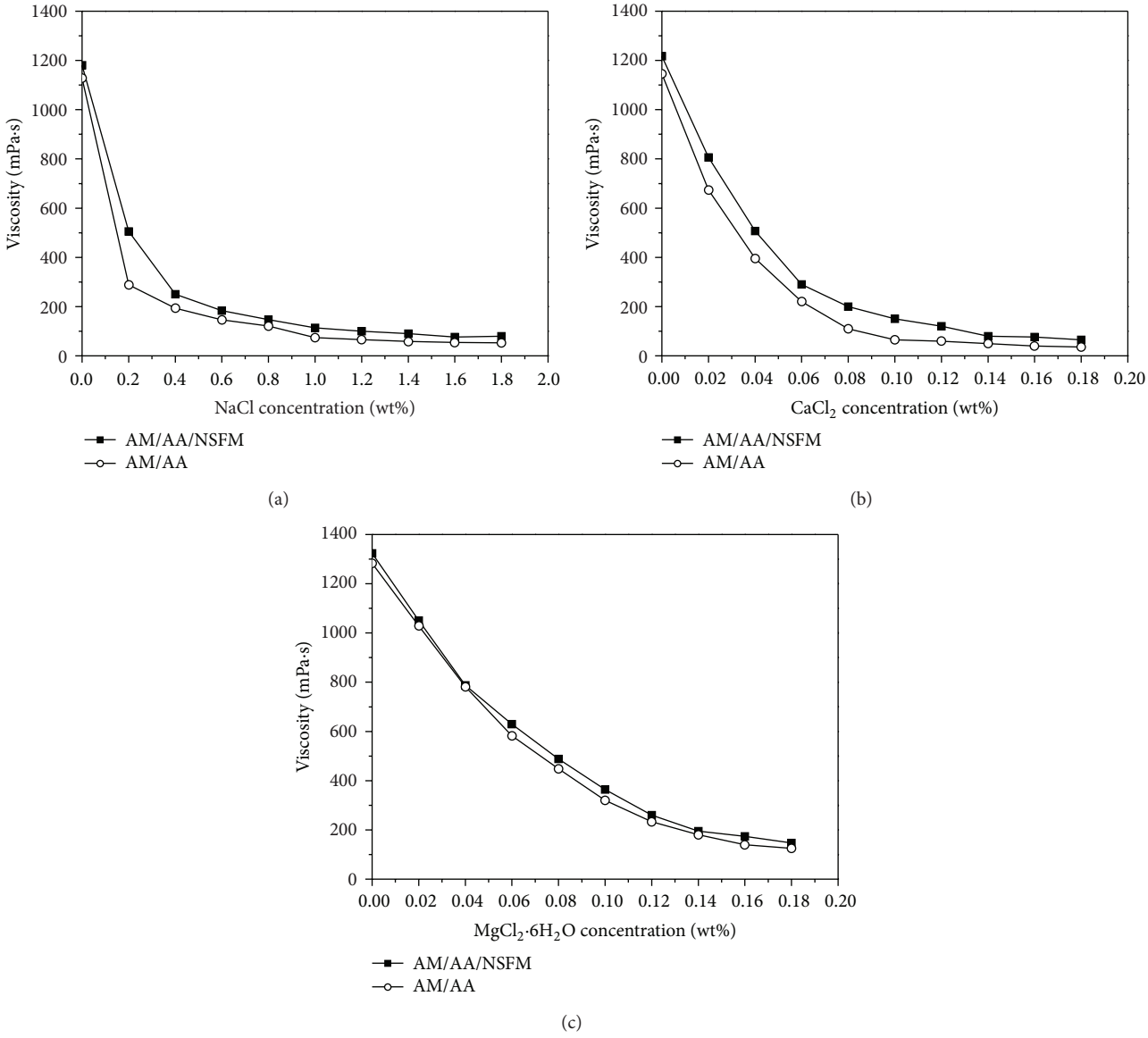

Figure 10: Salt tolerance ((a) NaCl, (b) $CaCl_2$, and (c) $MgCl_2 \cdot 6H_2O$) of AM/AA and AM/AA/NSFM solutions (0.5 wt%) at 20°C. The viscosity of copolymer solution was measured by Brookfiled DV-3 viscometer at 7.34 s^{-1} using number 62 rotor (rotation speed: 18.8 r/min) or number 61 rotor (rotation speed: 18.5 r/min).

pressure was collected by a pressure sensor with precision of 0.0001 MPa. The flow characteristic curves of AM/AA and AM/AA/NSFM in porous media are shown in Figure 11.

As shown in Figure 11, the AM/AA/NSFM solution could establish much higher RF and RRF than that of the AM/AA solution under the same conditions (RF: 16.52 versus 12.17, RRF: 3.63 versus 2.59). This is to say that the AM/AA/NSFM solution has stronger mobility control ability which is favorable to enhance oil recovery due to the higher viscosity retention rate and microstructure. In addition, it was found that AM/AA/NSFM revealed higher retention than AM/AA (83 mg versus 55 mg) by material balance calculations (for details, see Supporting Materials). This may support that the huge surface area of micro-nano structure units of AM/AA/NSFM can enhance the adsorption which may play an important role in improving mobility control.

3.12. Enhanced Oil Recovery. As shown in Table 2, the EOR of AM/AA/NSFM solution (0.2 wt%) was 20.10% compared with water flooding at 65°C. However, the EOR of AM/AA solution (0.2 wt%) was 14.22% under the same conditions. The EOR results showed that AM/AA/NSFM revealed more superior ability of oil displacement. As shown in Figure 12, compared with AM/AA, AM/AA/NSFM exhibited stronger ability of reducing water cut and establishing flow resistance in polymer flooding process. This phenomenon may support that the sweep efficiency is obviously improved

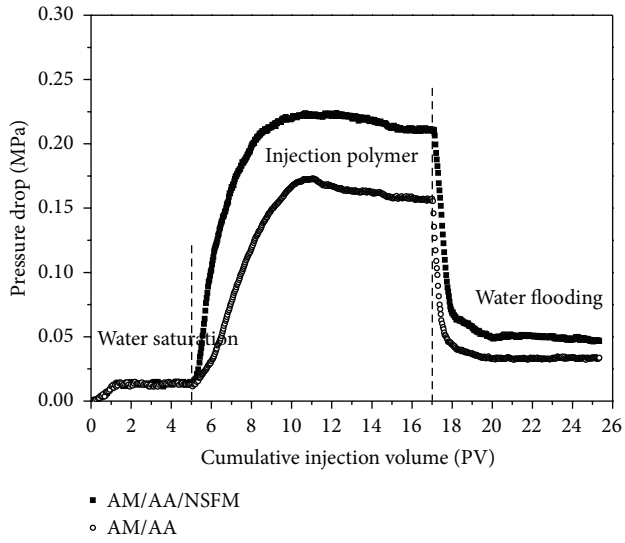

Figure 11: Flow characteristic curves of AM/AA and AM/AA/NSFM solution (0.2 wt%). The length and internal diameter of the core barrel were 25.0 cm and 2.5 cm, respectively.

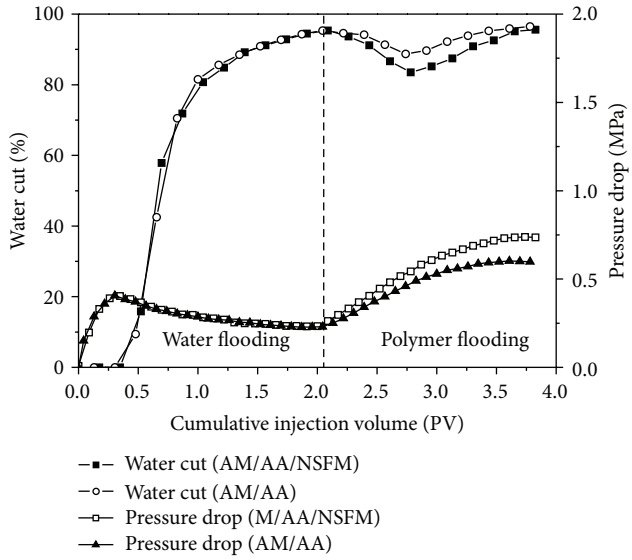

Figure 12: Core flooding experiments results of AM/AA/NSFM and AM/AA (0.2 wt%) at 65°C.

by AM/AA/NSFM due to the excellent mobility control capability in porous media.

4. Conclusions

A novel copolymer containing nano-SiO_2 was synthesized by free radical polymerization using AM, AA, and NSFM as raw materials. The AM/AA/NSFM copolymer was characterized by IR spectrum, ^{1}H NMR spectrum, elemental analysis, and scanning electron microscope. The solution properties, such as rheological property, viscoelasticity, temperature tolerance, salt tolerance, mobility control ability, and oil displacement efficiency of the copolymer, were investigated under different conditions. The results indicated that the copolymer containing nano-SiO_2 possessed moderate or good shear resistance, temperature tolerance, and mobility control ability as EOR chemical.

Conflict of Interests

The authors declare no possible conflict of interests.

Acknowledgments

This work was supported by the Open Fund (PLN1212) of State Key Laboratory of Oil and Gas Reservoir Geology and Exploitation (Southwest Petroleum University) and the Specialized Research Fund for the Doctoral Program of Higher Education (20125121120011).

References

[1] N. Mungan, F. W. Smith, J. L. Thompson, O. Sinclair, and C. Gas, "Some aspects of polymer floods," *Journal of Petroleum Technology*, vol. 18, no. 9, pp. 1143–1150, 1966.

[2] B. S. Shiran and A. Skauge, "Enhanced oil recovery (EOR) by combined low salinity water/polymer flooding," *Energy Fuels*, vol. 27, no. 3, pp. 1223–1235, 2013.

[3] C. Zhong, R. Huang, X. Zhang, and H. Dai, "Synthesis, characterization, and solution properties or an acrylamide-based terpolymer with butyl styrene," *Journal of Applied Polymer Science*, vol. 103, no. 6, pp. 4027–4038, 2007.

[4] T. Rho, J. Park, C. Kim, H. Yoon, and H. Suh, "Degradation of polyacrylamide in dilute solution," *Polymer Degradation and Stability*, vol. 51, no. 3, pp. 287–293, 1996.

[5] D. A. Z. Wever, F. Picchioni, and A. A. Broekhuis, "Polymers for enhanced oil recovery: a paradigm for structure-property relationship in aqueous solution," *Progress in Polymer Science*, vol. 36, no. 11, pp. 1558–1628, 2011.

[6] Z. B. Ye, G. J. Gou, S. H. Gou, W. C. Jiang, and T. Y. Liu, "Synthesis and characterization of a water-soluble sulfonates copolymer of acrylamide and N-Allylbenzamide as enhanced oil recovery chemical," *Journal of Applied Polymer Science*, vol. 128, no. 3, pp. 2003–2011, 2013.

[7] S. H. Chang and I. J. Chung, "Effect of shear flow on polymer desorption and latex dispersion stability in the presence of adsorbed polymer," *Macromolecules*, vol. 24, no. 2, pp. 567–571, 1991.

[8] L. Xue, U. S. Agarwal, and P. J. Lemstra, "Shear degradation resistance of star polymers during elongational flow," *Macromolecules*, vol. 38, no. 21, pp. 8825–8832, 2005.

[9] J. Zheng, P. Cui, X. Tian, and K. Zheng, "Pyrolysis studies of polyethylene terephthalate/silica nanocomposites," *Journal of Applied Polymer Science*, vol. 104, no. 1, pp. 9–14, 2007.

[10] L. I. Rueda, L. G. Hernandez, and C. C. Anton, "Effect of the textural characteristics of the new silicas on the dynamic properties of Styrene-Butadiene Rubber (SBR) vulcanizates," *Polymer Composites*, vol. 9, no. 3, pp. 204–208, 1988.

[11] H. Xia and Q. Wang, "Preparation of conductive polyaniline/nanosilica particle composites through ultrasonic irradiation," *Journal of Applied Polymer Science*, vol. 87, no. 11, pp. 1811–1817, 2003.

[12] X. Wang, X. Zhao, M. Wang, and Z. Shen, "The effects of atomic oxygen on polyimide resin matrix composite containing nano-silicon dioxide," *Nuclear Instruments and Methods in Physics Research B*, vol. 243, no. 2, pp. 320–324, 2006.

[13] Y. Li, J. Yu, and Z. Guo, "The influence of interphase on nylon-6/nano-SiO_2 composite materials obtained from in situ polymerization," *Polymer International*, vol. 52, no. 6, pp. 981–986, 2003.

[14] V. A. Bershtein, L. M. Egorova, P. N. Yakushev, P. Pissis, P. Sysel, and L. Brozova, "Molecular dynamics in nanostructured polyimide-silica hybrid materials and their thermal stability," *Journal of Polymer Science B*, vol. 40, no. 10, pp. 1056–1069, 2002.

[15] N. D. Alberola, K. Benzarti, C. Bas, and Y. Bomal, "Interface effects in elastomers reinforced by modified precipitated silica," *Polymer Composites*, vol. 22, no. 2, pp. 312–325, 2001.

[16] A. Voronov, A. Kohut, A. Synytska, and W. Peukert, "Mechanochemical modification of silica with poly(1-vinyl-2-pyrrolidone) by grinding in a stirred media mill," *Journal of Applied Polymer Science*, vol. 104, no. 6, pp. 3708–3714, 2007.

[17] H. Zou, S. Wu, and J. Shen, "Polymer/silica nanocomposites: preparation, characterization, propertles, and applications," *Chemical Reviews*, vol. 108, no. 9, pp. 3893–3957, 2008.

[18] G. Hsiue, W. Kuo, Y. Huang, and R. Jeng, "Microstructural and morphological characteristics of PS-SiO_2 nanocomposites," *Polymer*, vol. 41, no. 8, pp. 2813–2825, 2000.

[19] W. Wang and B. Gu, "Self-assembly of two- and three-dimensional particle arrays by manipulating the hydrophobicity of silica nanospheres," *Journal of Physical Chemistry B*, vol. 109, no. 47, pp. 22175–22180, 2005.

[20] B. J. Kim and K. S. Kang, "Fabrication of a crack-free large area photonic crystal with colloidal silica spheres modified with vinyltriethoxysilane," *Crystal Growth & Design*, vol. 12, no. 8, pp. 4039–4042, 2012.

[21] A. V. Biradar, A. A. Biradar, and T. Asefa, "Silica-dendrimer core-shell microspheres with encapsulated ultrasmall palladium nanoparticles: efficient and easily recyclable heterogeneous nanocatalysts," *Langmuir*, vol. 27, no. 23, pp. 14408–14418, 2011.

[22] Z. Meng, C. Xue, Q. Zhang, X. Yu, K. Xi, and X. Jia, "Preparation of highly monodisperse hybrid silica nanospheres using a one-step emulsion reaction in aqueous solution," *Langmuir*, vol. 25, no. 14, pp. 7879–7883, 2009.

[23] Z. Wu, H. Han, W. Han, B. Kim, K. H. Ahn, and K. Lee, "Controlling the hydrophobicity of submicrometer silica spheres via surface modification for nanocomposite applications," *Langmuir*, vol. 23, no. 14, pp. 7799–7803, 2007.

[24] A. Mehrdad and R. Akbarzadeh, "Effect of temperature and solvent composition on the intrinsic viscosity of poly(vinyl pyrrolidone) in water-ethanol solutions," *Journal of Chemical and Engineering Data*, vol. 55, no. 9, pp. 3720–3724, 2010.

[25] J. Lee and A. Tripathi, "Intrinsic viscosity of polymers and biopolymers measured by microchip," *Analytical Chemistry*, vol. 77, no. 22, pp. 7137–7147, 2005.

[26] L. Alagha, S. Wang, Z. Xu, and J. Masliyah, "Adsorption kinetics of a novel organic-inorganic hybrid polymer on silica and alumina studied by quartz crystal microbalance," *Journal of Physical Chemistry C*, vol. 115, no. 31, pp. 15390–15402, 2011.

[27] R. Ponnapati, O. Karazincir, E. Dao, R. Ng, K. K. Mohanty, and R. Krishnamoorti, "Polymer-functionalized nanoparticles for improving waterflood sweep efficiency: characterization and transport properties," *Industrial and Engineering Chemistry Research*, vol. 50, no. 23, pp. 13030–13036, 2011.

[28] C. Zhong, L. Ye, H. Dai, and R. Huang, "Flourescent probe and ESEM morphologies of a acrylamide-based terpolymer in aqueous solution," *Journal of Applied Polymer Science*, vol. 103, no. 1, pp. 277–286, 2007.

[29] L. Shi, Z. Ye, Z. Zhang, C. Zhou, S. Zhu, and Z. Guo, "Necessity and feasibility of improving the residual resistance factor of polymer flooding in heavy oil reservoirs," *Petroleum Science*, vol. 7, no. 2, pp. 251–256, 2010.

[30] X. Wang, X. Qiu, and C. Wu, "Comparison of the coil-to-globule and the globule-to-coil transitions of a single poly(N-isopropylacrylamide) homopolymer chain in water," *Macromolecules*, vol. 31, no. 9, pp. 2972–2976, 1998.

Hindawi Publishing Corporation
Journal of Chemistry
Volume 2013, Article ID 416328, 10 pages
http://dx.doi.org/10.1155/2013/416328

Research Article

Performance of Gel Treatments in Reservoirs with Multiscale Heterogeneity

Ji Ho Lee and Kun Sang Lee

Department of Natural Resources and Environmental Engineering, Hanyang University, Seoul 133-791, Republic of Korea

Correspondence should be addressed to Kun Sang Lee; kunslee@hanyang.ac.kr

Received 5 April 2013; Revised 3 August 2013; Accepted 7 August 2013

Academic Editor: Baojun Bai

Spatially correlated permeability fields are usually generated by single-scale correlation. To overcome the limitations of single-scale permeability fields in describing real situation, permeability fields should be generated by multiscale correlation. Multiscale heterogeneity results in the existence of various permeability magnitudes and spatial distributions of permeability. Gel treatment is applied on the heterogeneous permeability fields realized by multiscale correlation. Performance of gel treatment has been shown to depend on permeability distribution and permeability values, which are determined by correlation length, variance, and number of scales. Generally, spatially-correlated permeability fields generated with longer correlation length, higher variance, and multiscale lead to higher improvement in the performance of gel treatment. In addition, longer application of preflush as waterflooding results in larger reduction of water-oil ratio when the gel treatment is applied to heterogeneous permeability fields after preflush.

1. Introduction

Most of reservoirs are geologically complex and show the heterogeneity because of various distributions of porosity and permeability, deposition, and natural fractures. Among many heterogeneous petrophysical properties, permeability is the most important factor for reservoir engineering calculations. Heterogeneous permeability system leads to different flow movements in reservoir compared with the equivalent homogeneous system. Van Poolen [1] indicated that variations in permeability distribution caused a significant impact on the oil recovery and water production during enhanced oil recovery, which means that oil recovery by the injection of materials does normally not exist in the reservoir [2]. As long as heterogeneity of permeability distribution is increased, flow mechanism becomes more complex. Even though the average permeability of reservoir is the same, the distribution of permeability leads the performance of enhanced oil recovery makes totally different.

As the reservoirs have more severe heterogeneity, there is more severe permeability contrast. If waterflooding is applied on such highly heterogeneous fields, injected water flows mainly through high-permeability zones. This flow pattern makes the injected water unable to sweep substantial oil located in low-permeability zones, but it is produced directly at producer, the so-called conformance problem. According to Portwood et al. [3], parts of the Healdton Field in Carter County, Ok, USA, showed high watercut because of complex permeability distributions. Excessive water production could make the life of the well short because of high water disposal cost. For this reason, controlling of water production is of significant importance. To overcome excessive water production by improving volumetric sweep efficiency, especially vertical sweep efficiency, cross-linked polymer gel is widely used. Gel treatment uses polymer and cross-linker. Cross-linker makes polymer form networks, so that it has high capability to plug pore. Due to its promising permeability reduction capability, gel treatment is evidently of great conformance control [4, 5].

There are several types of gel treatment, such as the in situ bulk gel and microgel. In situ bulk gel is formed with high concentration of polymer and cross-linker representing substantial polymer network. Because of strong gel due to great amount of polymer network, it hardly flows well through small pores in matrix. Owing to relatively slow flow capacity, bulk gel is appropriate to treat high-permeability zones near well bores or reservoirs containing fractures. By contrast, in

situ microgel is formed with relatively low concentration of polymer and cross-linker. The microgel is able to penetrate deeper into a formation until its gelation mechanism is triggered. Therefore, it is appropriate for reservoirs that have in-depth high-permeability zones or that do not have fractures. Randomly heterogeneous reservoirs considered in this study have various locations of high-permeability zones without fractures; thus in situ microgel is selected.

In the recent years, preformed particle gels (PPGs) have been proposed and developed by Coste et al. and Bai et al. [6, 7]. They are oriented to overcome some distinct drawbacks inherent in the in situ gelation systems such as lack of gelation time, uncertainness of gelling due to shear, degradation, chromatographic fractionation, or change of gelant composition, and dilution by formation water [7]. They are categorized as preformed gels for conformance control, which is of great interest to several researchers [6–12]. There are also pH-triggered microgels and temperature-triggered microgels, called the Bright Water for application to specific reservoir conditions. However, this study utilizes in situ microgel to assess the performance of gel treatment with respect to not only water production but also gelation under general conditions.

According to the studies on the performance of gel treatment, heterogeneity of reservoir permeability has been revealed to be the most important factor among influential factors like other EOR methods. Also, previous investigations had been focused on layered permeability system in vertical direction [13–15]. It was revealed that high-permeability contrast of layered system significantly improves the performance of gel treatment [13, 14]. However, these layered reservoir systems are hard to be assumed as realistic reservoirs. In advance of researches for layered heterogeneous system, several researches for spatially correlated heterogeneous fields have been conducted in terms of enhanced oil recovery [16, 17]. However, these researches also assumed that heterogeneous permeability fields have single-scale correlation, so they still have limitation to generate various and proper realistic permeability fields.

In the field of groundwater flow, aquifer heterogeneity is important as much as reservoir heterogeneity in petroleum engineering. Groundwater and solute transport processes in the aquifer are considerably affected by the heterogeneity of the formation properties [18]. Many researchers developed theories based on the assumption that the spatial distributions of the medium properties can be characterized by one single-scale correlation [19]. However, when heterogeneity at any scale cannot be averaged out, nor can be treated as a deterministic trend, single-scale correlation approach is invalid [19]. In addition, as many subrandom fields compose of parent random field, that is, each layer, which has various geological conditions, gathers and consists of aquifer, single-scale correlation method lacks the ability to produce this model [19]. A number of reasons including deformation and solution could alter the characteristics of reservoir depending on scale. Therefore, generation of more proper fields should include both local and regional correlations, that is, multiscale correlation, so a few researchers investigated nonstationary multiscale correlation [19]. However, researches considering multiscale heterogeneity of permeability have not been conducted substantially, especially for EOR. This study accesses the performance of gel treatment applied on spatially correlated heterogeneous fields considering multiscale spatial correlation.

We neglect time-dependent term and suppose that stationary multiscale focuses on how the multiscale, combination of local scale and regional scale, affects heterogeneity and performance of gel treatment by comparing with single scale. In addition to multiscale effect, effect of spatial correlation, which is represented with correlation length and variance, on heterogeneity and performance of gel treatment is evaluated. The Dykstra-Parsons coefficient is used to quantify the level of heterogeneity of all permeability fields used in the simulations. Distribution of permeability and permeability reduction factor of gel placement are shown with figures, which could not been clarified through the Dykstra-Parsons coefficient. It is also investigated how preflush as waterflooding influences the performance of gel treatment applied on heterogeneous permeability field. Because preflush before gel treatment could control location of gelation, investigation of preflush is of importance.

2. Basic Theories

2.1. Gel Treatment. Due to pore-blocking mechanism, gel treatment improves sweep efficiency and is known as an effective conformance control. However, the exact mechanism is still uncertain. The uncertainty arises from whether gel mainly penetrates high-permeability zones as intended. Cozic et al. and Seright et al. suggested steric effect, which assumes that microgel solution acts as water flows during injection [20, 21]. Zaitoun et al. insisted that relatively large microgel size results in low amount of microgel penetration of low-permeability zones [22]. Several authors suggested and explained the disproportionate permeability reduction (DPR) effects or sometimes called relative permeability modification (RPM) effects [11, 23–26]. According to DPR, it reduces relative water permeability dominantly rather than relative oil permeability, even if gel solution penetrates both low- and high-permeability zones. However, major mechanisms of gel treatment are related to permeability reduction by pore plugging and DPR, which are considered as main mechanisms in this study.

This study models polymer/chromium chloride gel. In the process of polymer/chromium chloride gel, two reactions and kinetics, that is, redox and gelation reactions, occurred. Substantive gelation process is the reaction between trivalent chromium (Cr^{3+}) and polymer to form gel. Because this reaction process is so fast, an additional reaction, that is, redox reaction, is implemented to delay this fast reaction. Fast gelation misleads to placing the gel intensively near the well bore, not in high-permeability zones, and it could decrease injectivity and productivity. To control gelation time, two reactions usually participate to gelation. The first reaction of in situ gelation is redox reaction of sodium dichromate with reducing agent, that is, thiourea ($CS(NH_2)_2$) generating trivalent

chromium. For the second reaction, the generated trivalent chromium forms gel with polymer as follows:

$$\begin{aligned} &Cr_2O_7^{2-} + 6CS(NH_2)_2 + 8H^+ \\ &\xrightarrow{k} 2Cr^{3+} + 3\left[CS(NH_2)_2\right]_2 + 7H_2O, \end{aligned} \tag{1}$$

$$Cr^{3+} + \text{POLYMER} \longrightarrow \text{Gel}. \tag{2}$$

The kinetics for the reaction of polymer and trivalent chromium are implemented with the following expression of exponents:

$$\frac{d\left[Cr^{3+}\right]}{dt} = -k\frac{\left[Cr^{3+}\right]^{X14}[\text{polymer}]^{X4}}{\left[H^+\right]^{X16}}, \tag{3}$$

$$\frac{d\left[\text{gel}\right]}{dt} = -\frac{1}{n}\frac{d\left[Cr^{3+}\right]}{dt}, \tag{4}$$

where $X4$, $X14$, and $X16$ are exponents to be used for each component in gelation reaction and k is kinetic rate coefficient for gel.

Because gel reaction is extremely sensitive to temperature as other chemical reactions, temperature effect is very critical to decide whether gel treatment is applicable or not. The effect is reflected in kinetic rate coefficient shown in (3). Temperature dependence of kinetic rate coefficient is represented with the Arrhenius equation as follows:

$$k = k_{\text{ref}} \exp\left\{k_T\left(\frac{1}{T} - \frac{1}{T_{\text{ref}}}\right)\right\}, \tag{5}$$

where k_{ref} is kinetic reaction coefficient at reference temperature, k_T is parameter for calculating kinetic rate coefficient for gel as a function of reservoir temperature, T is the reservoir, temperature calculated from solving energy balance equation and T_{ref} is reference temperature assumed to be equal to reservoir temperature.

DPR, resulting by adsorption of gel onto surface of pore, is utilized due to its ability to compress/collapse/dehydrate in presence of water-oil capillary pressure. The adsorption is calculated by the Langmuir-type isotherm equation with gel concentration in the aqueous phase as follows:

$$\overline{C_{15}} = \frac{a_{15}C_{15,1}}{1 + b_{15}C_{15,1}}, \tag{6}$$

where $\overline{C_{15}}$ is the concentration of adsorbed gel and a_{15} and b_{15} are gel adsorption parameters.

The effect of gel on aqueous-phase permeability reduction reflecting pore plugging mechanism and DPR is represented with permeability reduction factor, which is an index of capacity to modify the flow in reservoirs. Permeability reduction factor, R_{RF}, is defined as effective aqueous-phase permeability ratio of the before-to-after gel treatment as follows;

$$\begin{aligned} R_{\text{RF}} &= 1 + \frac{\left(R_{\text{RF max}} - 1\right)A_{gk}C_{15,1}}{1 + B_{gk}C_{15,1}}, \\ R_{\text{RF max}} &= \left[1 - \frac{c_{rg}\left(A_{p1}C_{\text{SEP}}^{S_p}\right)^{1/3}}{\left(\sqrt{(k_xk_y)}/\phi\right)^{1/2}}\right]^{-4}, \\ C_{\text{SEP}} &= \frac{C_{5,1} + \left(\beta_p - 1\right)C_{6,1}}{C_{1,1}}, \end{aligned} \tag{7}$$

where $R_{\text{RF max}}$ is the maximum residual resistance factor, A_{gk} and B_{gk} are the permeability reduction parameters for the Langmuir correlation with gel concentration, $C_{15,1}$ is the concentration of gel in aqueous phase, c_{rg} is the constant depending on gel type, A_{p1} is the parameter to calculate polymer viscosity at zero shear rate, C_{SEP} is the effective salinity, S_p is the slope of viscosity versus effective salinity on a log-log plot, k_x and k_y are the permeabilities of x and y directions, ϕ is the porosity, $C_{5,1}$, $C_{6,1}$, and $C_{1,1}$ are the anion, divalent cation and water component concentrations in aqueous phase, and β_p is the parameter to combine divalent cation, salinity with anion salinity.

Increased viscosity of injection fluid by injected polymer or formed gel reduces conformance problem. The viscosity of aqueous phase containing gel and polymer is modeled with the Flory-Huggins equation as follows:

$$\begin{aligned} \mu_1 = \mu_w \Big[1 &+ \left(A_{p1}C_{4,1} + A_{p2}C_{4,1}^2 + A_{p3}C_{4,1}^3\right)C_{\text{SEP}}^{S_p} \\ &+ A_{g1}C_{15,1} + A_{g2}C_{15,1}^2\Big], \end{aligned} \tag{8}$$

where $C_{4,1}$ is the concentration of polymer, A_{p1}, A_{p2}, and A_{p3} are parameters to calculate polymer viscosity at zero shear rate, and A_{g1} and A_{g2} are the Flory-Huggins parameters for gel viscosity.

2.2. Random Field Generation. Recognition of permeability is critical to predict oil recovery process by numerical reservoir simulation. Permeability shows not perfectly random distribution but some correlation structures. Therefore, synthetic permeability fields could be realized in a stochastic method to simulate natural variety [27, 28]. Permeability is considered as a random variable and is assumed to have its own density function as log-normal distribution. To generate permeability random fields, second-order stationarity is assumed. Based on second-order stationarity, covariance function, correlation length, and variance are given. Correlation length is the lag distance at which the values at two locations are marginally dependent on each other [29].

Generation of heterogeneous permeability field is performed with the IGW software, which is developed for unified deterministic and stochastic groundwater modeling [30]. Based on efficient computational algorithms, IGW simulates complex flow and geological heterogeneity. Heterogeneous

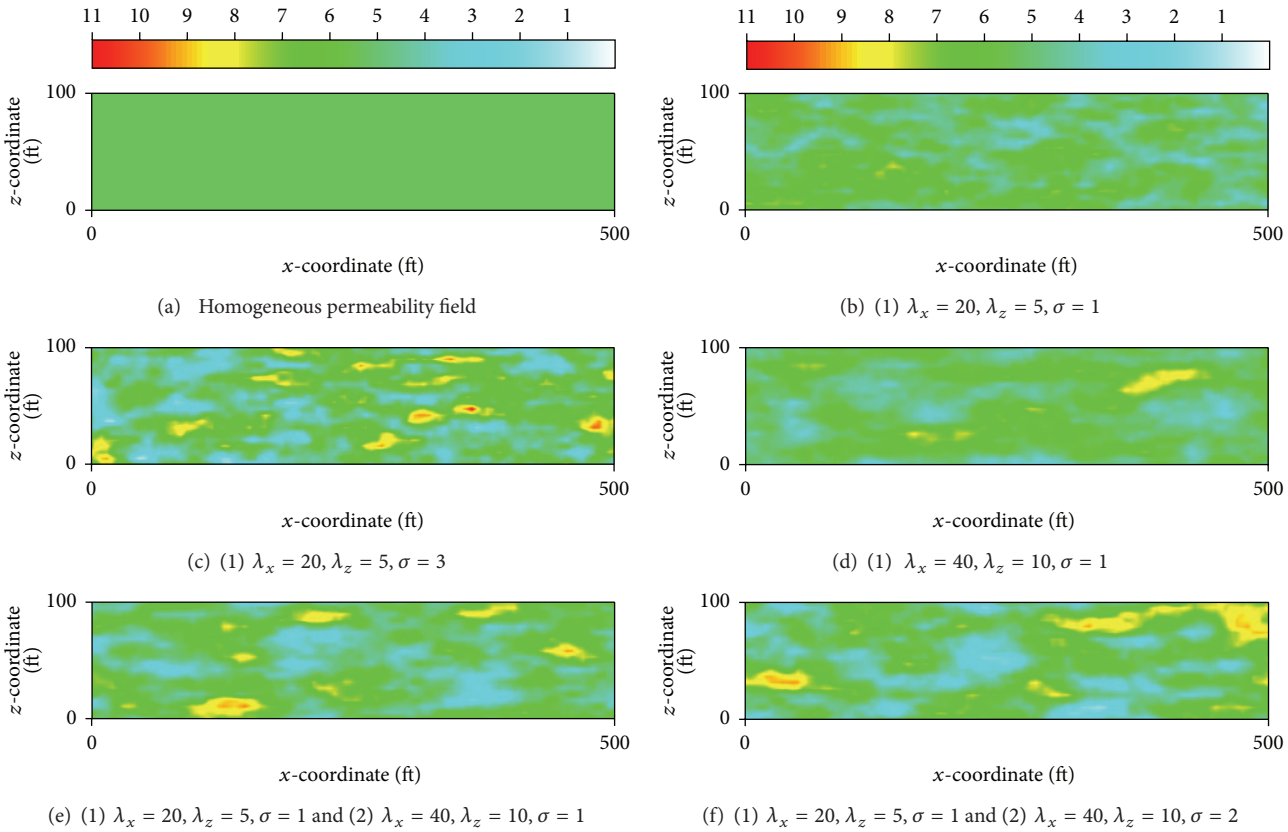

FIGURE 1: Homogeneous permeability field (a) and heterogeneous permeability fields depending on single-scale correlation ((b), (c), and (d)) and multiscale correlation ((e) and (f)) expressed with ln k.

permeability fields are generated by unconditional random process, given with correlation lengths for x and z directions (λ_x, λ_z), variances (σ), and several covariance functions.

This study aims to investigate multiscale correlation, correlation length, and variance, as shown in Figure 1. Permeability varies significantly in space, so the distribution is presented by natural logarithm of permeability (ln k).

3. Numerical Modeling

Modeling gel treatment on a spatially correlated heterogeneous permeability field is conducted with UTCHEM. UTCHEM performs a 3D, multicomponent, and multiphase compositional model of chemical flooding process considering complex phase behavior, chemical and physical transformation, and heterogeneous porous media properties [31]. It is known as one of the advanced simulators for chemical flooding process.

This study analyzes the heterogeneity and performance of gel treatment in multiscale heterogeneous permeability fields compared with those of single-scale heterogeneous fields. 2D cross-sectional model of reservoir is considered for the analysis. The hypothetical reservoir locates at 1,300 ft depth and has initial pressure and temperature as 200 psi and 103°F, respectively. The cross-sectional area is $500 \times 100\,\text{ft}^2$. There is a two-phase flow in the reservoir, so initial saturations of water and oil are assumed to be 0.3 and 0.7, respectively. Porosity has uniform value of 0.2 over the whole reservoir because the variation of porosity is not severe as much as that of the permeability. When vertical communication of fluid is high in the reservoirs, the efficiency of gel treatment decreases. In addition, geological processes make the vertical permeability much lower than horizontal permeability. Reflecting these observations, the ratio of vertical-to-horizontal permeability is set to be 0.01.

Effects of gel treatment are determined for the typical design of injection process. Injection of fluids and production are continued for 1,000 days. When enhanced oil recovery method is applied, preflush as waterflooding is usually recommended to get higher productivity, so preflush is applied before gel treatment. Rate of injection fluid is maintaind as 2,000 ft^3/day. After preflush is finished, injection of polymer and Cr^{3+} starts at in 510 days and continues until 525 days, as shown Figure 2. After that, postflush as also waterflooding is resumed. Concentrations of polymer and Cr^{3+} are shown in Figure 2. All detailed input data for petrophysical properties of the reservoir, kinetics of gelation, temperature effect on the reaction, permeability reduction factor, viscosity, and adsorption are summarized in Table 1.

Covariance function is required to realize spatially correlated heterogeneous permeability field. Single-scale correlation method needs just one covariance function, while

Table 1: Input data of reservoir property and gel reaction.

Parameters	
Reservoir	
Porosity, ϕ	0.2
Ratio of vertical-to-horizontal permeability, k_v/k_h	0.01
Depth (ft)	1,300
Temperature (°F)	103
Pressure (psi)	200
Compressibility, c_f (psi^{-1})	0
Initial saturation	
Water, S_{wi}	0.3
Oil, S_{oi}	0.7
Initial hydrogen ion concentration (meq/mL)	160
Kinetics of gelation	
$X4$	0.8
$X14$	1.32
$X16$	1
k_{ref} ((mole/m^3)$^{1-X14-X4+X16}$ days^{-1})	15
k_T (°K^{-1})	−22,344
SCR	0.25
Permeability reduction factor	
A_{gk}	0.06
B_{gk}	0.099
c_{rg} (m·wt.%$^{1/3}$)	4.9674×10^{-7}
A_{pl} (wt.%$^{-1}$)	80
C_{SEP}	
β_p	10
C_{SEPmin} (meq/m^3)	10,000
S_p	0.169
Viscosity	
A_{g1} (cp ppm^{-1})	0.008
A_{g2} (cp ppm^{-2})	2.7×10^{-5}
Adsorption	
a_{15} (vol. of water/ppm of chromium)	1,157
b_{15} (vol. of water/ppm of chromium)	100

multiscale correlation method requires two covariance functions. Similarly, one correlation length for each direction and one theoretical variance are needed to generate realization of single scale correlated random field. Multiscale-correlated random fields need two correlation lengths for each direction and two variances. Tables 2 and 3 summarize the variables used to generate permeability fields for Cases 1 to 5 in this study. With these variables, 50 equivalent realizations have been generated for each case, and heterogeneity has been investigated by means of heterogeneity index and visualized image. In addition, gel treatment is applied to heterogeneous permeability fields to investigate the effects of heterogeneity on the performance of gel treatment. Representative realized fields among a number of fields for each case are visualized in Figure 1 including homogeneous permeability field having equivalent permeability as 200 md. These representative example heterogeneous permeability fields for each case will be named as Ex 1 to 5 to differentiate Cases 1 to 5.

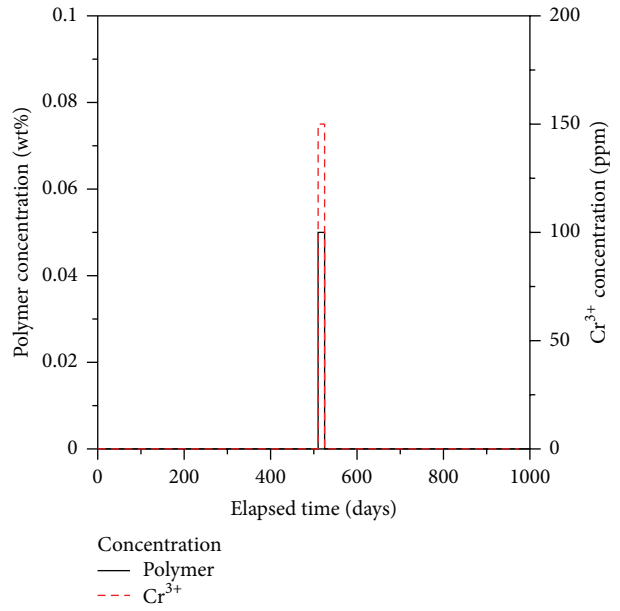

Figure 2: Injection history of concentrations for polymer and Cr^{3+}.

Table 2: Variables for single-scale correlation.

	Case 1	Case 2	Case 3
Covariance function	Bell	Bell	Bell
γ_x	20	20	40
γ_z	5	5	10
σ	1	3	1
Horizontal permeability (md)	200	200	200

Table 3: Variables for multiscale correlation.

	Case 4	Case 5
Covariance function	Bell	Bell
γ_x	20	20
γ_z	5	5
σ	1	1
Covariance function	Exponential	Exponential
γ_x	40	40
γ_z	10	10
σ	1	2
Horizontal permeability (md)	200	200

4. Results

4.1. Heterogeneity. Based on the preliminary simulation results, heterogeneities of five cases are investigated. As permeability is characterized as log-normal distribution, the Dykstra-Parsons coefficient is used to define permeability variation as follows:

$$V_k = \frac{k_{50} - k_{84.1}}{k_{50}}, \tag{9}$$

where k_{50} is the permeability value with 50% probability and $k_{84.1}$ is the permeability value with 84.1% probability.

Table 4: The Dykstra-Parsons coefficients of 50 fields for each case.

	Case 1	Case 2	Case 3	Case 4	Case 5
#1	0.636	0.785	0.632	0.764	0.780
#2	0.595	0.789	0.600	0.748	0.822
#3	0.753	0.831	0.623	0.764	0.804
#4	0.776	0.771	0.593	0.705	0.827
#5	0.818	0.792	0.513	0.740	0.847
#6	0.693	0.764	0.591	0.700	0.837
⋮	⋮	⋮	⋮	⋮	⋮
#49	0.814	0.803	0.619	0.729	0.831
#50	0.771	0.766	0.537	0.771	0.769

Although this is a useful tool for characterizing the degree of reservoir heterogeneity, it does not have information on the spatial distribution of fields. To analyze the reservoir heterogeneity quantitatively and to get information of distribution, not only the Dykstra-Parsons coefficient but also the images of permeability are utilized, as shown in Figure 1. Table 4 briefly shows the Dykstra-Parsons coefficients for each realized field for each case. Arithmetic mean of generated 50 geometric permeability means for each case and arithmetic mean of the realized Dykstra-Parsons coefficients for each case are introduced to analyze degrees of heterogeneity statistically and are represented in Table 5.

Table 5: Arithmetic means of geometric permeability means and the Dykstra-Parsons coefficients for each case.

	Geometric mean of permeability	The Dykstra-Parsons coefficient
Case 1	197	0.587
Case 2	197	0.788
Case 3	207	0.597
Case 4	202	0.733
Case 5	200	0.814

With respect to Dykstra-Parsons coefficient, generated heterogeneous permeability fields have various heterogeneities depending on the correlation length, the variance, and the number of scales. It is easily identified that higher variance and multiscale result in higher heterogeneity in a range of 0.6 to 0.85 from Table 4. Table 5 summarizes the simulation results of heterogeneous fields. Based on the heterogeneity index, V_k values of Cases 1 and 3 are over 0.5, so the two cases are moderately heterogeneous. Cases 2, 4, and 5, where V_k values are over 0.7, are extremely heterogeneous. From the results, it is concluded that impacts of variables, that is, correlation length, variance, and number of scales, are definitely different. Variance influences heterogeneity index more significantly than correlation length. In multiscale-correlated heterogeneous fields, heterogeneity index is higher than single-scale-correlated heterogeneous fields because of inclusion of locally correlated relation within regionally correlated relation as shown in comparison between Cases 3 and 4 or between Cases 1 and 4. In the comparison between Cases 2 and 4, single-scale cases show higher heterogeneity index than multiscale cases. This inconsistency resulted due to higher variance in single-scale cases. To evaluate the multiscale effect only, either of local scale or regional scale of multiscale should have the same spatial correlation with single scale. For this reason, comparison between Cases 3 and 4 or between Cases 1 and 4, not between Cases 2 and 4, is appropriate to assess multiscale effect.

Heterogeneity should be investigated with not only heterogeneity index but also visualized permeability image. Because the Dykstra-Parsons coefficient just arranges all permeabilities in order of magnitude to calculate heterogeneity quantitatively, it lacks spatial distribution information of permeability, as shown in Figure 1. For example, even though correlation lengths are different between Cases 1 and 3, the Dykstra-Parsons coefficients are similar. Accordingly, investigation of spatial permeability distribution on fields is conducted with permeability field images. From the Figures 1(b) and 1(d), longer correlation length produces spatial distribution to be more layered system in spite of the similar Dykstra-Parsons coefficients. It is due to longer x-direction correlation length for Case 3 than Case 1. From the comparison of permeability fields between Figures 1(b) and 1(c), it is clearly seen that extremely large values of permeability are shown easily in the higher variance case. However, both cases have the same correlation length, so the spatial distribution of both cases seems to be similar. Case 4 has two scales: the first one shows local correlation, and the second one shows regional correlation. Local correlation is the same with Case 1, and regional correlation is the same with Case 3. Because correlation length defines the spatial distribution of permeability, Case 4 follows similar spatial distribution of both Cases 1 and 3. It has more layered system than Case 1, but a less layered one than Case 3. Multiscale correlation shows local and regional relationship simultaneously. In addition, multiscale correlation has higher heterogeneity than both Cases 1 and 3. To make sure that higher variance could represent higher heterogeneity in multiscale correlation, the second scale of Case 5 is set to have higher variance than that of Case 4. As expected, higher variance leads to higher heterogeneity in multiscale correlation. From these results, multiscale correlation could broaden generation of synthetic heterogeneous fields variously.

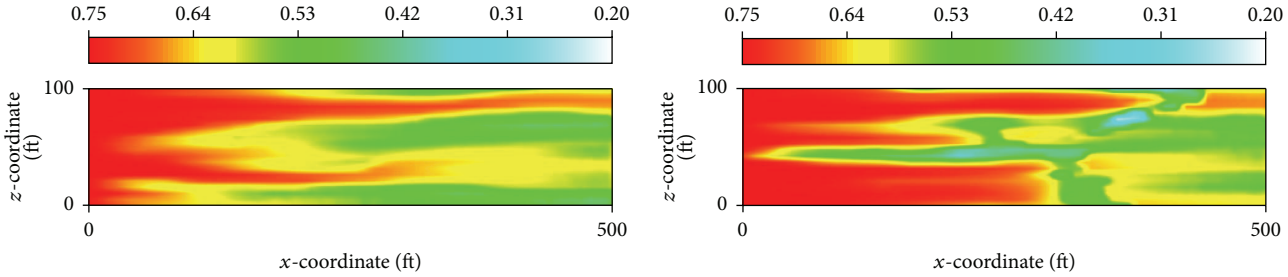

(a) Nontreated waterflooding

(b) Gel-treated waterflooding

Figure 3: Comparison of water saturations between nontreated waterflooding and gel-treated waterflooding at 640 days.

Table 6: Produced water-oil ratio after gel treatment at 1,000 days.

	Case 1	Case 2	Case 3	Case 4	Case 5	Homogeneous
#1	20	21	28	27	21	45
#2	29	32	45	27	10	
#3	52	11	27	12	32	
#4	31	24	21	24	22	
#5	57	11	34	17	6	
#6	33	17	19	28	30	
⋮	⋮	⋮	⋮	⋮	⋮	
#49	30	9	18	36	16	
#50	35	25	24	17	17	

4.2. Gel Treatment. Results from the previous study indicate that multiscale correlation usually generates more heterogeneous field than single-scale correlation. With these generated heterogeneous fields, analysis of gel treatment performance is conducted; that is, how much gel treatment improves productivity, reduction of water production, and when gel treatment is applied on single-scale- or multiscale-correlated heterogeneous permeability fields.

Because main purpose of gel treatment is to reduce excessive water production, gel treatment performance is mainly analyzed with water-oil ratio (WOR). Figure 3 presents comparison of water saturation between gel-treated and nontreated waterflooding at 640 days. The corresponding permeability field is an Ex 5, as shown in Figure 1(f). Figure 3 confirms that gel treatment is effective not only to delay the outbreak of water breakthrough at producer but also to improve vertical sweep efficiency.

Table 6 lists the results of water-oil ratio at the end of production. All realized heterogeneous fields have similar geometric mean of permeability of 200 md. To investigate all results statistically, arithmetic means of WOR and cumulative oil recovery for gel treatment on 50 generated permeability fields for all cases are analyzed and summarized in Table 7. To investigate the influence of heterogeneity on gel treatment performance, results from homogeneous permeability field are considered as a base. From the homogeneous field case, it is certain that gel treatment reduces water-oil ratio as much as 78%. In comparison with homogeneous field, all gel treatments on Cases 1 to 5 reduce water-oil ratio more than 17%, as illustrated in Tables 6 and 7. The best improvement of water-oil ratio is observed in Case 5 at the end of production, which is about 63% reduction of that for gel-treated homogeneous field case. Even though heterogeneous field has equivalent geometric mean of permeability to homogeneous field, application of gel treatment on heterogeneous field results in less water-oil ratio than on homogeneous field because of heterogeneity. Tables 6 and 7 also prove that gel treatment on heterogeneous field having higher heterogeneity index leads to lower water-oil ratio than on heterogeneous field having lower heterogeneity index. With respect to cumulative oil recovery, gel treatment does not have effectiveness due to DPR mechanism.

Table 7: Arithmetic means of water-oil ratio and cumulative oil recovery after gel treatment at the 1,000 days.

	Water-oil ratio	Cumulative oil recovery
Nontreated homogeneous field	206	0.62
Gel-treated homogeneous field	45	0.62
Case 1	31	0.59
Case 2	18	0.52
Case 3	37	0.59
Case 4	23	0.55
Case 5	17	0.51

Figures 4(b) to 4(f) present permeability reduction factor calculated from simulations by applying gel treatment to Ex 1 to 5 fields which are representative heterogeneous permeability fields shown in Figures 1(b) to 1(f). Figure 4(a) just

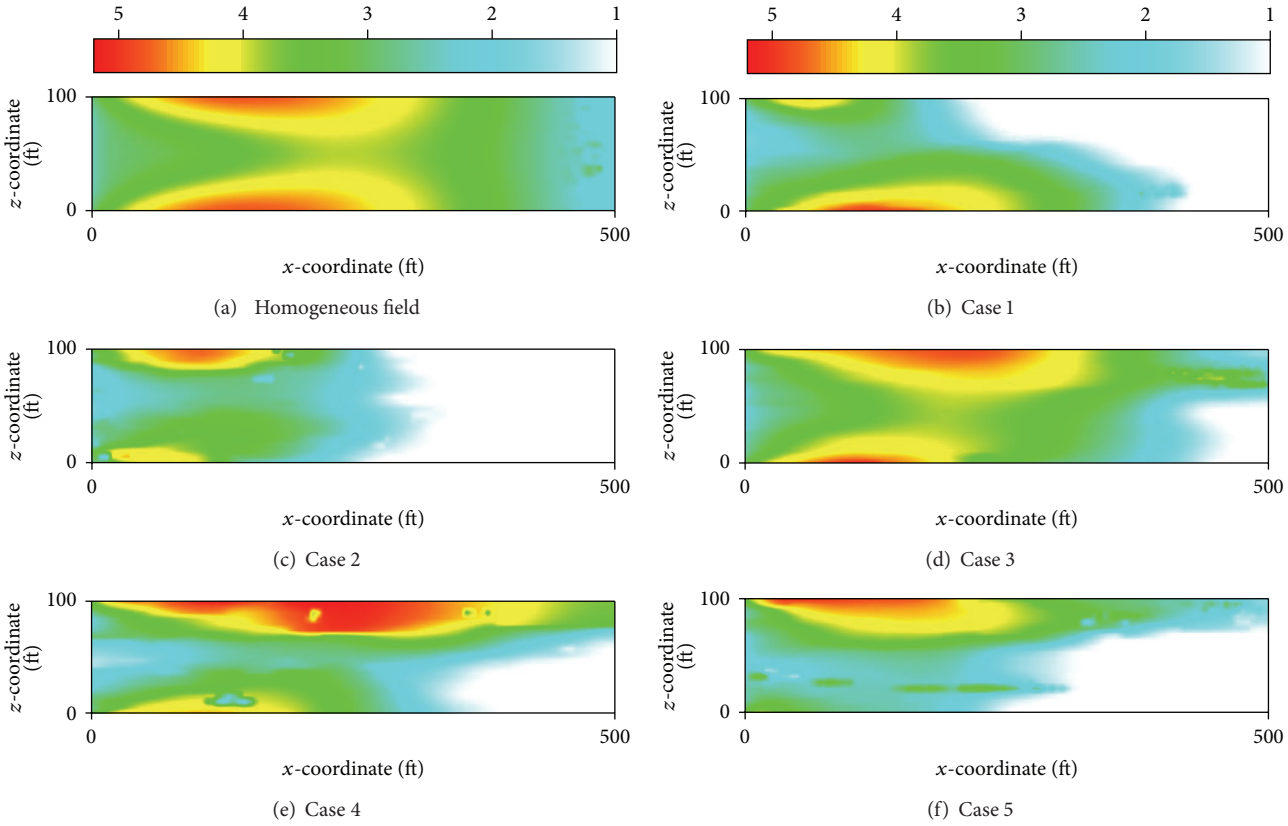

Figure 4: Permeability reduction factors depending on heterogeneity at 1,000 days.

shows the permeability reduction factor when gel treatment is applied on equivalent homogeneous permeability field. Successful gel treatment means placing gel in a proper location, that is, high-permeability zone. For the homogeneous field, nonperturbation of permeability sustains the front of gel solution to advance steady. Regarding heterogeneous fields, as shown in Figures 4(b) to 4(f), gel is placed in mainly high-permeability zone. Among heterogeneous fields, gel treats almost whole domain in multiscale correlation (Figures 4(e) and 4(f)) and single scale correlation field having longer correlation length (Figure 4(d)). The results are consistent with previous results in that correlation length controls spatial distribution of permeability, that is, degree of layered permeability system. For Case 3, gel could spread on whole domain in spite of single-scale correlation because of longer correlation length. In a multiscale correlation field, regional scale having longer correlation length induces more layered permeability field, so gel spreads on whole area of reservoir. By comparing Cases 3 and 4, adding local scale to regional scale makes heterogeneity more severe, so this makes gel present in high-permeability zones intensively.

Figure 5 shows improvements of water-oil ratio in gel-treated waterflooding compared with nontreated waterflooding as a function of time for Ex 1 to 5. It is hard to be certain that comparison among Ex 1 to 5 represents all information of every gel treatment on realized permeability field. However,

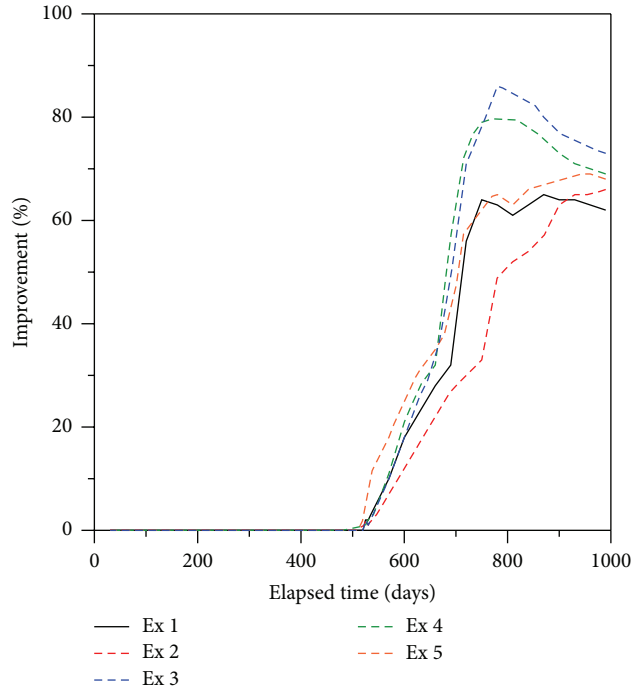

Figure 5: Improvements of water-oil ratio between nontreated waterflooding and gel-treated waterflooding according to elapsed time.

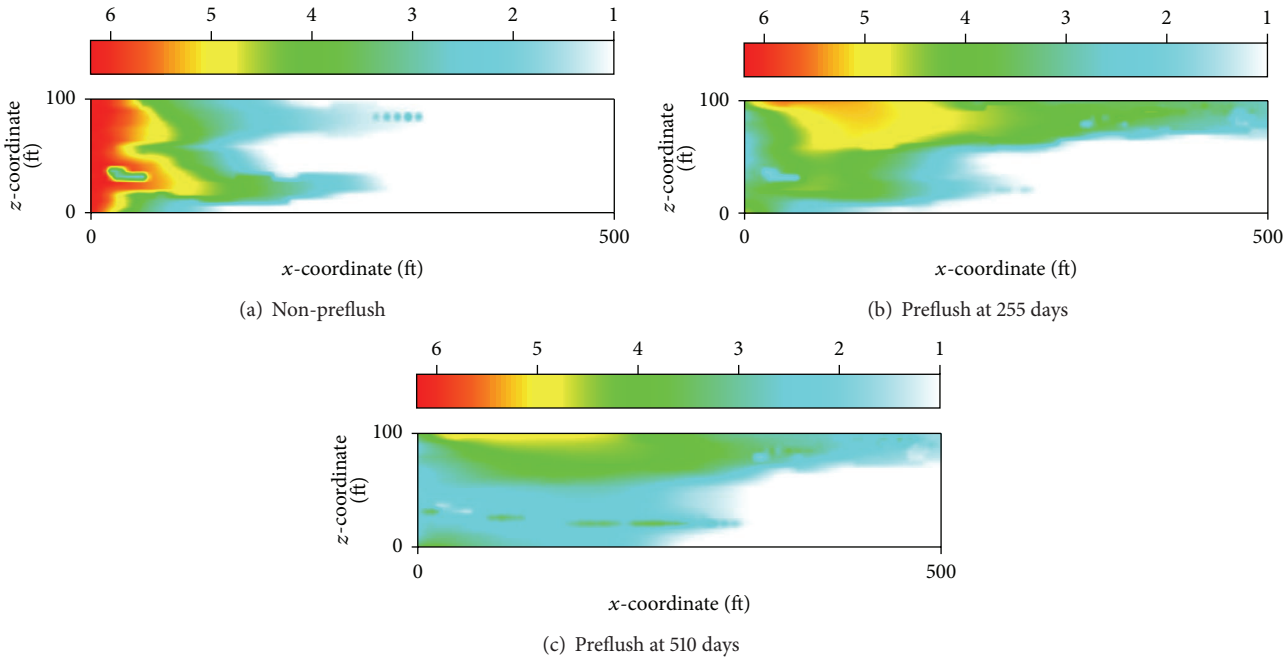

Figure 6: Permeability reduction factors depending on preflush at 1,000 days.

Table 8: Effects of gel treatment and preflush on water-oil ratio and cumulative oil.

	Preflush (days)	Water-oil ratio	Cumulative oil recovery
Nontreated waterflooding		54	0.56
Gel-treated waterflooding	0	24	0.55
	255	21	0.56
	510	17	0.54

it is pretty accurate and effective to explain trend for each case. From the results of Ex 1 and 4, we can conclude that higher heterogeneity index originating from multiscale leads to higher improvement of gel treatment performance on the fields. although Ex 2 and 4 show similar heterogeneity as 0.788 and 0.733, there is considerable difference in the improvements of gel treatment, up to 14% because of different spatial distribution of permeability. Ex 5 has the highest heterogeneity over 0.8, but improvement of water-oil ratio is not that much high due to less layered spatial distribution of permeability. The maximum improvement of Ex 5 does not exceed 70%. These results show that performance of gel treatment is affected by not only heterogeneity index but also spatial distribution of permeability.

To be a successful gel treatment, gel solution should travel to the whole domain of a field and locate at high-permeability zones intensively. To accomplish this goal, preflush as waterflooding is used as one of controllers. Usually, preflush is used to mitigate salinity effect, cation exchange, and so on. In addition, it regulates the placement of gel in fields. Except for preflush duration, all conditions are maintained to be the same as in previous study. Gel treatment is applied on the heterogeneous permeability field of Ex 5, as shown in Figure 1(f). As shown in Table 8, with more preflush, lower water-oil ratio was obtained at the end of the production. Figure 6 shows that the duration of preflush, that is, initiation time of injecting gelant, impacts the distribution of gel into reservoir. No improvement of cumulative oil recovery is observed. Although non-preflush case just reduces 56% of water-oil ratio, preflush cases for 255 and 510 days show 61% and 69% reduction of water-oil ratio.

5. Conclusions

(1) In stochastic random field generation, correlation length and number of scales describe spatial distribution of permeability, and variance defines appearance of high-permeability value. Multiscale correlation generally realizes severe heterogeneous permeability fields having higher heterogeneity index.

(2) Reduction of water-oil ratio by gel treatment is a function of heterogeneity index and spatial distribution of permeability originating from correlation length, variance, and number of scales. Generally, longer correlation length, higher variance, and multiscale lead to higher performance of gel treatment.

(3) Preflush influences location of gelation in the reservoir, so it determines performance of gel treatment, that is, reduction of water-oil ratio. Therefore, optimal design of preflush should be considered for successful application of gel treatment.

Acknowledgments

This work was supported by the Energy Efficiency & Resources of the Korea Institute of Energy Technology Evaluation and Planning (KETEP) Grant funded by the Korean Government, Ministry of Knowledge Economy (20122010300020).

References

[1] H. K. Van Poolen, *Fundamentals of Enhanced Oil Recovery*, PennWell, Tulsa, Okla, USA.

[2] L. W. Lake, *Fundamentals of Enhanced Oil Recovery*, The University of Texas, Austin, Tex, USA.

[3] J. T. Portwood, S. H. Lackey, and S. W. Abel, "Selective polymer treatments improve oil recovery in five mature Southern Oklahoma waterfloods," in *Proceedings of the 17th SPE Improved Oil Recovery Symposium (IOR '10)*, SPE 129796, Tulsa, Oklahoma, USA, April 2010.

[4] C. A. Norman and J. E. Smith, "Economics of in-depth polymer gel process," in *Proceedings of the SPE Rocky Mountain Regional Meeting*, SPE 55632-MS, pp. 15–18, Gillette, Wyo, USA, May1999.

[5] J. J. Sheng, *Modern Chemcial Enhanced Oil Recovery: Theory and Practice*, Elsevier, Oxford, UK.

[6] J. P. Coste, Y. Liu, B. Bai, Y. LI, and P. Shen, "In-depth fluid diversion by pre-gelled particleslaboratory study and pilot testing," in *Proceedings of the SPE/DOE Improved Oil Recovery Symposium (IOR '12)*, SPE 59362-MS, pp. 3–5, Tulsa, Okla, USA, April 2012.

[7] B. Bai, Y. Liu, J.-P. Coste, and L. Li, "Preformed particle gel for conformance control: transport mechanism through porous media," *SPE Reservoir Evaluation and Engineering*, vol. 10, no. 2, pp. 176–184, 2007.

[8] B. Bai, L. Li, Y. Liu, H. Liu, Z. Wang, and C. You, "Preformed particle gel for conformance control: factors affecting its properties and applications," *SPE Reservoir Evaluation and Engineering*, vol. 10, no. 4, pp. 415–422, 2007.

[9] R. S. Seright, "Use of preformed gels for conformance control in fractured systems," *SPE Production & Facilities*, vol. 12, no. 1, pp. 59–65, 1997.

[10] R. S. Seright, "Gel propagation through fractures," *SPE Production & Facilities*, vol. 16, no. 4, pp. 225–231, 2001.

[11] R. S. Seright, "Disproportionate permeability reduction with pore-filling gels," *SPE Journal*, vol. 14, no. 1, pp. 5–13, 2009.

[12] G. Chauveteau, A. Omari, R. Tabary, M. Renard, J. Veerapen, and J. Rose, "New size-controlled microgels for oil production," in *Proceedings of the SPE International Symposium on Oilfield Chemistry*, SPE 64988-MS, pp. 111–118, Houston, Tex, USA, February 2001.

[13] H. W. Gao and T. E. Burchfield, "The effects of crossflow and layer permeability contrast on the effectiveness of gel treatments in polymer floods and waterfloods," *SPE Reservoir Engineering*, vol. 10, no. 2, pp. 129–135, 1995.

[14] B. Bai, Q. Wang, Y. Du, and Y. Z. Liu, "Factors affecting in-depth gel treatment for reservoirs with thick heterogeneous oil layers," in *Proceedings of the Canadian International Petroleum Conference 55th Annual Technical Meeting*, SPE 2004-140, Alberta, Canada, June 2004.

[15] R. S. Seright, G. Zhang, O. O. Akanni, and D. Wang, "A comparison of polymer flooding with in-depth profile modification," in *Proceedings of the Canadian Unconventional Resources Conference (CURC '11)*, pp. 128–140, Alberta, Canada, November 2011.

[16] R. B. Gharbi, E. J. Peters, A. Elkamel, and N. Afzal, "Effect of heterogeneity on the performance of EOR processes with horizontal wells," in *Proceedings of the SPE Western Regional Meeting*, SPE 38320, Long Beach, Calif, USA, June 1997.

[17] S. Murata, A. Ashida, S. Takahashi, and H. Okabe, "Numerical study on effective in-depth profile modification to heterogeneous reservoir," in *Proceeding of the 33rd IEA EOR Annual Symposium*, Saskatchewan, Canada, 2012.

[18] B. X. Hu, J. Wu, A. K. Panorska, D. Zhang, and C. He, "Stochastic study on groundwater flow and solute transport in a porous medium with multi-scale heterogeneity," *Advances in Water Resources*, vol. 26, no. 5, pp. 541–560, 2003.

[19] B. X. Hu, J. Wu, and C. He, "On stochastic modeling of groundwater flow and solute transport in multi-scale heterogeneous formations," *Computational and Applied Mathematics*, vol. 23, no. 2-3, pp. 121–151, 2004.

[20] C. Cozic, D. Rousseau, and R. Tabary, "Novel insights into microgel systems for water control," *SPE Production & Operations*, vol. 24, no. 4, pp. 590–601, 2009.

[21] R. S. Seright, G. Zhang, O. O. Akanni, and D. Wang, "A comparison of polymer flooding with in-depth profile modification," in *Canadian Unconventional Resources Conference (CURC '11)*, SPE 146087-MS, Alberta, Canada, November 2011.

[22] A. Zaitoun, R. Tabary, D. Rousseau et al., "Using microgels to shut off water in a gas storage well," in *Proceedings of the SPE International Symposium on Oilfield Chemistry*, SPE 106042-MS, Houston, Tex, USA, March 2007.

[23] J. Liang, H. Sun, and R. S. Seright, "Reduction of oil and water permeabilities using gels," in *Proceedings of the SPE/DOE Enhanced Oil Recovery Symposium (IOR '92)*, SPE 24195-MS, pp. 22–24, Society of Petroleum Engineers, Tulsa, Okla, USA, April.

[24] J.-T. Liang and R. S. Seright, "Further investigations of why gels reduce water permeability more than oil permeability," *SPE Production & Facilities*, vol. 12, no. 4, pp. 225–230, 1997.

[25] G. Chauveteau, R. Tabary, N. Blin, M. Renard, D. Rousseau, and R. Faber, "Disproportionate permeability reduction by soft preformed microgels," in *Proceedings of the SPE/DOE 4th Inproved Symposium Oil Recovery*, SPE 89390, Tulsa, Oklahoma, USA, April 2004.

[26] D. Rousseau, G. Chauveteau, M. Renard et al., "Rheology and transport in porous media of new water shutoff/conformance control microgels," in *Proceedings of the SPE International Symposium on Oilfield Chemistry*, SPE 93254, pp. 435–446, Houston, Tex, USA, February 2005.

[27] S. G. Ghori and J. P. Heller, "Computed effect of heterogeneity on well-to-well tracer results," in *Proceeding of 5th Canadian/American Conference on Hydrology*, Alberta, Canada, 1990.

[28] L. Smith and R. A. Freeze, "Stochastic analysis of steady state groundwater flow in a bounded domain. I. One-dimensional simulations," *Water Resources Research*, vol. 15, no. 3, pp. 521–528, 1979.

[29] S. G. Ghori, J. P. Heller, and A. K. Singh, "An efficient method of generating random permeability fields by the source point method," *Mathematical Geology*, vol. 25, no. 5, pp. 559–572, 1993.

[30] S.-G. Li and Q. Liu, "Interactive ground water (IGW)," *Environmental Modelling & Software*, vol. 21, no. 3, pp. 417–418, 2006.

[31] Center for Petroleum and Geosystems Engineering, *UTCHEM-9: 0 A Three-Dimensional Chemical Flood Simulator*, University of Texas, Austin, Tex, USA, 2000.

Hindawi Publishing Corporation
Journal of Chemistry
Volume 2013, Article ID 927519, 8 pages
http://dx.doi.org/10.1155/2013/927519

Research Article

Laboratory Study on the Potential EOR Use of HPAM/VES Hybrid in High-Temperature and High-Salinity Oil Reservoirs

Dingwei Zhu,[1,2] Jichao Zhang,[3] Yugui Han,[3] Hongyan Wang,[3] and Yujun Feng[1,3,4]

[1] *Chengdu Institute of Organic Chemistry, Chinese Academy of Sciences, Chengdu 610041, China*
[2] *University of Chinese Academy of Sciences, Beijing 100039, China*
[3] *EOR Laboratory, Geological Scientific Research Institute, Shengli Oilfield Company of SINOPEC, Dongying 257013, China*
[4] *State Key Laboratory of Polymer Materials Engineering, Polymer Research Institute, Sichuan University, Chengdu 610065, China*

Correspondence should be addressed to Yujun Feng; yjfeng@cioc.ac.cn

Received 6 April 2013; Revised 12 July 2013; Accepted 12 July 2013

Academic Editor: Ibnelwaleed Ali Hussien

Polymer flooding represents one of the most efficient processes to enhance oil recovery, and partially hydrolyzed polyacrylamide (HPAM) is a widely used oil-displacement agent, but its poor thermal stability, salt tolerance, and mechanical degradation impeded its use in high-temperature and high-salinity oil reservoirs. In this work, a novel viscoelastic surfactant, erucyl dimethyl amidobetaine (EDAB), with improved thermal stability and salinity tolerance, was complexed with HPAM to overcome the deficiencies of HPAM. The HPAM/EDAB hybrid samples were studied in comparison with HPAM and EDAB in synthetic brine regarding their rheological behaviors and core flooding experiments under simulated high-temperature and high-salinity oil reservoir conditions (T: 85°C; total dissolved solids: 32,868 mg/L; $[Ca^{2+}] + [Mg^{2+}]$: 873 mg/L). It was found that the HPAM/EDAB hybrids exhibited much better heat- and salinity-tolerance and long-term thermal stability than HPAM. Core flooding tests showed that the oil recovery factors of HPAM/EDAB hybrids are between those of HPAM and EDAB. These results are attributed to the synergistic effect between HPAM and EDAB in the hybrid.

1. Introduction

Among all the chemically enhanced oil recovery (CEOR) processes, polymer flooding represents one of the most efficient methods to produce residual oil from depleted and water-flooded reservoirs [1, 2]. In this process, the increased viscosity of the displacing fluid by the added water-soluble polymer will improve the mobility ratio between the injected fluid and the reservoir oil, mobilizing the capillary trapped water-flooded oil in the secondary stage, leading to better vertical and areal sweep efficiencies and thus higher oil recovery efficiencies [2]. In China, around 13 million tons of oil is produced additionally per year by this chemical flooding technique.

Partially hydrolyzed polyacrylamide (HPAM) is the most widely used oil displacement agent and has been successfully employed in polymer flooding worldwide [2–4]. As an anionic polyelectrolyte, HPAM is easily to be dissolved in water and shows strong thickening ability in fresh water at relatively lower dosage. Nevertheless, the notorious congenital drawbacks of HPAM also limit its applications in hostile environment, in particular, the high-temperature, high-salinity, and low-permeability oil reservoirs [5], such as the Class III reserve of Shengli Oil Field in China where the temperature is above 85°C and the salinity (total dissolved solids, TDS) is higher than 30,000 mg/L in which the total amount of Ca^{2+} and Mg^{2+} exceeds 800 mg/L. In such a harsh environment, the interaction of metal ions in the oil field brines largely shields the mutual repulsion from the carboxylic groups along the HPAM skeleton, leading the polymer coils to collapse, decreasing hydrodynamic volume, and thus ultimately lowering solution viscosity [2]. Efficiency loss of HPAM aqueous solution at elevated temperature becomes further serious as more amide groups undergo extensive hydrolysis into carboxylic characters, and the resulting hydrolyzed products precipitated when contacting Ca^{2+} and Mg^{2+} [6], commonly present in oil reservoir brines or hard water.

Another major limitation of HPAM is its flow-induced mechanical degradation. As a synthetic polymer, HPAM is intrinsically linear, flexible, high-molecular weight (generally higher than ten million), and highly polydispersible in molecular weight (polydispersity index normally between 2 and 3). When it is mixed and dissolved in tanks, or it is passing through chokes, pipes, valves, nozzles, pumps, perforations near wellbore, or the pore throat in the porous media, HPAM chains are subjected to both shear flows and elongation flows [7]. In pure shear flows where the shear rate is perpendicular to the flow direction, HPAM molecules rotate and are thus subjected to periodic extensional and compressional stresses. As shear rate increases, hydrodynamic stresses increase and their effects are nonnegligible compared with those of Brownian motion when rotation time becomes smaller than the longest rotational relaxation time. In pure elongational flows where the elongation rate is parallel to flow direction, the effective deformation that occurs in the flow direction may be very large for the flexible HPAM and a full stretching is achieved only if the macromolecule remains in the elongational flow over a sufficiently long time. When submitted to shear, macromolecules do not stretch significantly, whereas when submitted to extension, they can elongate drastically and break. The first consequence of macromolecule stretching in elongational flows is a strong increase in viscosity. For high-molecular-weight HPAM used in EOR, the elongational viscosity may be as high as 10^4 times the zero-shear-rate viscosity. The second consequence is that the macromolecule is subjected to an internal tensile. It has been shown that elongation force could possibly be high enough to exceed the carbon-carbon bond force and thus may cause chain breakage, that is, mechanical degradation of HPAM chains [7]. This degradation process essentially breaks the larger molecules up into smaller fragments and thus changes the molecular weight distribution of the HPAM, which hinders the efficiency of the EOR technique [8, 9].

Facing these severe challenges, two options were naturally used to improve the properties of HPAM in high-temperature and high-salinity environment; one is introducing thermostable and more salt-tolerant monomer or groups such as SO_3^- onto the HPAM backbone [10], and the second is increasing molecular weight of HPAM (maximum 35×10^6 g/mol to date) to get higher viscosity retention. However, the main portion in the first case is still the acrylamide segment which shows poor long-term thermal stability and salt tolerance, and in the second case, the increased molecular weight of HPAM will bring about easier mechanical degradation [7] and the plugging of the smaller pore throat in the low-permeability oil reservoirs. Thus, we shifted our attention to seek other alternatives with better salt tolerance and thermal stability, as well as improved mechnical stability, and we found recently that viscoelastic surfactant (VES) is one of such choices amongst others.

Viscoelastic surfactants are formed from the entanglement of worm-like micelles (WLMs) by certain surfactants in the presence of an organic or inorganic hydrotrope [11]. WLMs are long flexible aggregates of surfactant molecules in aqueous solution, and above a surfactant concentration threshold, WLMs entangle into a transient network that is constantly breaking and reforming, for which they are also referred to as "living" or "equilibrium" polymers [12, 13]. The entanglement of WLMs imparts strong thickening ability of water and remarkable viscoelastic properties to the solution. These peculiar rheological properties of VES, including reversible breaking and formation, viscoelastic response analogous to polymer solutions, and strong viscosifying ability, may furnish them to be applied in CEOR process.

Up to date, most of the VES systems are composed of cationic surfactants whose hydrophobic tail is normally shorter than C18. The strong adsorption between these cationic amphiphiles and negatively charged sandstone, as well as high dosage needed to thicken injection fluid, impeded their practical use in EOR process. To overcome these deficiencies of cationic VES, we recently developed ultra-long chain particularly C22-tailed zwitterionic [14–19], anionic [20, 21], nonionic [22] surfactants which are capable of forming WLMs at much lower concentration; that is, the overlapping concentration (C^*) is much lower than those of C16 cationic counterparts. Apart from these advantages, the C22-tailed zwitterionic surfactants—3-(nerucamidopropyl-*N,N*-dimethyl ammonium) propane sulfonate (EDAS) [14–17, 19] also show additional advantages such as insensitivity to inorganic salt, sufficient stability over the whole pH range [14], and long-term thermal stability [15]. These unique properties of EDAS make it suitable for potential use in high-temperature and high-salinity reservoirs. Nevertheless, the betaine agent to prepare EDAS, 1,3-propanesultone, is extremely poisonous and carcinogenic, restricting the scale-up production and industrial use of EDAS in tertiary oil recovery.

Thus, in this work, a newly synthesized carboxylate counterpart of EDAS, erucyl dimethyl amidopropyl betaine (EDAB), was chosen for the study of its possible use in chemical EOR process. Compared with its saturated-chain counterparts, EDAB shows improved water solubility and much lower critical micelle concentration [18]. However, we found that the oil recovery factor from single VES solution is quite low. Therefore, HPAM was used to complex with EDAB to form hybrids which were systematically examined to see their potential in CEOR process. Reported here are the rheological behaviors and preliminary core flooding results of these hybrids under simulated high-temperature and high-salinity oil reservoirs of Shengli oil Field. For comparison, HPAM and EDAB were also tested under the same experimental conditions.

2. Experimental

2.1. Materials. HPAM (Scheme 1) with viscosity-averaged molecular weight of 1.2×10^7 g/mol was obtained from Beijing Hengju Chemical Group Co., Ltd. The hydrolysis degree and active content of this polymer are 24% and 89.9%, respectively. EDAB (Scheme 1) was prepared by the reaction of the corresponding fatty acids with *N,N*-dime-thyl-1,3-propanediamine, followed by quaternization with sodium chloroacetate of the obtained intermediates [18]. All other

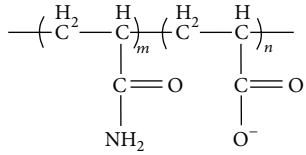

HPAM

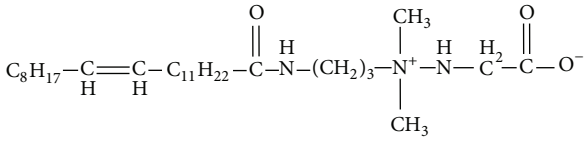

EDAB

Scheme 1: Molecular structures of HPAM and EDAB used in this work.

Table 1: The nomenclature and compositions of chemicals used in this work.

Sample name	HPAM (wt%)	EDAB (wt%)
P30	0.3	0
E30	0	0.3
P25E5	0.25	0.05
P20E10	0.20	0.10
P15E15	0.15	0.15
P5E25	0.05	0.25

chemicals used are analytical grade, and the water used is doubly distilled.

2.2. Preparation of Hybrid Samples. The HPAM or EDAB stock solutions with concentration of 0.3% were separately prepared by dissolving designed amount of powders into synthetic brine (TDS: 32,868 mg/L; $[Ca^{2+}] + [Mg^{2+}]$: 873 mg/L) with gentle stirring at room temperature. The TDS and hardness of the brine are close to those of connate water in the Reserve III of Shengli Oil Field. The hybrid samples were prepared by mixing EDAB solution with HPAM solution following the designed recipe and gently stirred for 3 days, and then left to stand for 1 day prior to test. The sample code "PxEy" refers to the concentration of the two chemicals in the mixture (Table 1).

2.3. Rheology Test. All rheological measurements were carried out on a Physica MCR301 (Anto-Paar, Austria) rotational rheometer equipped with concentric cylinder geometry CC27. The radii of the measuring bob and the measuring cup are 13.33 and 14.46 mm, respectively. The temperature was controlled by a Peltier system that provides fast and precise adjustment of the temperature during heating. A solvent trap was used to prevent evaporation of the solvents during measurement.

The apparent viscosity (η_{app}) of the samples was measured at 85°C with a fixed shear rate ($\dot{\gamma}$) of 7.34 s^{-1}. Steady shear viscosity was recorded during temperature scans going from 20 to 85°C (heating rate = 2°C/min). The elastic and storage moduli of the samples were registered during the angular frequency scans from 0.05 to 100 rad·s^{-1} at 85°C with the same rheometer.

2.4. Long-Term Thermal Stability Test. 0.05% $Na_2S_2O_3$ is added into all the samples as an oxygen scavenger, and the sample solutions were distributed into 120-mL glass bottles, and then sealed with a cover, followed by placing them into an oven and aged at 85°C. At consecutive time intervals, the samples were taken out for viscosity monitoring.

2.5. Core Flooding Test. The core flooding tests were performed under the simulated high-temperature and high-salinity oil reservoirs in Shengli Oil Field of China and followed a previously reported procedure [23]. A steel cylinder with 2.5 cm in inner diameter and 25 cm in height was packed with several sizes of silica sand in model. The porosity of sandstone core was 32.6%. The sand pack was initially saturated with the synthetic brine, followed by injecting the dehydrated Shengli oil to ~70%. The density of dehydrated Shengli oil was 0.95 g/cm^3 and the viscosity was 40.1 mPa·s. The core was then injected with the synthetic brine until the water content was higher than 98% in the output fluid, and the injection of 30% pore volume (PV) of the sample solution was followed. The total oil recovery and the oil recovery by water flooding were calculated, respectively, and the difference between them was the tertiary oil recovery factor by polymer or polymer/surfactant hybrid flooding. The injection rate of the sample was maintained at 0.23 mL/min, and the cylindrical sand pack was placed in a chamber and heated at 85°C throughout the test.

3. Results and Discussion

3.1. Rheological Behaviors of HPAM/EDAB Hybrid Samples. It is well accepted that apparent viscosity of polymer solution plays a crucial role in displacing less viscous oil in the EOR process [24]. Therefore, it is necessary to investigate the viscous properties of the hybrid samples before flooding test.

Exhibited in Figure 1 are the apparent viscosities of different samples plotted against temperature. As expected, η_{app} of HPAM solution (P30) decreases continuously upon increasing temperature, with a general trend following Arrhenius laws. The final η_{app} at 85°C is just one-third of the original value at room temperature, which implies that the HPAM solution shows pure thermothinning behavior. However, η_{app} of EDAB solution (E30) decreases sharply before 25°C, following an unstable increase until 56°C, after which the viscosity drops again. Typically, its viscosity between 70 and 85°C remains unchanged. But if one compares the η_{app} of EDAB at 30 and 85°C, you will find that there is no change between them. This means that EDAB is less thermosensitive than HPAM. Interestingly, the HPAM/EDAB hybrid samples such as P15E15 and P10E20 exhibit more similar behavior to EDAB rather than HPAM solution. Both of the two hybrid samples show inverted "V" shape in viscosity-temperature curves, all of which have a viscosity peak 55°C, analogous

Table 2: Apparent viscosity of the samples measured at simulated high-temperature and high-salinity oil reservoirs (TDS = 32,868 mg/L, $[Ca^{2+}] + [Mg^{2+}] = 873$ mg/L, $T = 85^{\circ}C$, $\dot{\gamma} = 7.34\ s^{-1}$).

Sample	P30	P25E5	P20E10	P15E15	P10E20	P5E25	E30
η_{app} (mPa·s)	17.93	11.34	8.59	11.25	30.61	18.29	28.04

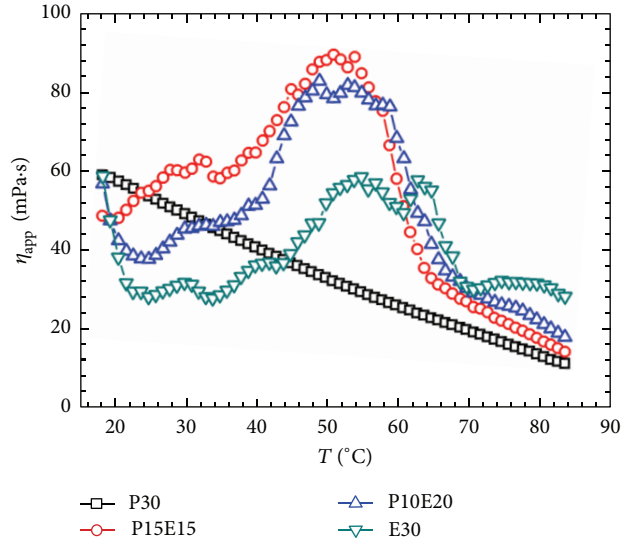

Figure 1: Effect of temperature on apparent viscosity of the samples (TDS = 32,868 mg/L, $[Ca^{2+}] + [Mg^{2+}] = 873$ mg/L, $\dot{\gamma} = 7.34\ s^{-1}$, heating rate: 2°C/min).

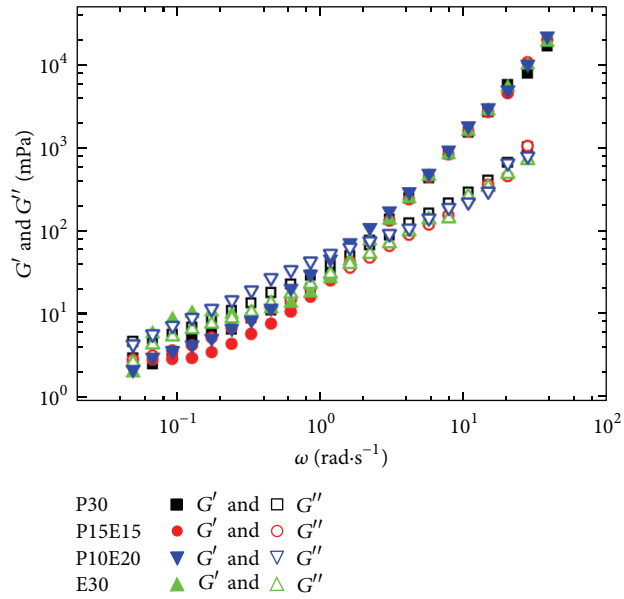

Figure 2: Storage modulus (G') and loss modulus (G'') plotted as a function of angular frequency (ω) for the samples (TDS = 32,868 mg/L, $[Ca^{2+}] + [Mg^{2+}] = 873$ mg/L, $T = 85^{\circ}C$).

to that of EDAB. But it is worth noting that the higher the polymer fraction, the higher the viscosity peak. It is also noteworthy that the hybrid samples show stronger thermo-thinning behaviors after the viscosity maximum compared to EDAB.

To pick out the optimized formulation used for oil displacement under the simulated oil reservoir condition, it is utmost important to compare all the hybrid samples, as well as the pure HPAM and EDAB solutions, at the target temperature. Summarized in Table 2 are the apparent viscosities of all the samples. It is quite surprising that there is no direct correlation between viscosity and the content of EDAB or HPAM. Although the viscosity of 0.3% EDAB is 10 mPa·s higher than that of 0.3% HPAM, the apparent viscosity of the 0.3% hybrid samples decreases first followed by continuous increase upon increasing the content of EDAB in the hybrid samples. Exceptionally, the sample P10E20 composed of 0.10% HPAM and 0.20% EDAB displays the apparent viscosity as high as 30.61 mPa·s, while P5E25 with 0.05% HPAM and 0.25% EDAB possesses viscosity of only 18.29 mPa·s, and P15E15 only has 11.25 mPa·s. In the following studies, the two hybrid samples, P15E15 and P10E20, will be employed for long-term thermostability and core flooding studies.

In order to distinguish whether HPAM undergo micro-structural changes with the addition of EDAB, dynamic rheological experiments were performed at 85°C as well. Figure 2 shows the plots of storage modulus (G') and loss modulus (G'') as a function of oscillatory shear frequency (ω) for the HPAM/EDAB hybrid samples. For the HPAM sample (P30), both moduli are strong functions of shear frequency over the entire frequency. When EDAB is added, the G' and G'' of the hybrid samples P15E15 and P10E20 remain nearly unchanged, especially at high frequencies. But it is worth noting that there are crossovers between G' and G'' for all the samples, indicative of the formation of network structures in the solution. These results suggest that HPAM does not undergo microstructural changes when EDAB is added and it still has the ability of increasing the oil recovery factor. Therefore, the hybrid samples have great potential to enhance oil recovery from high-temperature and high-salinity oil reservoirs because EDAB shows excellent heat and salinity tolerance.

3.2. Long-Term Thermal Stability. The remaining viscosity at high temperature represents a primary criterion for any chemicals to be used in hostile environment. For instance, the continuous aging of the displacing fluid is detrimental to tertiary oil recovery [25], particularly in high-temperature oil reservoirs. Therefore, high-temperature aging is crucial to EOR chemicals, and long-term thermal stability experiment of HPAM/EDAB hybrid samples is inescapably necessary.

Figure 3 shows the variation of η_{app} as a function of aging time for the HPAM/EDAB hybrid samples and sole HPAM

Table 3: Core parameters, displacement process, and recovery factors.

Core no.	Permeability (mDarcy)	Pore volume (cm^3)	Saturated oil (cm^3)	Slug	Slug injected (PV)	Water flooding recovery (%)	Ultimate recovery (%)	Enhanced oil recovery (%)
1	1059	53.4	43.0	P30	0.3	55.10	70.95	15.85
2	1480	50.6	42.0	P15E15	0.3	60.85	71.05	10.20
3	1496	50.0	41.0	P10E20	0.3	45.10	52.20	7.10
4	1494	49.0	41.0	E30	0.3	35.95	37.85	1.90

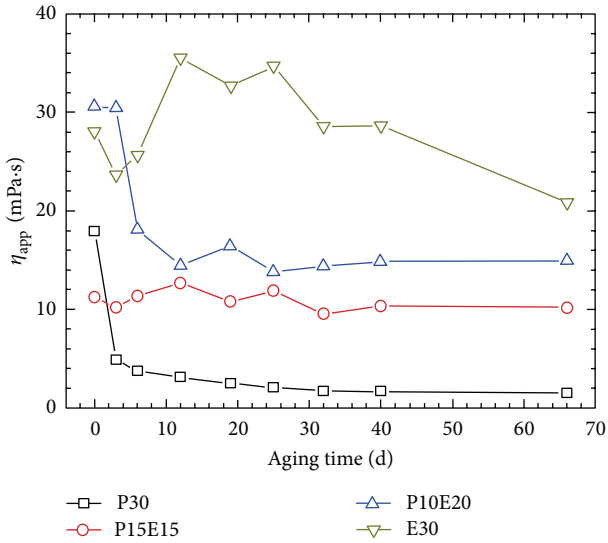

Figure 3: Long-term thermal stability of HPAM/EDAB hybrid samples in comparison with EDAB and HPAM (TDS = 32,868 mg/L, $[Ca^{2+}] + [Mg^{2+}] = 873$ mg/L, $\dot{\gamma} = 7.34\ s^{-1}$). Both the aging and measuring temperature is 85°C.

or EDAB after aging at 85°C. One can clearly find a sharp reduction in η_{app} for HPAM (P30) after aging: the initial η_{app} (0 d) is 17.93 mPa·s, but is only 4.88 mPa·s left for the same sample after 3 days of aging! There is also a sharp reduction in η_{app} for P10E20 in 6 days: its η_{app} decreases to 18.11 mPa·s, and 41% of loss in viscosity. However, after more than 25 days of aging, the η_{app} of P10E20 begins to increase other than decrease. Unlike P30 and P10E20, the η_{app} of P15E15 maintains a constant value regardless of aging time, showing improved long-term thermal stability over HPAM. Meanwhile, as shown in Figure 3, EDAB (E30) exhibits a much better thermal stability than HPAM after 66 days of aging. These results clearly demonstrate that the ultra-long-chain zwitterionic surfactant EDAB possesses much better long-term thermal stability over HPAM, and the addition of EDAB into HPAM solutions will improve the thermal stability of HPAM solutions.

3.3. Oil Displacement Test. To our knowledge, there are no published data concerning chemical flooding using HPAM or EDAB under the simulated high temperature and salinity oil reservoir conditions. Although the HPAM/EDAB hybrid samples show promising potential for chemical EOR in high-temperature and high-salinity oil reservoirs, no core flooding test so far has been performed yet.

Plotted in Figure 4 are the recovery factors, water cut, and flooding pressure as a function of injected volume of the sample solutions under the simulated high-temperature and high-salinity oil reservoir environment. Table 3 shows core parameters, displacement process, and the results of these oil displacement tests. It was found that 15.85% oil recovery factor by HPAM (P30) flooding was obtained at these conditions (Figure 4(a)), whereas the oil recovery factor of EDAB (E30) was only 1.90% (Figure 4(b)). As shown in Figures 4(c) and 4(d), the oil recovery factor of P15E15 was 10.20% and the factor of P10E20 was 7.10%; both of them are smaller than that of HPAM, but much higher than that of EADB. The main reason to get a higher oil recovery factor with the hybrid samples can be ascribed to strengthened micelles by the added HPAM long chains which are not as easy as that of micelles to be disrupted. It is worth emphasizing that the synergistic effect between HPAM and EDAB enables the hybrid sample to show an excellent long-term thermal stability and get a relatively high oil recovery factor. Under long-term propagation in the simulated high-temperature and high-salinity oil reservoirs, the apparent viscosity of the HPAM/EDAB hybrid sample is relatively stable, thus effectively improving water-to-oil mobility ratio to make more oil produced.

In spite of its poor long-term thermal stability, the 0.3% HPAM solution can still enhance oil recovery to a higher extent in the relative short period (10 hours) of oil displacement test. On the contrary, the oil recovery factor of EDAB is extremely low though it has much stronger thickening ability and much better long-term thermal stability under the simulated high-temperature and high-salinity oil reservoirs. The poor oil recovery efficiency may be attributed to the collapse of the micelles upon contacting oil, and the disassembled micelles by the shear and elongation force at the pore throats cannot be recovered when they reach the next throat. However, such a hypothesis should be further verified quantitatively in future studies.

The propagation of the different chemicals in porous media is schematically illustrated in Figure 5. In the flooding process, all the samples are subjected to shear and stretch in the pores of porous reservoir media. In this case, WLMs are destroyed and cannot form micelles in a short time (Figure 5(a)). However, HPAM molecular chains orient the flow direction and reform polymer coils after going through

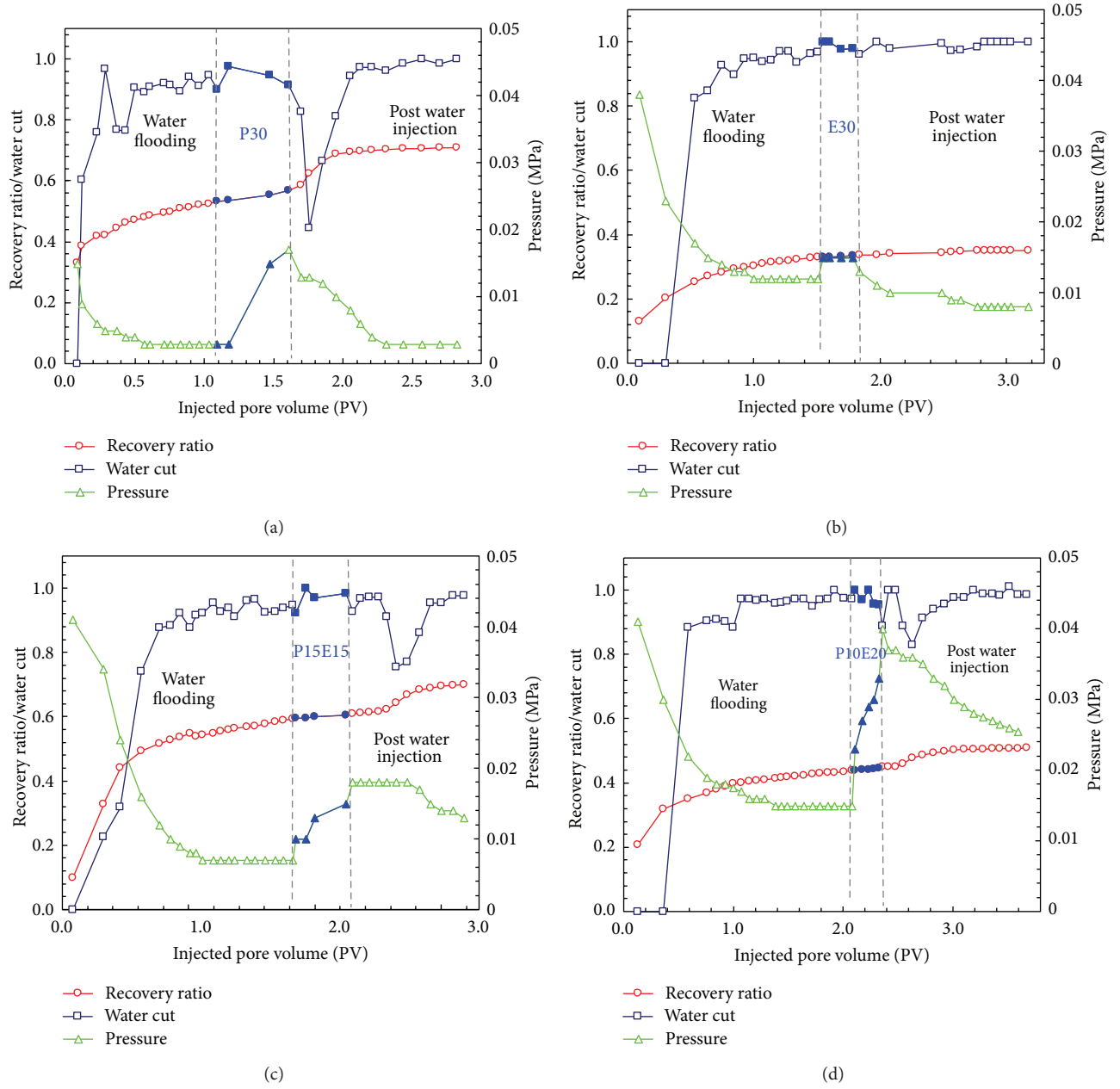

Figure 4: Recovery factor, water cut, and flooding pressure plotted as a function of injected volume of the samples: (a) P30, (b) E30, (c) P15E15, and (d) P10E20 (TDS = 32,868 mg/L, $[Ca^{2+}] + [Mg^{2+}]$ = 873 mg/L; injected volume = 30% PV; injected rate = 0.23 mL/min).

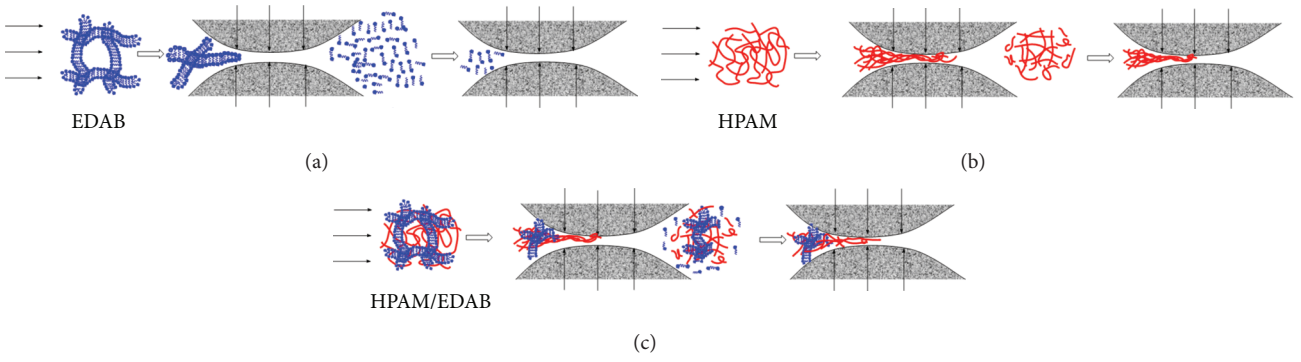

Figure 5: Schematic description of the chemical flooding processes for the samples: (a) EDAB, (b) HPAM, and (c) HPAM/EDAB hybrid.

the porous media (Figure 5(b)). For the HPAM/EDAB hybrid samples, HPAM assists WLMs in going across the pores and prevents them from being destroyed (Figure 5(c)). Therefore, the oil recovery factor of the HPAM/EDAB hybrid sample is smaller than that of HPAM, but much higher than that of EADB.

4. Conclusion Remarks

The rheological behaviors of partially hydrolyzed polyacrylamide/amidobetaine surfactant hybrid and core flooding experiments under simulated high temperature and salinity oil reservoirs conditions were preliminarily examined. It was found that the HPAM/EDAB hybrid samples (P15E15 and P10E20) exhibited improved salt tolerance and long-term thermal stability. In addition, 10.20% and 7.10% of oil recovery factors were achieved from the HPAM/EDAB hybrid samples in the laboratory core flooding test. Along with their improved salt tolerance and long-term thermal stability, these hybrid samples show great potential to enhance oil recovery from hostile oil reservoir environment. However, it is necessary to further investigate the mechanism of the HPAM/EDAB hybrid and the optimum ratio between HPAM and EDAB for economic consideration.

Acknowledgments

The authors are grateful to the financial support from Shandong Provincial government through the "Taishan Scholar" project, Science and Technology Department of Sichuan Province (2012NZ0006, 2010JQ0029), as well as Natural Science Foundation of China (21173207, 21273223), and Chinese Academy of Sciences.

References

[1] S. Thomas, "Enhanced oil recovery—an overview," *Oil & Gas Science and Technology—Revenue d'IFP Energies Nouvelles*, vol. 63, no. 1, pp. 9–19, 2008.

[2] K. S. Sorbie, *Polymer-Improved Oil Recovery*, Baca Raton, Fla, USA, 1991.

[3] J. C. Jung, K. Zhang, B. H. Chon, and H. J. Choi, "Rheology and polymer flooding characteristics of partially hydrolyzed polyacrylamide for enhanced heavy oil recovery," *Journal of Applied Polymer Science*, vol. 127, no. 6, pp. 4833–4839, 2013.

[4] Q. Chen, Y. Wang, Z. Lu, and Y. Feng, "Thermoviscosifying polymer used for enhanced oil recovery: rheological behaviors and core flooding test," *Polymer Bulletin*, vol. 70, no. 2, pp. 391–401, 2013.

[5] Y. Wang, Z. Lu, Y. Han, Y. Feng, and C. Tang, "A novel thermoviscosifying water-soluble polymer for enhancing oil recovery from high-temperature and high-salinity oil reservoirs," *Advanced Materials Research*, vol. 306-307, pp. 654–657, 2011.

[6] A. Zaitoun and B. Poitie, "Limiting conditions for the use of hydrolysed polyacrylamides in brines containing divalent ions," in *Proceedings of the SPE International Oilfield and Geothermal Chemistry Symposium*, Paper SPE 11785, Denver, Colo, USA, June 1983.

[7] G. Chauveteau and K. S. Sorbie, "Mobility control by polymers," in *Basic Concepts in Enhanced Oil Recovery Process*, M. Bavière, Ed., vol. 33 of *Critical Reports on Applied Chemistry*, pp. 44–87, Elsevier, London, UK, 1991.

[8] A. Dupas, I. Hénaut, J. F. Argillier, and T. Aubry, "Mechanical degradation onset of polyethylene oxide used as a hydrosoluble model polymer for enhanced oil recovery," *Oil & Gas Science and Technology—Revenue d'IFP Energies Nouvelles*, vol. 67, no. 6, pp. 931–940, 2012.

[9] C. Noïk, P. Delaplace, and G. Müller, "Physico-chemical characterics of polyacrylamide solutions after mechanical degradation through a porous medium," in *Proceedings of the SPE International Symposium on Oilfield Chemistry*, Paper SPE 28954, San Antonio, Tex, USA, February 1995.

[10] G. Dupuis, D. Rousseau, R. Tabary, J.-F. Argillier, and B. Grassl, "Hydrophobically modified sulfonated polyacrylamides for IOR: correlations between associative behavior and injectivity in the diluted regime," *Oil & Gas Science and Technology—Revenue d'IFP Energies Nouvelles*, vol. 67, no. 6, pp. 903–920, 2012.

[11] J. Yang, "Viscoelastic wormlike micelles and their applications," *Current Opinion in Colloid & Interface Science*, vol. 7, no. 5-6, pp. 276–281, 2002.

[12] C. A. Dreiss, "Wormlike micelles: where do we stand? Recent developments, linear rheology and scattering techniques," *Soft Matter*, vol. 3, no. 8, pp. 956–970, 2007.

[13] Z. Chu, C. A. Dreiss, and Y. Feng, "Smart wormlike micelles," *Chemical Society Review*, vol. 42, pp. 7174–7203, 2013.

[14] Z. Chu, Y. Feng, X. Su, and Y. Han, "Wormlike micelles and solution properties of a C22-tailed amidosulfobetaine surfactant," *Langmuir*, vol. 26, no. 11, pp. 7783–7791, 2010.

[15] Z. Chu, Y. Feng, H. Sun et al., "Aging mechanism of unsaturated long-chain amidosulfobetaine worm fluids at high temperature," *Soft Matter*, vol. 7, no. 9, pp. 4485–4489, 2011.

[16] Z. Chu and Y. Feng, "Amidosulfobetaine surfactant gels with shear banding transitions," *Soft Matter*, vol. 6, no. 24, pp. 6065–6067, 2010.

[17] Z. Chu and Y. Feng, "A facile route towards the preparation of ultra-long-chain amidosulfobetaine surfactants," *Synlett*, no. 16, pp. 2655–2658, 2009.

[18] D. Feng, Y. Zhang, Q. Chen, J. Wang, B. Li, and Y. Feng, "Synthesis and surface activities of amidobetaine surfactants with ultra-long unsaturated hydrophobic chains," *Journal of Surfactants and Detergents*, vol. 15, no. 5, pp. 657–661, 2012.

[19] Z. Chu and Y. Feng, "Empirical correlations between Krafft temperature and tail length for amidosulfobetaine surfactants in the presence of inorganic salt," *Langmuir*, vol. 28, no. 2, pp. 1175–1181, 2012.

[20] Y. Han, Y. Feng, H. Sun, Z. Li, Y. Han, and H. Wang, "Wormlike micelles formed by sodium erucate in the presence of a tetraalkylammonium hydrotrope," *The Journal of Physical Chemistry B*, vol. 115, no. 21, pp. 6893–6902, 2011.

[21] Y. Han, Z. Chu, H. Sun, Z. Li, and Y. Feng, "'Green' anionic wormlike micelles induced by choline," *RSC Advances*, vol. 2, no. 8, pp. 3396–3402, 2012.

[22] J. Wang, J. Wang, B. Wang, S. Guo, and Y. Feng, "Synthesis and aqueous solution properties of polyoxyethylene surfactants with ultra-long unsaturated hydrophobic chains," *Journal of Dispersion Science and Technology*, vol. 34, no. 4, pp. 504–510, 2013.

[23] H. Wang, X. Cao, J. Zhang, and A. Zhang, "Development and application of dilute surfactant-polymer flooding system for Shengli oilfield," *Journal of Petroleum Science and Engineering*, vol. 65, no. 1-2, pp. 45–50, 2009.

[24] H. K. Kotlar, O. Selle, and O. Torsaeter, "Enhanced oil recovery by COMB-flow: polymer floods revitalized," in *Proceedings of the SPE International Symposium on Oilfield Chemistry*, Paper SPE 106421, pp. 540–545, Houston, Tex, USA, February-March 2007.

[25] J. L. Cayias, M. E. Hayes, R. S. Schechter, and W. H. Wade, "Surfactant aging—possible detriment to the tertiary oil recovery," *Journal of Petroleum Technology*, vol. 28, pp. 985–988, 1976.

Hindawi Publishing Corporation
Journal of Chemistry
Volume 2013, Article ID 370543, 4 pages
http://dx.doi.org/10.1155/2013/370543

Research Article

Evaluation and Injection Parameter Optimization for Polymer Flooding with Different Kinds of Profile Control Agents

Yikun Liu,[1] Qingjun Deng,[1,2] Gang Chen,[2] Shuang Liang,[1] and Lingyun Chen[1]

[1] *Northeast Petroleum University, Daqing, Heilongjiang 163318, China*
[2] *Daqing Oilfield Limited Company, Daqing, Heilongjiang 163000, China*

Correspondence should be addressed to Gang Chen; 43973502@qq.com

Received 5 April 2013; Revised 26 June 2013; Accepted 1 August 2013

Academic Editor: Baojun Bai

Injecting profile control agent (PCA) into deep reservoir can decrease the inefficient circulation of injected water effectively, which is critical to improve polymer flooding in heterogeneous reservoir. Polymer flooding contrast experiments were carried out with three PCAs, respectively; the influence of different injection times on recovery is analyzed, and the best injection rate of PCA is determined. The result shows that the effect of compound ion PCA, anionic delay-action cross-linking PCA, and luminum citrate cross-linking PCA gets worse in turn. The effect of injecting PCA before polymer flooding is better than that of injecting it during and after the procedure. As the PCA rate increases, the recovery increment raises, but the increasing ranges decrease. The best rate of PCA is 0.10PV, considering technical and economic effects.

1. Introduction

To reduce the inefficient circulation of injected water in the formation, reduce production cost, and improve oilfield development, the effect of profile control on improving polymer flooding development has been explored since 1996 when polymer flooding began to be applied on largescale [1, 2]. But the research on contrast, application condition, and the best injection time and injection rate optimization for different PCAs is still in an exploratory stage [3–5].

From research before, we can know some information about these PCAs. Compound ion PCA [6] is a kind of compound ion cross-linker system made up with compound ion polymer, cross-linker, and assistant with certain proportion. It performs well in injection and gelation and has certain shear resistance, thus it can have an effect in profile control. Anionic delay-action cross-linking PCA uses anionic polymer as cross-linker. It has notable elasticity, large absorption, high residual resistance factor, and obvious profile control effect. Aluminum citrate cross-linking PCA [7] does not contain sulfate radical, nitrate radical, and metallic iron, whose mass fraction for aluminum ions is more than 4.17%. In some ranges of polymer concentration, aluminum citrate cross-linking system (HPAM) can form polymer jelly with high strength.

2. Experiment

2.1. Experimental Conditions. Quartz sand epoxy cementation artificial cores and three cores in parallel connection with positive rhythm are used, whose water phase permeability is 0.2 μm^2, 0.5 μm^2, and 0.8 μm^2 and core size is 30 cm × 4.5 cm × 4.5 cm. The viscosity of oil in experiment is 10 mPa·s (45°C). The water is drained after filtration. The polymer is APAM, whose relative molecular mass is 13 million. The PCAs are, respectively, compound ion PCA, anionic delay-action cross-linking PCA, and aluminum citrate cross-linking PCA.

2.2. Experimental Program

2.2.1. Basic Flooding Experiment. (a) Saturated with oil, water flooding until 98% water cut + 0.69PV 1500 mg/L polymer with medium molecular weight + subsequent water flooding until 98% water cut; (b) saturated with oil, water flooding until 98% water cut + 0.74PV 1500 mg/L polymer with medium molecular weight + subsequent water flooding until

Table 1: Result of basic polymer flooding experiment.

Injected slug	Water phase permeability (10^{-3} μm^2)	Porosity (%)	Oil saturation (%)	Water flooding recovery (%)	Polymer flooding EOR (%)
0.69PV	512	24.35	73.36	45.36	13.07
0.74PV	516	24.50	73.44	45.02	13.81
0.84PV	509	24.51	73.69	45.05	14.19

98% water cut; (c) saturated with oil, water flooding until 98% water cut + 0.84PV 1500 mg/L polymer with medium molecular weight + subsequent water flooding until 98% water cut.

2.2.2. Profile Control Experiment before Polymer Flooding. (a) Saturated with oil, water flooding until 98% water cut + 0.05PV PCA + 0.64PV 1500 mg/L polymer with medium molecular weight + subsequent water flooding until 98% water cut; (b) saturated with oil, water flooding until 98% water cut + 0.10PV PCA + 0.64PV 1500 mg/L polymer with medium molecular weight + subsequent water flooding until 98% water cut; (c) saturated with oil, water flooding until 98% water cut + 0.20PV PCA + 0.64PV 1500 mg/L polymer with medium molecular weight + subsequent water flooding until 98% water cut.

2.2.3. Profile Control Experiment in the Middle of Polymer Flooding. (a) Saturated with oil, water flooding until 98% water cut + 0.10PV 1500 mg/L polymer with medium molecular weight + 0.05PV PCA + 0.54PV 1500 mg/L polymer with medium molecular weight + subsequent water flooding until 98% water cut; (b) saturated with oil, water flooding until 98% water cut + 0.10PV 1500 mg/L polymer with medium molecular weight + 0.10PV PCA + 0.54PV 1500 mg/L polymer with medium molecular weight + subsequent water flooding until 98% water cut; (c) saturated with oil, water flooding until 98% water cut + 0.10PV 1500 mg/L polymer with medium molecular weight + 0.20PV PCA + 0.54PV 1500 mg/L polymer with medium molecular weight + subsequent water flooding until 98% water cut.

2.2.4. Profile Control Experiment After Polymer Flooding. (a) Saturated with oil, water flooding until 98% water cut + 0.64PV 1500 mg/L polymer with medium molecular weight + 0.05PV PCA + subsequent water flooding until 98% water cut; (b) saturated with oil, water flooding until 98% water cut + 0.64PV 1500 mg/L polymer with medium molecular weight + 0.10PV PCA + subsequent water flooding until 98% water cut; (c) saturated with oil, water flooding until 98% water cut + 0.64PV 1500 mg/L polymer with medium molecular weight + 0.20PV PCA + subsequent water flooding until 98% water cut.

3. Results Analysis

3.1. Effect of Basic Polymer Flooding. From Table 1, we can see that the extent of polymer flooding EOR increases with the increase of polymer quantity.

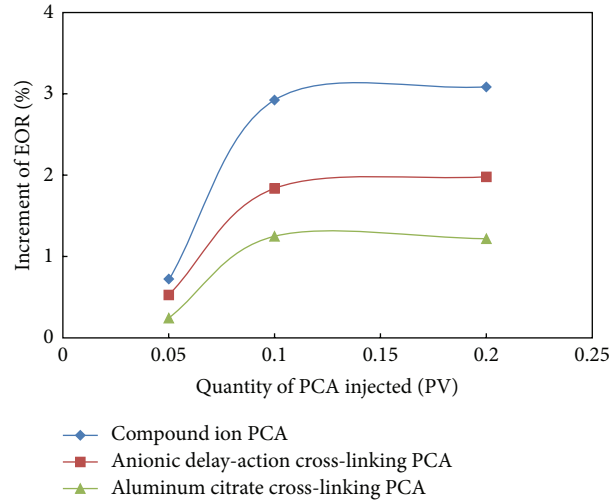

Figure 1: The relation between injected PV of PCA and recovery increment before polymer flooding.

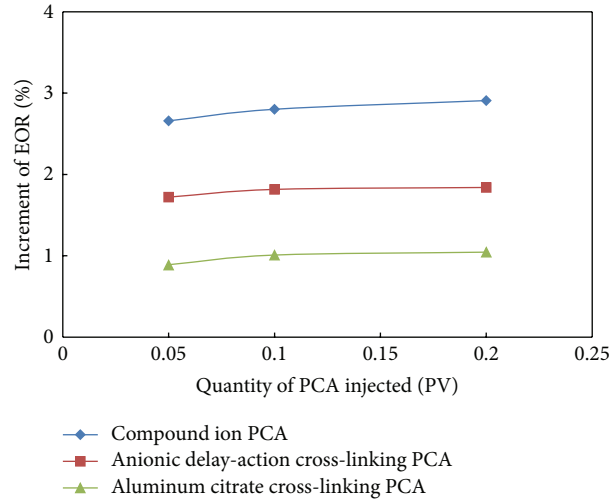

Figure 2: The relation between injected PV of PCA and recovery increment during polymer flooding.

The result of polymer flooding experiment will be the standard to contrast between displacement effects with different PCAs, different injection times, and different injection rates.

3.2. Result of Polymer Flooding with PCA. From Figures 1, 2, and 3, we can see that compound ion PCA, anionic delay-action cross-linking PCA, and aluminum citrate cross-linking PCA get worse in sequence and the effect of injecting

Table 2: Prediction on output increment and economic benefit analysis for different PCA flooding.

PCA types	Injection time	Injection rate (PV)	EOR (%)	Output increment prediction $(cm)^3$	Output ($\times 10^6$ RMB)	Input ($\times 10^6$ RMB)	Input/output ratio
Compound ion PCA	Before	0.05	0.67	0.49	759.5	320.35	1 : 2.37
		0.10	2.91	2.14	3317	640.7	1 : 5.18
		0.20	3.09	2.27	3518.5	1281.4	1 : 2.75
	Middle	0.10	2.87	2.11	3270.5	640.7	1 : 5.10
	After	0.05	0.46	0.34	527	320.35	1 : 1.65
		0.10	2.03	1.49	2309.5	640.7	1 : 3.60
		0.20	2.58	1.90	2945	1281.4	1 : 2.30
Anionic delay-action cross-linking PCA	Before	0.05	0.49	0.36	558	255.35	1 : 2.19
		0.10	1.83	1.35	2092.5	510.7	1 : 4.10
		0.20	1.95	1.43	2216.5	1021.4	1 : 2.17
	Middle	0.10	1.62	1.19	1844.5	510.7	1 : 3.61
	After	0.05	0.18	0.13	201.5	255.35	1 : 0.79
		0.10	1.76	1.29	1999.5	510.7	1 : 3.92
		0.20	1.70	1.25	1937.5	1021.4	1 : 1.90
Aluminum citrate cross-linking PCA	Before	0.05	0.24	0.18	279	155.35	1 : 1.80
		0.10	1.24	0.91	1410.5	310.7	1 : 4.54
		0.20	1.26	0.93	1441.5	621.4	1 : 2.32
	Middle	0.10	1.40	1.03	1596.5	310.7	1 : 5.14
	After	0.05	0.11	0.08	124	155.35	1 : 0.80
		0.10	0.45	0.33	511.5	310.7	1 : 1.65
		0.20	0.90	0.66	1023	621.4	1 : 1.65

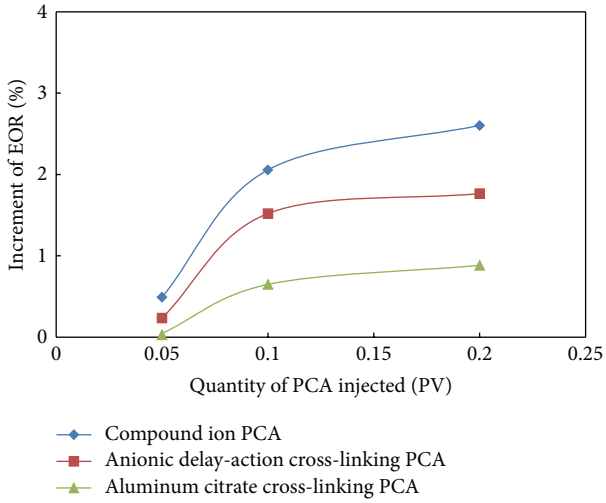

Figure 3: The relation between injected PV of PCA and recovery increment after polymer flooding.

PCA before polymer flooding is better than that of injecting it during and after the procedure. As PCA injection increases, recovery increment increases as well, but the increment gets smaller when PCA quantity is greater than 0.1PV.

3.3. Economic Benefit Analysis. From Table 2, we can see that when crude oil output price is 2,000 Yuan/ton and the cost is 450 Yuan/ton, the best injection rate of PCA is 0.10PV, when the input/output ratio reaches a maximum.

4. Conclusions

The effect of compound ion PCA, anionic delay-action cross-linking PCA, and aluminum citrate cross-linking PCA gets worse in sequence, and the effect of injecting PCA before polymer flooding is better than that of injecting it during and after the procedure. The best injection rate of PCA is 0.10PV, when input/output ratio reaches a maximum. The increment of EOR gets smaller when PCA quantity is bigger than 0.10PV. Thus, it is important to further analyze the effect of different PCAs, and the best injection time and quantity upon the establishment and application of PCA injecting scheme in situation.

Acknowledgments

This work is financially supported by National Natural Science Foundation of China (51074035) and Major Projects of National Science and Technology of China (2011ZX05010-002-05 and 2011ZX05052-12).

References

[1] Z. Sun, Y. Zheng, M. Li, M. Lin, and Z. Wu, "Study on mechanism of plugging porous media of linked polymer solution,"

Polymeric Materials Science & Engineering, vol. 21, no. 2, pp. 225–228, 2005.

[2] L. He, W. Xin, and L. Guo, "Enhanced oil recovery technology continually after polymer-flooding," in *Proceedings of the SPE Enhanced Oil Recovery Conference (EORC '11)*, 144250, Kuala Lumpur, Malaysia, July 2011.

[3] Q. You, Y. Tang, and C. Dai, "Research on a new profile control agent: dispersed particle gel," in *Proceedings of the SPE Enhanced Oil Recovery Conference (EORC '11)*, 143514, Kuala Lumpur, Malaysia, July 2011.

[4] M.-Y. Li, M.-Q. Lin, X.-Y. Zheng, and Z.-L. Wu, "Linked polymer solution as in-depth permeability control agent: laboratory study and field test," *Oilfield Chemistry*, vol. 17, no. 2, pp. 144–147, 2000.

[5] K. Wang, Y. Ding, Y. Yan et al., "Physical simulation of oil displacement effect by using ASP composite PCA," *Northeast Petroleum University Press*, vol. 29, no. 1, pp. 31–32, 2005.

[6] Z. Yue, "Aluminum citrate crosslinker preparation and research on its crosslinking system," *Special Oil & Gas Reservoirs*, vol. 15, no. 1, 2008.

[7] B. Wu, "Laboratory research on water plugging and control for exploiting potentialities in injection and production wells," *Oil Drilling & Production Technology*, vol. 34, no. 3, 2012.

Hindawi Publishing Corporation
Journal of Chemistry
Volume 2013, Article ID 938237, 8 pages
http://dx.doi.org/10.1155/2013/938237

Research Article

Influence of Oil Viscosity on Alkaline Flooding for Enhanced Heavy Oil Recovery

Yong Du,[1,2] Guicai Zhang,[1] Jijiang Ge,[1] Guanghui Li,[1] and Anzhou Feng[3]

[1] *College of Petroleum Engineering, China University of Petroleum, Qingdao 266555, China*
[2] *Zhuangxi Oil Production Plant, Shengli Oilfield, Sinopec, Dongying 257237, China*
[3] *Xinchun Production Plant, Shengli Oilfield, Sinopec, China*

Correspondence should be addressed to Jijiang Ge; gejijiang@163.com

Received 21 March 2013; Accepted 25 June 2013

Academic Editor: Ibnelwaleed Ali Hussien

Oil viscosity was studied as an important factor for alkaline flooding based on the mechanism of "water drops" flow. Alkaline flooding for two oil samples with different viscosities but similar acid numbers was compared. Besides, series flooding tests for the same oil sample were conducted at different temperatures and permeabilities. The results of flooding tests indicated that a high tertiary oil recovery could be achieved only in the low-permeability (approximately 500 mD) sandpacks for the low-viscosity heavy oil (Zhuangxi, 390 mPa·s); however, the high-viscosity heavy oil (Chenzhuang, 3450 mPa·s) performed well in both the low- and medium-permeability (approximately 1000 mD) sandpacks. In addition, the results of flooding tests for the same oil at different temperatures also indicated that the oil viscosity put a similar effect on alkaline flooding. Therefore, oil with a high-viscosity is favorable for alkaline flooding. The microscopic flooding test indicated that the water drops produced during alkaline flooding for oils with different viscosities differed significantly in their sizes, which might influence the flow behaviors and therefore the sweep efficiencies of alkaline fluids. This study provides an evidence for the feasibility of the development of high-viscosity heavy oil using alkaline flooding.

1. Introduction

Thermal methods are the primary ways to develop heavy oil reservoirs. However, severe heat losses reduce the effectiveness of thermal processes in deep or thin heavy oil reservoirs and increase the production cost. Inexpensive alkaline reagents can react with the organic acids in heavy oil and form massive amounts of surfactant *in situ* at the oil/water interface, by which the interface tension (IFT) can be reduced greatly [1–5]. In recent years, a new mechanism proposed by Ding et al. [6] has attracted the attention of researchers. He described the interfacial reaction between the oil phase and the alkaline solution in detail and proposed two stages related to the reaction during the alkaline flooding process. The first stage was the occurrence of water columns that resulted from the penetration of the alkaline solution into the crude oil. The second stage was the division of these water columns into small discontinuous water droplets due to the nonuniform enrichment of surfactants at the oil/water interface. The viscous fingering effect was significantly reduced by the presence of water drops inside the oil phase. In contrast, the water in oil (W/O) emulsion was simply a byproduct of alkaline liquid penetration rather than the basic mechanism of enhanced oil recovery (EOR) during alkaline flooding. They also observed differences of water breakthrough and alkaline breakthrough. In water flooding, after water breaks through, several connected water channels are created diagonally and little oil can be recovered by continued water flooding. Consequently, most of the oil is bypassed, due to the viscous fingering caused by the adverse mobility ratio between the oil and the water. In alkaline flooding, after alkaline breaks through, it can be seen that relatively uniform degree oil saturation is distributed over the entire model. Oil is subsequently displaced in the form of the "water drop" with little viscous fingering. Therefore, it is the "water drop" mechanism that reduces the mobility of water phase and diverts the injected alkaline solution to the unswept region of micromodel to improve the sweep efficiency.

The mechanism of "water drops" flow allowed the successful interpretation to some phenomena in alkaline flooding.

Many factors influence the performance of alkaline flooding. Arhuoma et al. [7] investigated the influence of alkaline concentration on the alkaline flooding for Alberta heavy oil through sandpack flooding tests using NaOH as the alkaline reagent. Their results indicated that the recovery initially increased with the increase of alkaline concentration; afterwards, the variation became very slight or even decreased, which suggests that an optimum concentration exists for enhancing the oil recovery. Almalik et al. [8] have studied the influence of the alkaline type and the injection mode on oil recovery. They observed that NaOH performed better than $Na_3PO_4{\cdot}12H_2O$ and KOH under identical conditions, and the continuous alkaline flooding yielded a higher recovery than when slugs were used. Previous research has been primarily focused on these dynamic injection conditions. However, a few static reservoir conditions have been also studied in some reports. Chiwetelu et al. [9] and Trujillo [10] have investigated the influence of reservoir temperature on alkaline flooding, the results showed that about 12% more oil was recovered at 65°C than at 25°C, and the IFT values were significantly greater at higher temperatures which was considered as the main reason for the change regulation.

The static conditions of heavy oil reservoirs are complicated and different with each other, which can also influence the effectiveness of alkaline flooding significantly. Among these static conditions, oil viscosity may exhibit the largest variation range in heavy oil reservoirs. However, the previous study about this aspect is insufficient to satisfy the requirement to design a good EOR plan. Therefore, the influence of oil viscosity on alkaline flooding in heavy oil reservoirs is investigated here by sandpack flooding experiments.

2. Experimental

2.1. Fluids and Chemicals. Oil samples were collected from the heavy oil reservoirs of Zhuangxi, Chenzhuang, Xia-8 and Binnan in Shengli Oilfield; their viscosities were measured by a rotary viscometer, and the viscosity-temperature properties are shown in Figure 1. The acid-number of these four oil samples were measured by potentiometric titration method, and the results are listed in Table 1. All the aqueous phase was brine that contained 0.5 wt% NaCl. Chemicals used in this study, such as NaOH and NaCl, were all analytical-grade reagents supplied by Sinopharm.

2.2. IFT Measurements. The dynamic IFT values between heavy oil and alkaline solutions were measured at 50°C using an American Texas-500 spinning drop tensiometer according to the following:

$$\sigma = 1.2336\left(\rho_w - \rho_o\right)\omega^2\left(\frac{D}{n}\right)^3, \qquad \frac{L}{D} \geq 4, \tag{1}$$

where σ is the interfacial tension (mN/m), ρ_w is the density of the water phase (g/cm^3), ρ_o is the density of the oil phase (g/cm^3), ω is the rotational velocity (rpm), D is the measured drop width (mm), L is the length of the oil drop (mm), and n is the refractive index of the water phase.

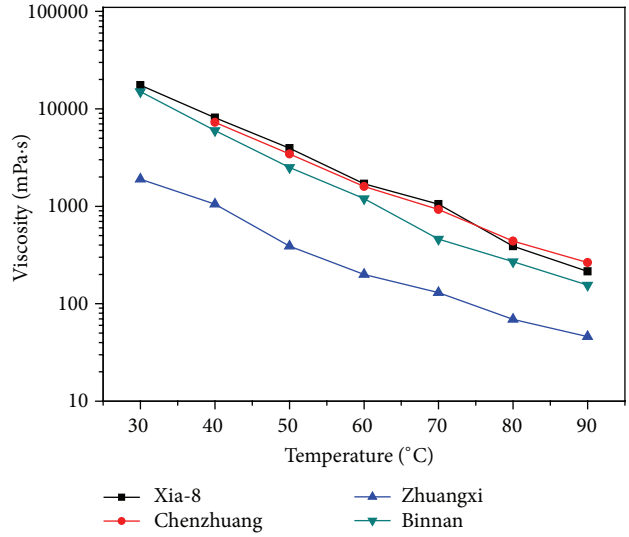

Figure 1: Viscosity-temperature curves of four types of heavy oil.

2.3. Microscopic Flooding Tests. The glass-etched micromodel was used to investigate the displacement mechanisms of alkaline flooding. The micromodel was made by the two same glass plates which were impacted tightly, and the pore throats were etched on the interface by special corrosive substances. The procedure of the microscopic flooding test was described as follows: the micromodel was first saturated with brine after being vacuumed, and it was subsequently displaced by heavy oil until no more brine was produced. The alkaline solution was then injected at a constant flow rate of 0.003 mL/min. The flooding tests can be visualized using a video recorder and camera apparatus.

2.4. Sandpack Flooding Tests. The sandpacks used in this study were 30 cm in length and 2.45 cm in diameter. They were wet-packed as follows: first, fresh quartz sand with 100–200 and 80–100 mesh sizes was blended at a weight ratio of 3 : 1. The sandpack was positioned vertically, and the sand was then added into the sandpack filled with brine water in several increments. In each step, the sand in the sandpack was shaken slightly after being added. The water surface was kept above the sand surface to avoid the intrusion of air.

The sandpack displacement was conducted at 50°C using the following procedure: first, the sandpack was saturated with brine solution, and then the permeability was measured and the porosity was calculated. Afterward, the sandpack was subsequently saturated with the heavy oil until no more water was produced (the water cut was less than approximately 1 vol%). After the oil injection, water flooding was conducted until the oil cut was less than 1 vol%, and then a chemical slug of 0.3 pore volume (PV) was injected. The injection of the chemical slug was followed by an extended period of water flooding until the oil production became negligible (oil cut

Table 1: Basic properties of four types of heavy oil.

Heavy oil	Density at 50°C (g/cm^3)	Viscosity at 50°C (mPa·s)	Acid number (mg KOH per g sample)
Zhuangxi	0.9302	390	1.85
Chenzhuang	0.9778	3450	2.02
Binnan	0.9632	2500	3.85
Xia-8	0.9712	3950	4.66

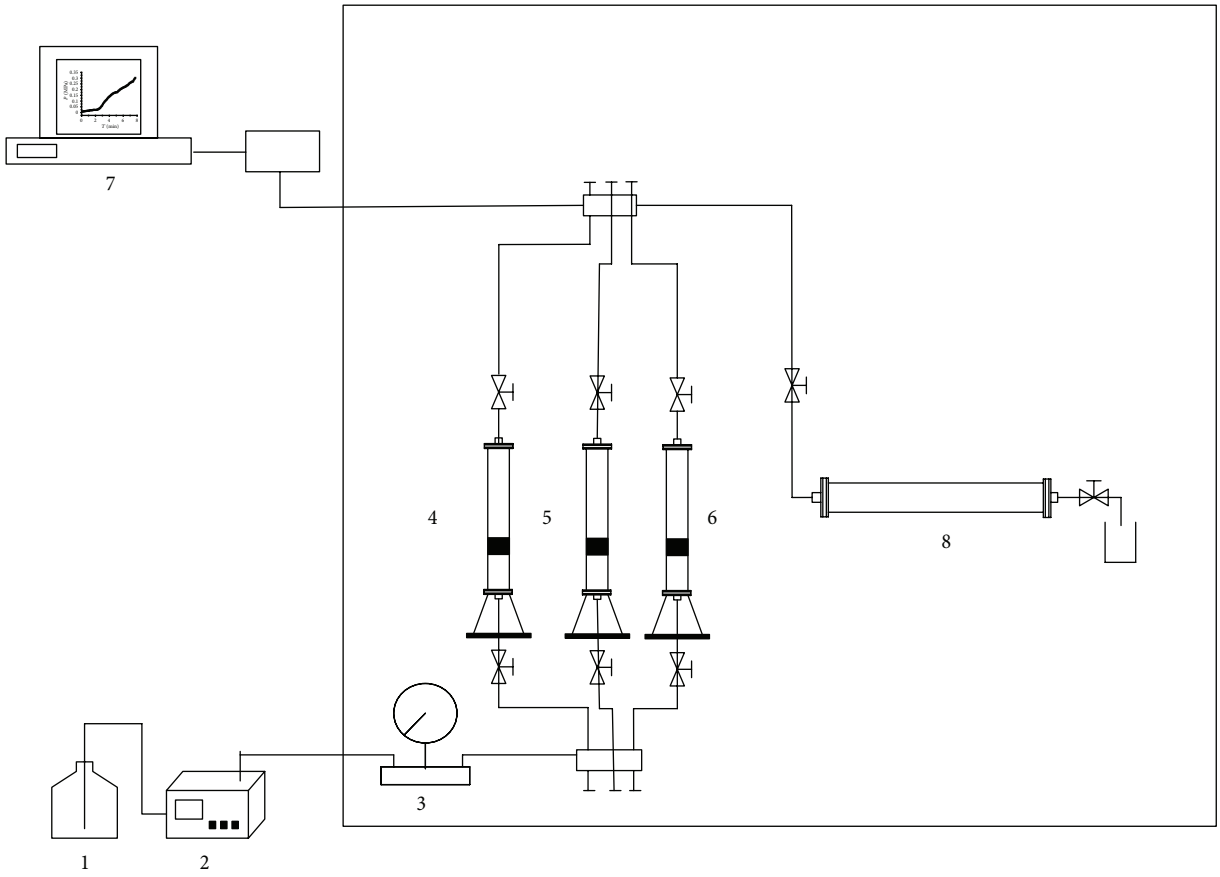

Figure 2: The equipment for sandpack flooding. 1, distilled water; 2, pump; 3, pressure meter; 4, brine water container; 5, crude oil container; 6, alkaline solution container; 7, pressure collection system; 8, Sandpack model.

< 1 vol%). The injection rate of the brine solution and the chemical slug was set at 0.5 mL/min.

The equipment for the sandpack flooding is shown in Figure 2.

3. Results and Discussion

3.1. Performance of Alkaline Flooding for Oils with Different Viscosities. To investigate the influence of oil viscosity on the performance of alkaline flooding, alkaline flooding for two oil samples with different viscosities, and similar acid numbers were compared. Then, series flooding tests for the same oil sample were conducted at different temperatures.

Zhuangxi and Chenzhuang heavy oil were selected for their similar acid numbers and different viscosities, as shown in Figure 1 and Table 1. 18 alkaline flooding tests (Runs 1 ~ 18) were conducted in sandpacks with three levels of permeability: low-permeability (approximately 500 mD), medium-permeability (approximately 1000 mD), and high-permeability (approximately 2000 mD). Three alkaline concentrations were investigated at each permeability level. The parameters of the sandpacks, the chemical formulas, and the flood results are summarized in Table 2.

The alkaline flooding performances of these two oil samples were significantly different, as shown in Figures 3 and 4. The correspondingly dynamic recovery with the production is shown in Figure 5. For the Zhuangxi heavy oil with a relative low-viscosity, the incremental oil recovery was greater than 20% when the sandpack permeability was approximately 500 mD; however, it declined significantly as the permeability increased, and the tertiary oil recovery was only 5 ~ 10% in the high-permeability sandpacks. For the Chenzhuang heavy oil, which exhibits a higher

Table 2: Summary of sandpack flooding tests for different heavy oils.

Run no.	Heavy oil	Permeability (mD)	Initial oil saturation (%)	Chemical formula	Equilibrium IFT (mN/m)	Recovery (%)		
						Water flooding	Alkaline flooding	Total
1	Zhuangxi	570	90.0	0.25% NaOH + 0.5% NaCl	0.600	29.0	22.9	51.9
2	Zhuangxi	488	82.4	0.5% NaOH + 0.5% NaCl	0.064	36.7	26.7	63.4
3	Zhuangxi	570	84.9	1% NaOH + 0.5% NaCl	0.200	23.1	29.7	52.8
4	Zhuangxi	1120	83.7	0.25% NaOH + 0.5% NaCl	0.600	36.7	7.2	43.9
5	Zhuangxi	985	88.1	0.5% NaOH + 0.5% NaCl	0.064	37.5	12.4	49.9
6	Zhuangxi	1075	84.5	1% NaOH + 0.5% NaCl	0.200	35.5	16.5	52.0
7	Zhuangxi	1875	88.0	0.25% NaOH + 0.5% NaCl	0.600	39.4	5.6	45.0
8	Zhuangxi	2080	87.4	0.5% NaOH + 0.5% NaCl	0.064	39.9	9.3	49.2
9	Zhuangxi	2125	89.5	1% NaOH + 0.5% NaCl	0.200	40.6	10.4	51.0
10	Chenzhuang	558	85.1	0.25% NaOH + 0.5% NaCl	0.122	31.8	14.7	46.5
11	Chenzhuang	577	82.6	0.5% NaOH + 0.5% NaCl	0.096	33.2	20.1	53.3
12	Chenzhuang	543	86.3	1% NaOH + 0.5% NaCl	0.180	35.3	21.3	56.6
13	Chenzhuang	1025	84.4	0.25% NaOH + 0.5% NaCl	0.122	35.8	15.3	51.1
14	Chenzhuang	1180	85.7	0.5% NaOH + 0.5% NaCl	0.096	37.3	21.4	58.7
15	Chenzhuang	1065	84.2	1% NaOH + 0.5% NaCl	0.180	37.8	23.9	61.7
16	Chenzhuang	2135	89.1	0.25% NaOH + 0.5% NaCl	0.122	40.2	8.6	48.8
17	Chenzhuang	2110	86.1	0.5% NaOH + 0.5% NaCl	0.096	39.8	12.9	52.7
18	Chenzhuang	2240	88.5	1% NaOH + 0.5% NaCl	0.180	40.2	13.5	53.7

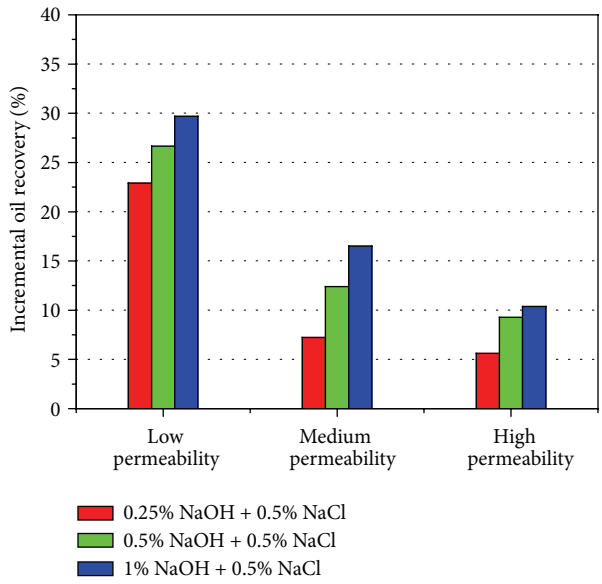

Figure 3: Alkaline flooding performance of Zhuangxi heavy oil.

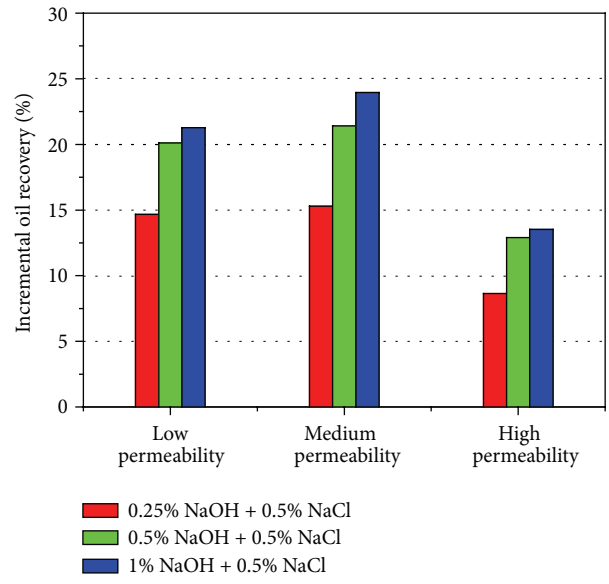

Figure 4: Alkaline flooding performance of Chenzhuang heavy oil.

viscosity, the tertiary oil recovery was as high as 20% at both low- and medium-permeabilities, but it also decreased when the permeability was approximately 2000 mD. These results demonstrate that oil with a higher viscosity exhibits a wider range of applicable permeability and that only in the low-permeability sandpacks can the low-viscosity heavy oil such as Zhuangxi oil achieve a high tertiary oil recovery.

Subsequently, temperature was changed to achieve different oil viscosities for the same oil sample. Xia-8 and Binnan heavy oil were selected for these tests, and their basic properties are also shown in Table 1.

For the Xia-8 heavy oil, the sandpack flooding tests were conducted at viscosity values of 18,235 mPa·s (30°C), 3950 mPa·s (50°C), and 1083 mPa·s (70°C). Similarly, the tests were performed at viscosity values of 15,030 mPa·s (30°C),

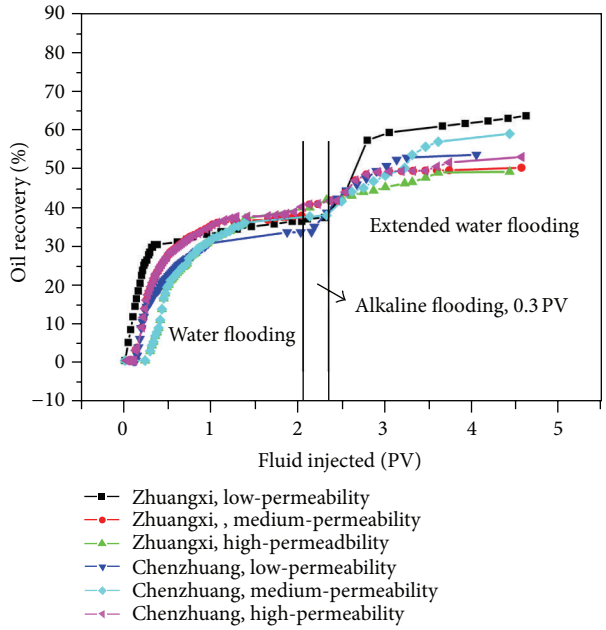

FIGURE 5: Oil recovery curves for different permeability sandpacks (alkaline concentration = 0.5 wt%).

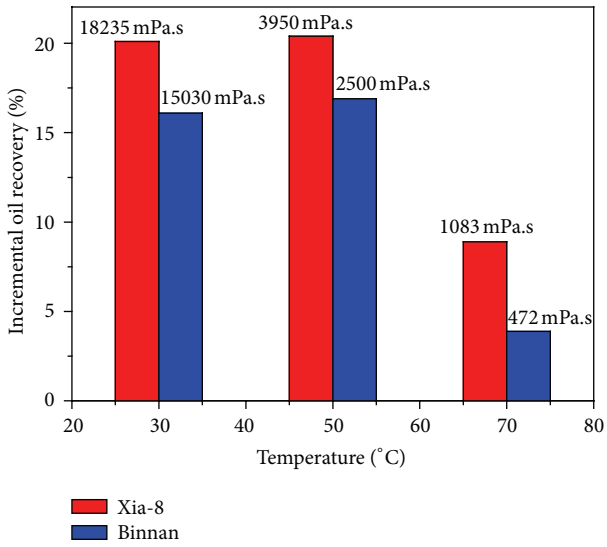

FIGURE 6: Influence of oil viscosity on the alkaline flooding efficiency.

2500 mPa·s (50°C), and 472 mPa·s (70°C) for the Binnan heavy oil. The chemical formula of 0.5% NaOH + 0.5% NaCl was used for all of the sandpack flooding tests. The test parameters and flood results are summarized in Table 3.

The incremental oil recoveries of the sandpack flooding tests are shown in Figure 6. The results lead to the conclusion that the behaviors of tertiary oil recovery for the two oil samples are similar with the variation of oil viscosity. The incremental oil recovery reached 20% at 30°C and 50°C for the oil with high-viscosity, and it declined intensively at 70°C for the oil with low-viscosity.

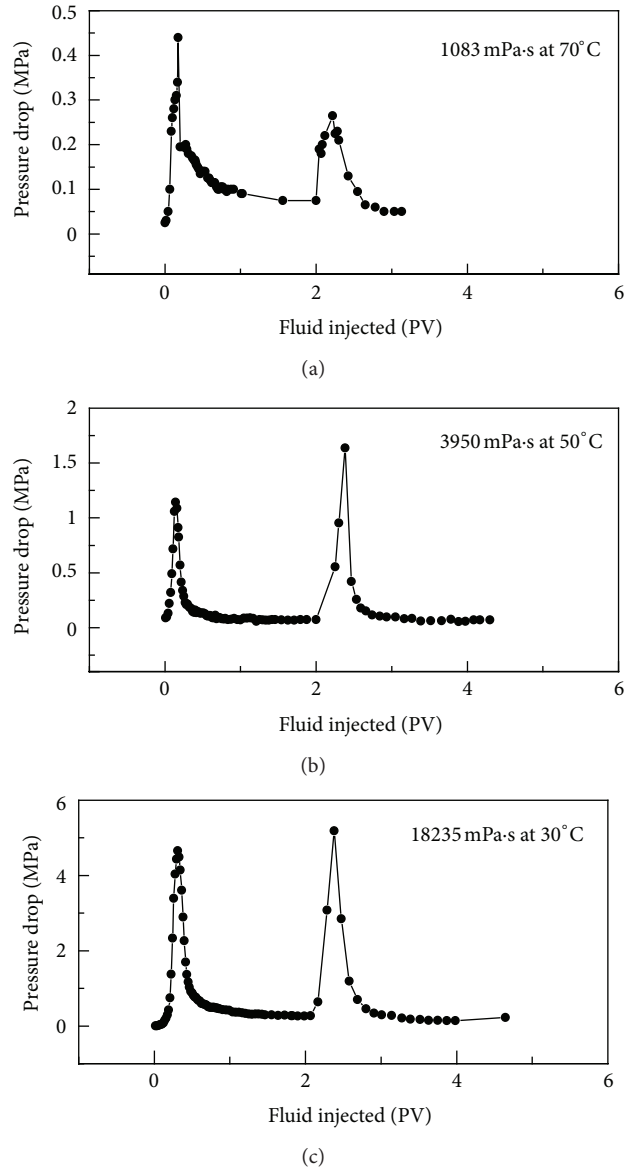

FIGURE 7: Pressure changes during alkaline flooding for Xia-8 heavy oil with different viscosities.

In Figure 7, the displacement pressure drop is plotted as a function of the injected volume. It shows that the peak pressure drop during alkaline flooding is higher than that during water flooding for the Xia-8 heavy oil, except for the oil at low-viscosity (70°C). It means that the plugging effect of water drops formed by injected alkaline solution is weakened for the low-viscosity oil sample. This result is consistent with the results of the sandpack flooding tests. Pictures of the effluent in these tests are shown in Figure 8. It can be seen that the interface of the produced fluid is clear, and the upper phase is the water drops inside the oil phase when the oil viscosity is high (30°C and 50°C). However, because the formation of water drops inside the oil phase cannot be implemented easily for the oil with low-viscosity (70°C), the alkaline solution injected into the

Table 3: Summary of sandpack flooding tests for Xia-8 and Binnan heavy oil.

Run no.	Heavy oil	Viscosity (mPa·s)	Permeability (mD)	Initial oil saturation (%)	Recovery (%)		
					Water flooding	Alkali flooding	Total
1	Xia-8	18235	1425	83.4	34.7	20.1	54.8
2	Xia-8	3950	1380	82.7	37.6	20.4	58.0
3	Xia-8	1083	1580	85.9	43.3	8.9	52.2
4	Binnan	15030	1380	82.9	37.8	16.1	53.9
5	Binnan	2500	1425	83.7	39	16.9	55.9
6	Binnan	472	1380	87.1	42.9	3.9	46.8

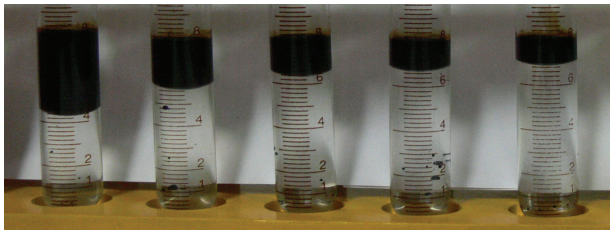

(a) 18235 mPa·s at 30°C

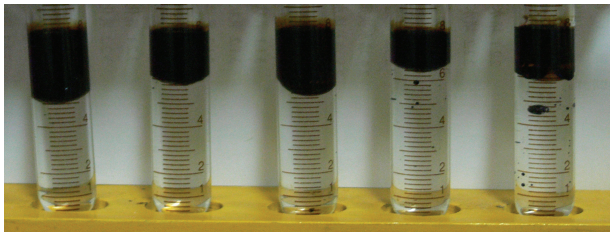

(b) 3950 mPa·s at 50°C

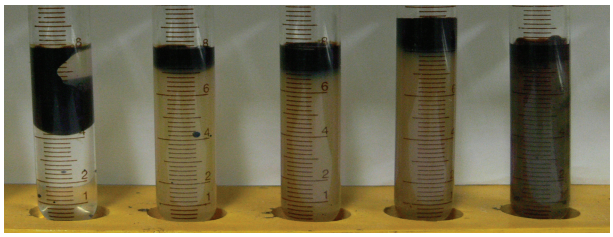

(c) 1083 mPa·s at 70°C

Figure 8: Pictures of the fluid produced during the displacement tests of Xia-8 heavy oil with different viscosities. (Effluents during alkali injection and the extended water flooding were collected in the tubes from left to right in turn. The pictures show their appearances at the end of flooding, without demulsification.)

sandpack mainly streams forward along the water channels and forms a muddy oil in water (O/W) emulsion, as shown in Figure 8(c). Consequently, heavy oil with a relative low-viscosity is unfavorable for alkaline flooding.

3.2. Mechanism of Oil Viscosity on the Performance of Alkaline Flooding. In conventional oil reservoirs, high-permeability and low oil viscosity are both favorable for development. However, the results of sandpack flooding tests indicate that this behavior is different for alkaline flooding in heavy oil reservoirs. Microscopic flooding tests were conducted to investigate the mechanism of this anomalous phenomenon, and the images intercepted from the flooding process are shown in Figure 9. It can be seen that there are a lot of water drops inside the oil phase existing in the models for both Chenzhuang and Zhuangxi heavy oils. These drops can plug the pore throats and improve the sweep efficiency for displacing phase. Compared to Chenzhuang heavy oil, the size of water drops formed in Zhuangxi heavy oil is obviously smaller, and numerous drops can exist in the same pore throat. These smaller water drops can effectively plug the small pores in the low-permeability cores, but this capacity decreases intensively in the high-permeability sandpacks. Therefore, good flooding performance could be achieved only in the low-permeability sandpacks. Figure 10 shows the pressure changes during the flooding process for the Zhuangxi heavy oil in the cores with different permeabilities. The displacement pressure increased significantly when the alkaline solution was injected into the low-permeability sandpacks; however, it changed little in the medium- and high-permeability sandpacks, which indicated that the water drops cannot plug the pores effectively.

In contrast, when the alkaline solution penetrated into the oil with a higher viscosity, that is, the Chenzhuang heavy oil shown in Figures 9(d), 9(e), and 9(f), the water drops were large, and even the throat could be occupied by only one drop. These water drops could plug the pores in both the low- and medium-permeability sandpacks and resulted in the high tertiary oil recoveries, as shown in Figure 4. In conclusion, the high-viscosity of heavy oil is favorable for the improvement of sweep efficiency in alkaline flooding.

The results of the sandpack flooding tests discussed in Section 3.1 indicated that the two oil samples could exhibit similar behaviors when these tests were conducted at different temperatures. However, the changing temperature may influence the dynamic water/oil IFT, which is very important for chemical flooding in conventional oil reservoirs. Therefore, dynamic IFT between the alkaline solutions and crude oils was measured. The results are shown in Figures 11 and 12, and little change is observed as the temperature varies. These results are inconsistent with the conclusions of Chiwetelu et al. [9] and Trujillo [10] as described in Section 1. Besides, it can be seen from Table 2 that the efficiency of alkaline flooding has little relation to the equilibrium IFT. So, we think many factors must be considered to design an alkaline flooding plan for heavy oil besides the IFT.

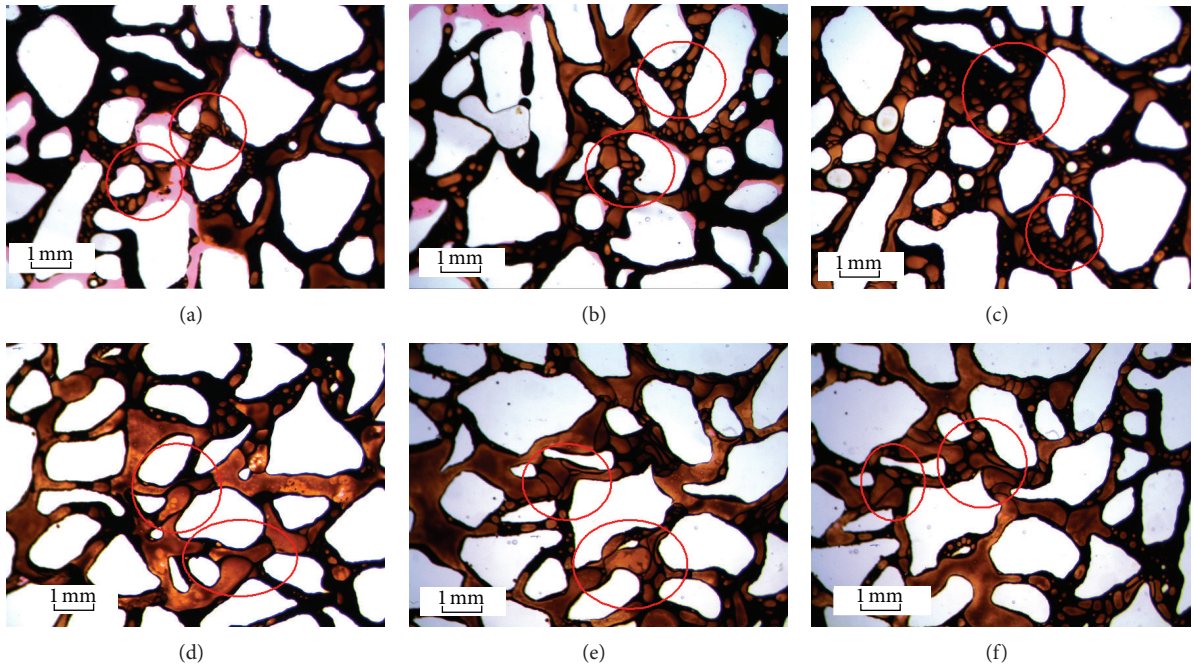

FIGURE 9: Microscopic images of alkaline flooding for different types of oil samples: (a), (b), and (c) Zhuangxi and (d), (e), and (f) Chenzhuang.

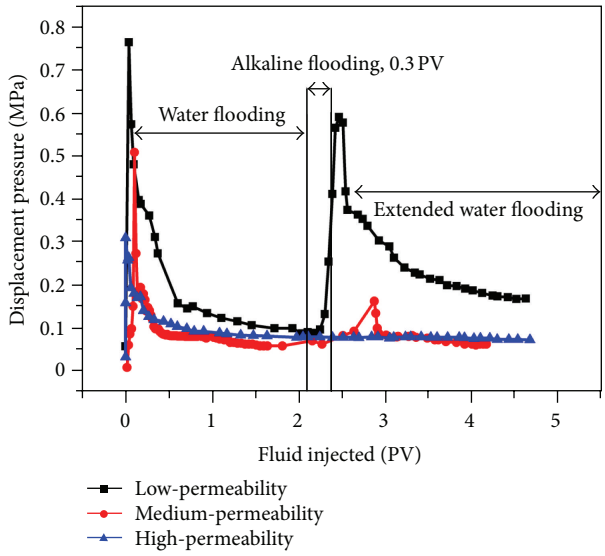

FIGURE 10: Pressure changes during alkaline flooding for Zhuangxi heavy oil (alkaline concentration = 0.5 wt%).

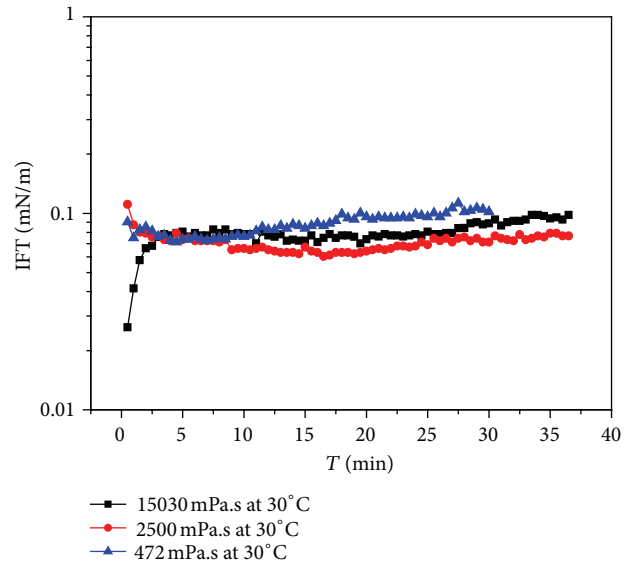

FIGURE 11: Dynamic IFT curves of Binnan heavy oil/0.5% NaOH + 0.5% NaCl.

As previously discussed, two stages occur in the water-drop formation process. The first stage is the penetration of the alkaline solution into the heavy oil and the occurrence of water columns covered with oil film. This process is related to the fast reduction in the oil/water IFT, which is difficult to measure using drop-spinning method. The second stage is the formation of discontinuous water droplets from the breakup of the water columns, which is caused by the non-uniform enrichment of *in situ* surfactant [11]. High temperature accelerates the reaction and diffusion rate between alkaline solution and heavy oil, which reduces the degree of non-uniform enrichment of *in situ* surfactant. The water columns then cannot be easily divided into small discontinuous water droplets. Therefore, the temperature militates the performance of alkaline flooding.

4. Conclusions

(1) The results of flooding tests indicated that a high tertiary oil recovery could be achieved only in the low-permeability sandpacks for the low-viscosity heavy

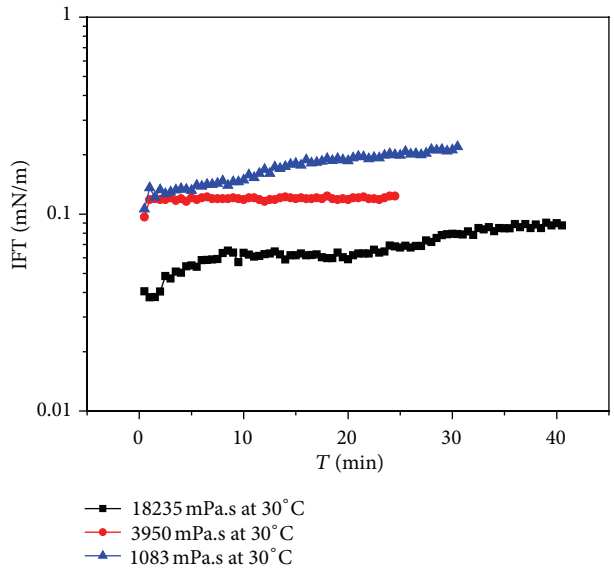

FIGURE 12: Dynamic IFT curves of Xia-8 heavy oil/0.5% NaOH + 0.5% NaCl.

oil; however, the high-viscosity heavy oil performed well in both the low- and medium-permeability sandpacks. In addition, the results of flooding tests for the same oil at different temperatures also indicated that the oil viscosity put a similar effect on alkaline flooding, and oil with a high-viscosity was favorable for alkaline flooding.

(2) Microscopic flooding tests were conducted to elucidate the influence of oil viscosity on the alkaline flooding. It indicated that the water drops produced during alkaline flooding for oils with different viscosities differed significantly in their sizes, which might influence the flow behaviors and therefore the sweep efficiencies of alkaline fluids.

Acknowledgments

Financial support from the National Natural Science Foundation of China (51104170), the National Natural Science Foundation of Shandong Province (ZR2011EEQ001), "Taishan Scholars" Construction Engineering (ts20070704), the Fok Ying Tung Education Foundation (114016), and the Research on the Displacement Mechanisms of Chemical Flooding for Water Flooding Heavy Oil from the State Key Laboratory of Heavy Oil Processing is gratefully acknowledged.

References

[1] C. E. Johnson Jr., "Status of caustic and emulsion methods," *Journal of Petroleum Technology*, vol. 28, pp. 85–92, 1976.

[2] H. Y. Jennings Jr., C. E. Johnson Jr., and C. D. McAuliffe, "Caustic waterflooding process for heavy oilscaustic waterflooding process for heavy oils," *Journal of Petroleum Technology*, vol. 26, pp. 1344–1352, 1974.

[3] C. E. Cooke Jr., R. E. Williams, and P. A. Kolodzie, "Oil recovery by alkaline waterflooding," *Journal of Petroleum Technology*, vol. 26, pp. 1365–1374, 1974.

[4] M. Dong, Q. Liu, and A. Li, "Micromodel study of the displacement mechanisms of enhanced heavy oil recovery by alkaline flooding," in *Proceedings of the International Symposium of the Society of Core Analysts*, pp. 2007–2047, Calgary; SCA, Alberta, Canada, September 2007.

[5] J. Bryan and A. Kantzas, "Enhanced heavy-oil recovery by alkali-surfactant flooding," in *Proceedings of the SPE Annual Technical Conference and Exhibition (ATCE '07)*, pp. 3642–3654, Anaheim, Calif, USA, November 2007.

[6] B. Ding, G. Zhang, J. Ge, and X. Liu, "Research on mechanisms of alkaline flooding for heavy oil," *Energy and Fuels*, vol. 24, no. 12, pp. 6346–6352, 2010.

[7] M. Arhuoma, D. Yang, M. Dong, and R. Idem, "Numerical simulation of displacement mechanisms for enhancing heavy oil recovery during alkaline flooding," in *Proceedings of the Canadian International Petroleum Conference (CIPC '09)*, pp. 2009–2053, Calgary; SPE, Alberta, Canada, June 2009.

[8] M. S. Almalik, A. M. Attia, and L. K. Jang, "Effects of alkaline flooding on the recovery of Safaniya crude oil of Saudi Arabia," *Journal of Petroleum Science and Engineering*, vol. 17, no. 3-4, pp. 367–372, 1997.

[9] C. I. Chiwetelu, G. H. Neale, V. Hornof, and A. E. George, "Recovery of a saskatchewan heavy oil using alkaline solution," *Journal of Canadian Petroleum Technology*, vol. 33, no. 4, pp. 37–42, 1994.

[10] E. M. Trujillo, "Static and dynamic interfacial tensions between crude oils and caustic solutions," *Society of Petroleum Engineers Journal*, vol. 23, no. 4, pp. 645–656, 1983.

[11] H. Pei, G. Zhang, J. Ge, L. Jin, and X. Liu, "Analysis of microscopic displacement mechanisms of alkaline flooding for enhanced heavy-oil recovery," *Energy and Fuels*, vol. 25, no. 10, pp. 4423–4429, 2011.

Hindawi Publishing Corporation
Journal of Chemistry
Volume 2013, Article ID 275943, 6 pages
http://dx.doi.org/10.1155/2013/275943

Research Article

Alkali/Surfactant/Polymer Flooding in the Daqing Oilfield Class II Reservoirs Using Associating Polymer

Ru-Sen Feng,[1,2] Yong-Jun Guo,[1,2] Xin-Min Zhang,[1,2] Jun Hu,[1,2] and Hua-Bing Li[1,2]

[1] *State Key Laboratory of Oil and Gas Reservoirs Geology and Exploration, Southwest Petroleum University, Chengdu, Sichuan 610500, China*
[2] *School of Chemistry and Chemical Engineering of Southwest Petroleum University, Chengdu, Sichuan 610500, China*

Correspondence should be addressed to Ru-Sen Feng; gs_frs@163.com and Yong-Jun Guo; gyfzgyj@126.com

Received 4 April 2013; Accepted 20 June 2013

Academic Editor: Ibnelwaleed Ali Hussien

Hydrophobically modified associating polyacrylamide (HAPAM) has good compatibility with the Daqing heavy alkylbenzene sulfonate surfactant. The HAPAM alkali/surfactant/polymer (ASP) system can generate ultralow interfacial tension in a wide range of alkali/surfactant concentrations and maintain stable viscosity and interfacial tension for 120 days. The HAPAM ASP system has good injectivity for the Daqing class II reservoirs ($100–300 \times 10^{-3}$ μm^2) and can improve oil recovery by more than 25% on top of water flooding. In the presence of both the alkali and the surfactant, the surfactant interacts with the associating groups of the polymer to form more micelles, which can significantly enhance the viscosity of the ASP system. Compared with using HPAM (Mw = 2.5 MDa), using HAPAM can reduce the polymer use by more than 40%.

1. Introduction

ASP flooding is the chemical flooding method that gives the highest oil recovery rate [1–5]. Despite the controversies on its technical and economic feasibilities [6, 7], pilot on-site experiments and examination of its industrial application are continuously carried out [8–12]. The technical issues of ASP flooding mainly include (1) formation damage due to the use of strong base, (2) scale buildup in the injection and production equipment, and (3) difficulties in processing the produced fluid [13–15]. In addition, compared with the already industrialized polymer flooding technology, ASP flooding is considerably more costly [10], mainly because the used polymer has poor resistance against alkali. Currently, new trends in ASP flooding include (1) the use of alkali-resistant polymer to reduce costs [16]; (2) developing weak-alkali ASP flooding system to alleviate problems associated with using strong base [17]; (3) developing ASP flooding system suitable for reservoirs with low/medium permeability. Field test indicated that hydrophobically modified associating polyacrylamide (HAPAM) can be a suitable flooding agent for high-temperature high-salinity reservoirs due to its excellent characteristics in temperature, salt, and shear resistance and so forth, [18]. Nevertheless, the ASP flooding system based on HAPAM has not been reported yet. This paper describes the latest research progress on using strongly basic ASP flooding system consisting of the HAPAM associating polymer at the Daqing Class II reservoirs ($100–300 \times 10^{-3}$ μm^2).

2. Experimental

2.1. Materials. HAPAM (Figure 1) was synthesized according to the literature [19] using 0.5% mol/mol cetyl dimethylallyl ammonium chloride (C_{16}DMAAC) as the hydrophobic monomer. The synthesized HAPAM has an intrinsic viscosity of 1388 mL/g and a hydrolysis degree of 24.5% (w/w).

HPAM (average molecular mass, 25,000 kDa; hydrolysis degree, 21.6% w/w) was provided by Daqing Refining and Chemical Company. C_{16}DMAAC was supplied by Southwest Petroleum University. Other reagents were purchased from Chengdu Kelong Chemical Reagents Corporation (China). All reagents were used as received without further purification. Heavy alkylbenzene sulfonate and the crude oil (ρ = 0.85 g/cm^3) were obtained from the Daqing oilfield.

To simulate the injected water in the pilot test, inorganic salts were added to distilled water and the solution was used

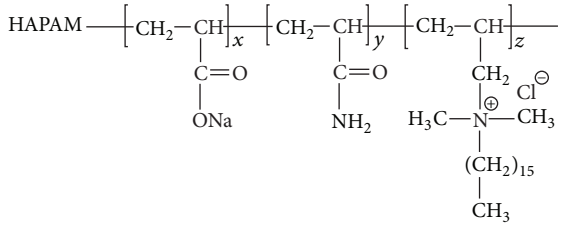

Figure 1: The structure of HAPAM.

Table 1: Composition of the simulated injection water.

Ion style	Ion concentration (mg L^{-1})
K^+ and Na^+	1044.87
Ca^{2+}	56.51
Mg^{2+}	24.90
HCO_3^-	2351.91
SO_4^{2-}	148.12
Cl^-	256.46
Total dissolved substance (TDS)	3882.77

in the subsequent experiments. The composition and salinity of the simulated injection water are given in Table 1. No precipitate was present in any formation water.

2.2. Solution Preparation. The stock solution of the surfactant or polymer (5000 mg/L) was prepared by dissolving the surfactant or polymer in brine. The ASP dilute solution was prepared by mixing the stock solutions to obtain the desired surfactant and polymer concentrations.

2.3. Measurement of Oil/Water Interfacial Tension. The oil/water interfacial tension between the solution and crude oil was measured using a Texas-500C spinning drop tensiometer (Bowing, USA) for 30 min at 45°C. The instrument could automatically record the interfacial tension with an image monitoring device and an image acquisition software.

2.4. Measurement of Viscosity. Solution viscosity was measured using a Brookfield DV-III viscometer (Brookfield, USA) at 45°C with a shear rate of 7.34 s^{-1}.

2.5. Injectivity Test. The cores saturated with brine were inserted into three core holders connected in series, each having a test point. The flooding solutions were injected into the cores at a constant rate of 1.0 mL/min until the pressure stabilized. Subsequently, brine was injected into the cores that had absorbed the polymer and the surfactant, and the experiment was finished when the pressure drop stabilized across the cores. All tests were run at 45°C. The pressures were recorded by a data terminal.

2.6. Core Flooding Test. Crude oil was injected continuously with a positive-displacement pump and an air bath held at 45°C until no more water was produced. Water flooding was then started until initial oil saturation was reached. Afterwards, chemical flooding was carried out by injecting a 0.3 PV displacement plug and then flooding with chase water

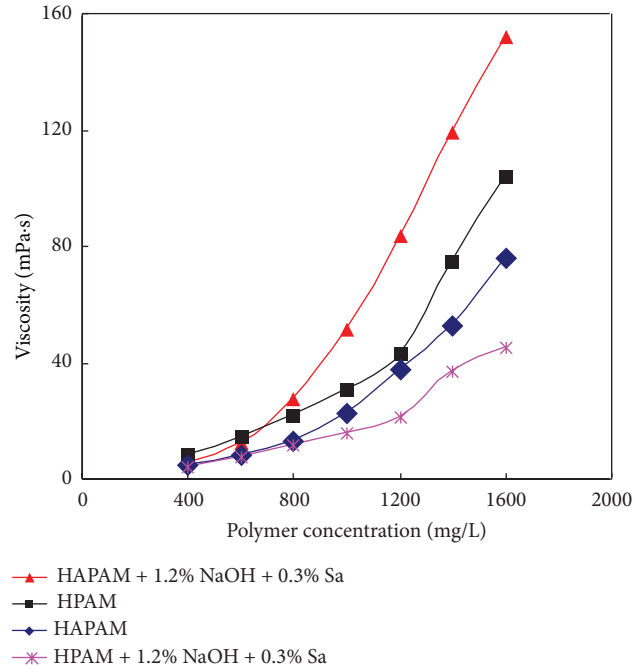

Figure 2: Viscosity-concentration curves of four flooding systems.

until the water cut of the produced fluid approached 98%. The oil recoveries and water cuts were calculated every 0.15 PV during the experiment.

3. Results and Discussion

3.1. Viscosity Enhancement. Figure 2 shows that, in the presence of alkali and surfactant, the HAPAM ASP flooding system has significantly better viscosity than using HPAM (Mw = 2.5 MDa) and can reduce the polymer use by more than 40%.

3.2. Compatibility between the Associating Polymer and the Surfactant. Figures 3 and 4 show the interfacial tension of the ASP systems containing HAPAM and HPAM, respectively.

The experimental comparison of the dynamic interfacial tension of the two ASP flooding systems is shown in Figure 5.

The results in Figures 3 and 4 indicate that the associating polymer HAPAM has better compatibility with heavy alkylbenzene sulfonate than HPAM and can enable ultralow interfacial tension in a wide alkali/surfactant concentration range. Figure 5 shows that HAPAM can quickly generate ultralow interfacial tension with heavy alkylbenzene sulfonate and remain stable for 120 min.

3.3. Aging Stability of HAPAM ASP Flooding System. Figure 6 shows that, within an aging period of 120 days, the viscosity of the HAPAM ASP system was always greater than 40 mPa·s and the interfacial tension remained stable.

3.4. Conductivity in Porous Media. The injectivity and conductivity of the sample were evaluated by the core flow experiment using three cores connected in series. The water

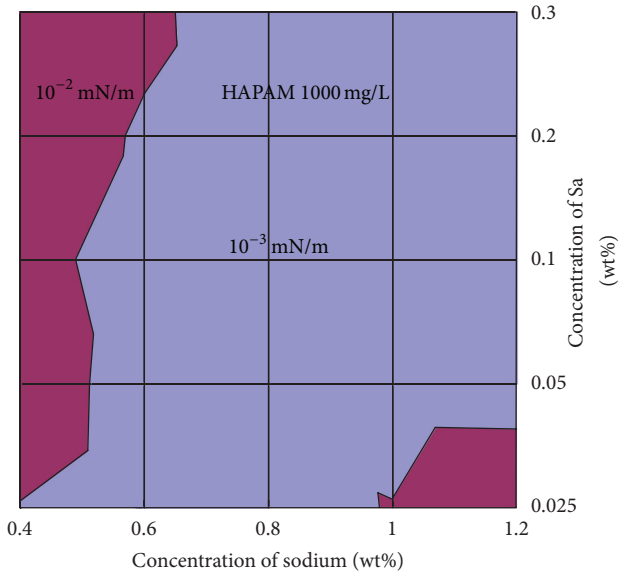

Figure 3: Interfacial tension of the ASP flooding system containing HAPAM.

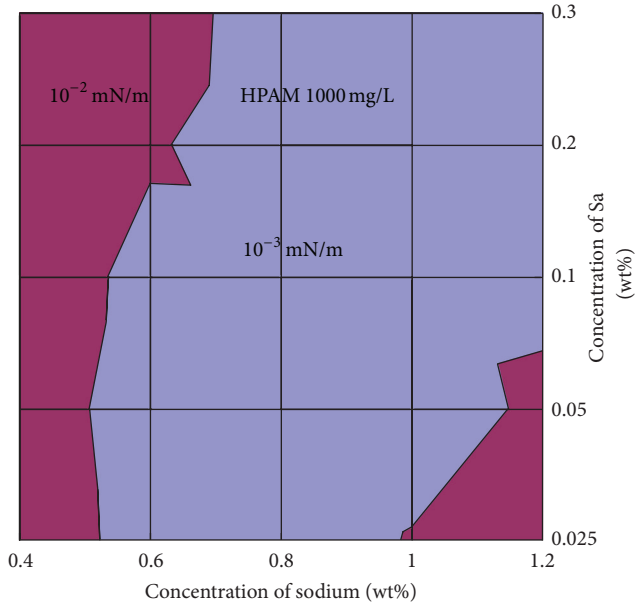

Figure 4: Interfacial tension of the ASP flooding system containing HPAM.

permeability of the three cores was 249 × 10^{-3} μm^2, 270 × 10^{-3} μm^2, and 256×10^{-3} μm^2, respectively, the concentration of the associating polymer was 1000 mg/L, the surfactant concentration was 0.3%, and the NaOH concentration was 1.2%.

Figure 7 shows that the HAPAM ASP system can penetrate into the 200 × 10^{-3} μm^2 core. The pressure gradient between the measurement points is relatively uniform, which suggests good pressure-conduction performance.

3.5. Core Flooding Experiment. Core flooding experiment was carried out using the HAPAM ASP system (1000 mg/L

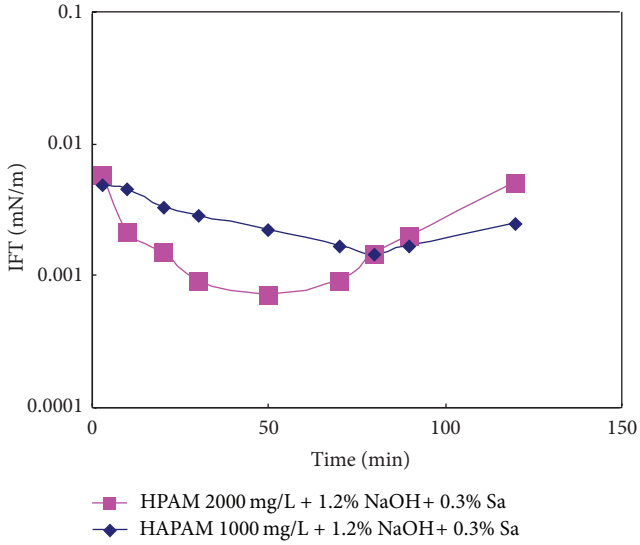

Figure 5: Dynamic interfacial tension of the two ASP systems.

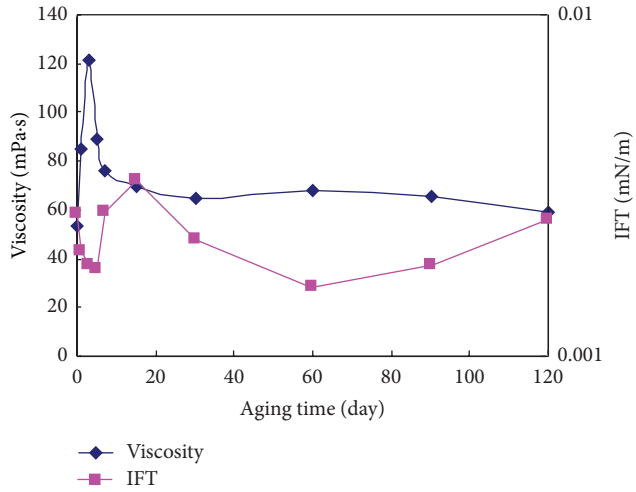

Figure 6: Variation of viscosity and interfacial tension with time.

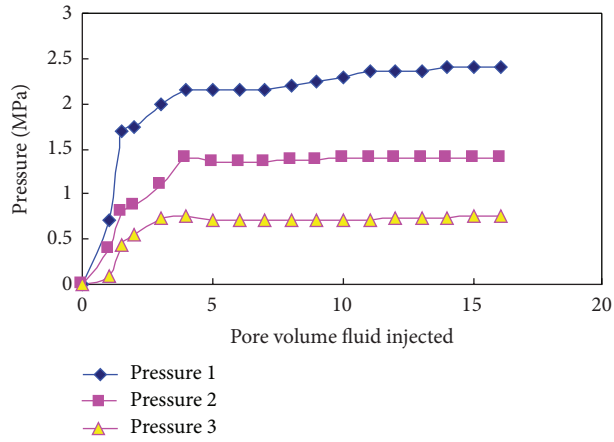

Figure 7: Conductivity of the HAPAM ASP flooding system in porous medium.

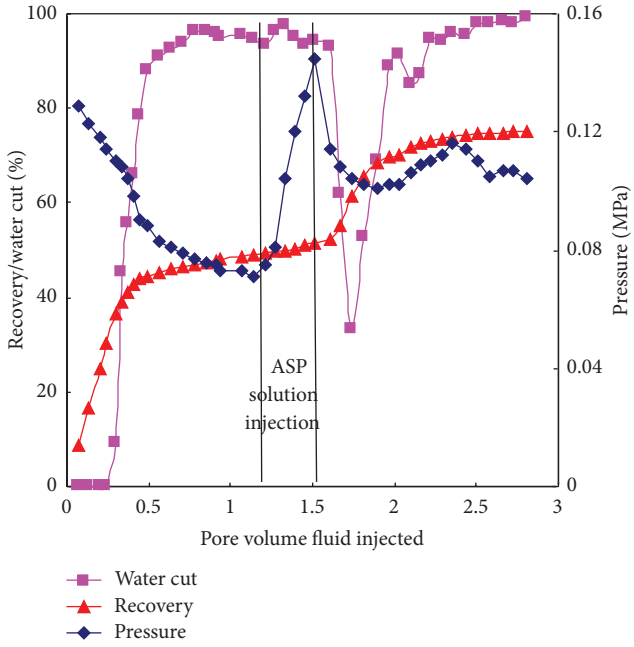

Figure 8: Flooding curve of the ASP flooding system.

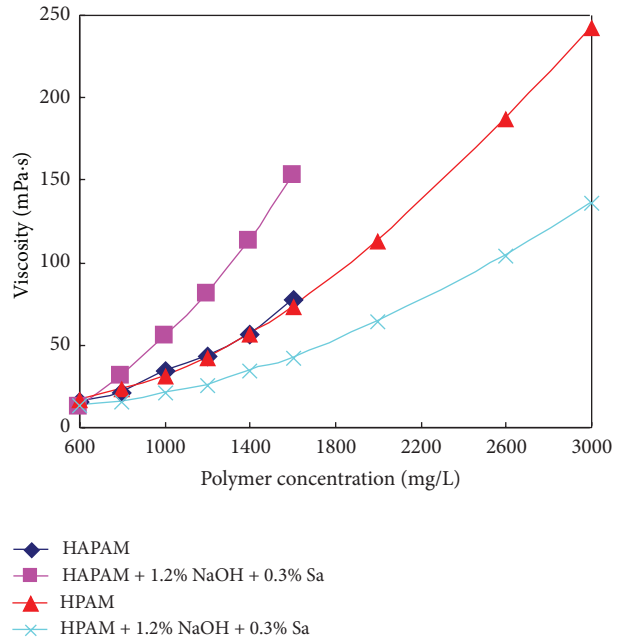

Figure 9: Viscosity-concentration curves of four flooding systems (in on-site injection water).

associating polymer HAPAM + 1.2% NaOH + 0.3% heavy alkylbenzene sulfonate) and 30 cm homogeneous square cores ($184 \times 0^{-3}\ \mu m^2$). The experimental results are shown in Figure 8.

The results in Figure 8 show that using 0.3 PV ASP flooding fluid can further improve oil recovery by 26% on top of water flooding.

3.6. Performance of ASP System under Field Conditions. The on-site injection water and surfactant were used to further investigate the performance of the HAPAM ASP flooding system.

The mother liquor was prepared at 20°C for a dissolution time of 2 h using on-site water of the oil production plant and the on-site dehydrated crude oil. The surfactant (effective content 50%) and NaOH were all on-site industrial products.

3.6.1. Viscosity. The ASP systems containing HAPAM and HPAM (Mw = 2.5 MDa) were prepared. The polymer concentration was 1000 mg/L, the surfactant concentration was 0.3%, and the NaOH concentration was 1.2%. The change of the different systems with the concentration is shown in Figure 9.

Figure 9 shows that, after the addition of base and surfactant, the HAPAM ASP system has clearly better viscosity under field conditions compared with other systems.

3.6.2. Interfacial Tension. The interfacial tension was measured at a fixed HAPAM concentration of 1000 mg/L and varying concentrations of surfactant and base. The experimental results are shown in Figure 10.

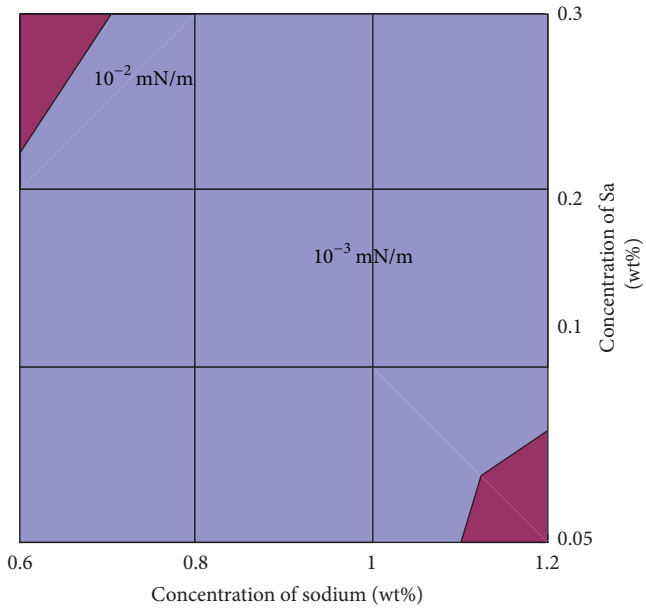

Figure 10: Interfacial tension of the HAPAM ASP system (in on-site injection water).

3.7. Discussions on the Viscosity Enhancement of the HAPAM ASP System. The prominent feature of the HAPAM ASP system is that, in the presence of both the base and the surfactant, the viscosity of the ASP system is significantly higher than that of the polymer solution alone, indicating a viscosity enhancing effect of the associating polymer under the given conditions. In this paper, the mechanism of this viscosity enhancement is analyzed and discussed (see Figure 11).

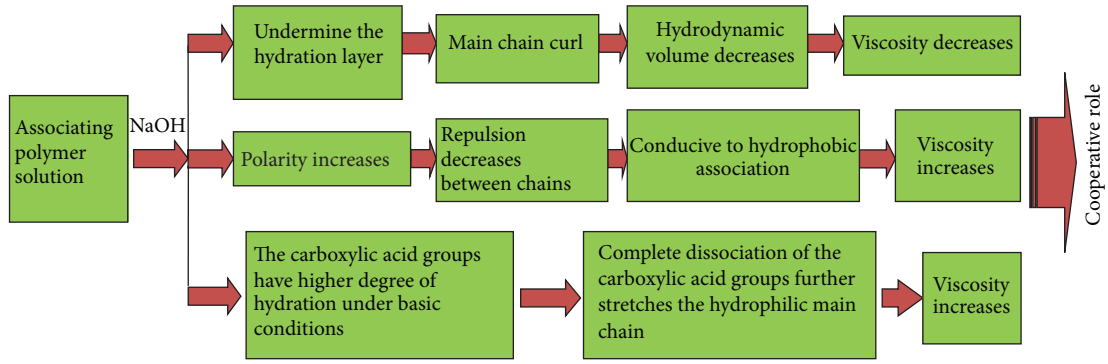

Figure 11: The effect of alkali on the viscosity of the associating polymer solution.

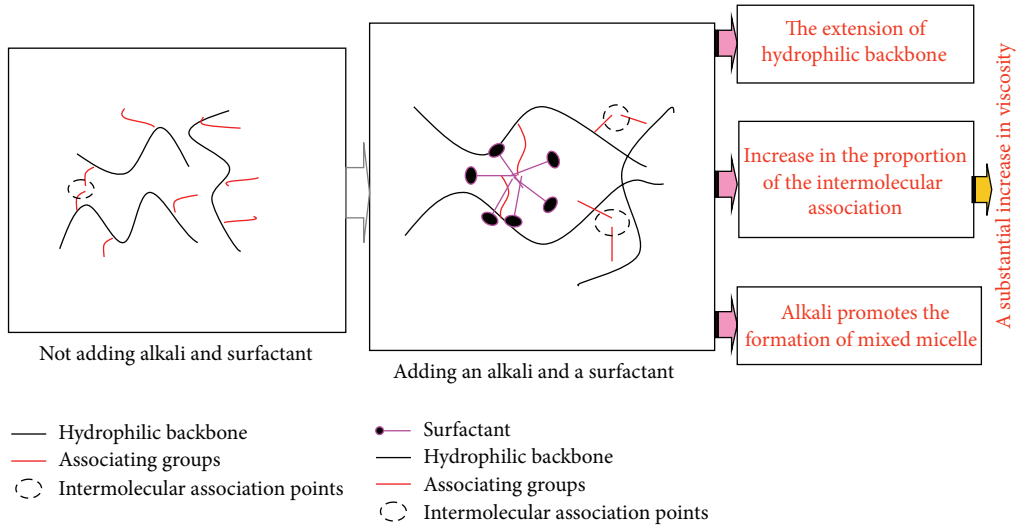

Figure 12: The effect of alkali mixed surfactant on the status of the associating polymer solution.

Because the base can promote the hydrolysis of the amide groups on the main chain of the associating polymer [20], it has less influence than NaCl on the viscosity of the associating polymer solution.

In the presence of both the base and the surfactant, the viscosity of the resulting ASP system is increased substantially. This is mainly because, under basic conditions, the carboxylic acid groups on the hydrophilic main chain have a higher hydration degree, the carboxylic acid groups are completely dissociated, and the molecular chain is more extended. Consequently, the surfactant interacts with the associating groups to form more intermolecular associating micelles, which substantially increases the solution viscosity (see Figure 12). This viscosity enhancement is closely related to the type and composition of the surfactant. Because the heavy alkylbenzene sulfonate surfactant used in this study has a very complicated composition, the mechanism of viscosity enhancement in the ASP system needs to be further studied.

4. Conclusions

The associating polymer HAPAM has good compatibility with the Daqing surfactant. The HAPAM ASP flooding system has good interfacial tension. After the addition of base and surfactant, the viscosity of the HAPAM ASP flooding system is increased significantly. Compared with using the HPAM polymer (Mw = 2.5 MDa), using HAPAM gives much better viscosity and can reduce polymer use by more than 40%. The core series injection experiment shows that the HAPAM ASP flooding system has good injectivity for the Daqing class II reservoirs ($100–300 \times 10^{-3}$ μm^2). The pressure gradient is uniform between the measurement points. The oil recovery can be improved by more than 25% on top of water flooding. Under basic conditions, the carboxylic acid groups on the hydrophilic main chain have a higher hydration degree, the carboxylic acid groups are completely dissociated, and the molecular chain is more extended. This promotes the interaction between the surfactant and the associating groups to form more intermolecular associating micelles, which substantially increase the solution viscosity.

Acknowledgments

This work was carried out as a part of the National Science and Technology Major Project, China (2011ZX05010-004). The authors are grateful for the financial support.

References

[1] Y. J. Guo, J. X. Liu, X. M. Zhang et al., "Solution property investigation of combination flooding systems consisting of gemini-non-ionic mixed surfactant and hydrophobically associating polyacrylamide for enhanced oil recovery," *Energy and Fuels*, vol. 26, no. 4, pp. 2116–2123, 2012.

[2] M. F. Nazar, S. S. Shah, and M. A. Khosa, "Microemulsions in enhanced oil recovery: a review," *Petroleum Science and Technology*, vol. 29, no. 13, pp. 1353–1365, 2011.

[3] G. Shutang and G. Qiang, "Recent progress and evaluation of ASP flooding for EOR in Daqing oil field," in *Proceedings of the SPE EOR Conference at Oil and Gas West Asia*, pp. 48–54, Muscat, Oman, April 2010.

[4] H. Dijk, M. A. Buijse, J. Nieuwerf et al., "Salym Chemical EOR Project, integration leads the way to success," in *Proceedings of the SPE Russian Oil and Gas Technical Conference and Exhibition*, pp. 885–900, Moscow, Russia, October 2010.

[5] M. A. Buijse, R. M. Prelicz, J. R. Barnes, and C. Cosmo, "Application of internal olefin sulfonates and other surfactants to EOR. Part 2: the design and execution of an ASP field test," in *Proceedings of the 17th SPE Improved Oil Recovery Symposium (IOR '10)*, pp. 706–717, Tulsa, Okla, USA, April 2010.

[6] J. Hou, Z. Liu, S. Zhang, X. Yue, and J. Yang, "The role of viscoelasticity of alkali/surfactant/polymer solutions in enhanced oil recovery," *Journal of Petroleum Science and Engineering*, vol. 47, no. 3-4, pp. 219–235, 2005.

[7] H. Zhang, M. Dong, and S. Zhao, "Which one is more important in chemical flooding for enhanced court heavy oil recovery, lowering interfacial tension or reducing water mobility?" *Energy and Fuels*, vol. 24, no. 3, pp. 1829–1836, 2010.

[8] W. M. Stoll, H. Al Shureqi, J. Finol et al., "Alkaline/surfactant/polymer flood: from the laboratory to the field," *SPE Reservoir Evaluation and Engineering*, vol. 14, no. 6, pp. 702–712, 2011.

[9] C. S. Gregersen, M. Kazempour, and V. Alvarado, "ASP design for the Minnelusa formation under low-salinity conditions: impacts of anhydrite on ASP performance," *Fuel*, vol. 105, pp. 368–382, 2013.

[10] Q. Hou, G. Jian, M. A. Desheng, and Z. Wang, "Current development and application of chemical combination flooding technique," *Petroleum Exploration and Development*, vol. 40, no. 1, pp. 96–103, 2013.

[11] K. Panthi and K. K. Mohanty, "Effect of alkaline preflush in an alkaline-surfactant-polymer flood," *Energy & Fuels*, vol. 27, no. 2, pp. 764–771, 2013.

[12] R. Kumar and K. K. Mohanty, "ASP flooding of viscous oils," in *Proceedings of the SPE Annual Technical Conference and Exhibition (ATCE '10)*, pp. 4493–4503, Florence, Italy, September 2010.

[13] M. A. Bataweel and H. A. Nasr-El-Din, "Minimizing scale precipitation in carbonate cores caused by alkalis in ASP flooding in high salinity/high temperature applications," in *Proceedings of the SPE International Symposium on Oilfield Chemistry*, pp. 849–863, The Woodlands, Tex, USA, April 2011.

[14] K. Zhang and J. S. Qin, "The effect of alkali and surfactant on polymer molecular structure," *Petroleum Science and Technology*, vol. 29, no. 2, pp. 183–191, 2011.

[15] B. Wang, T. Wu, Y. Li et al., "The effects of oil displacement agents on the stability of water produced from ASP (alkaline/surfactant/polymer) flooding," *Colloids and Surfaces A*, vol. 379, no. 1–3, pp. 121–126, 2011.

[16] L. Daoshan, L. Shouliang, L. Yi, and W. Demin, "The effect of biosurfactant on the interfacial tension and adsorption loss of surfactant in ASP flooding," *Colloids and Surfaces A*, vol. 244, no. 1–3, pp. 53–60, 2004.

[17] F. Chen, H. Jiang, X. Bai, and W. Zheng, "Evaluation the performance of sodium metaborate as a novel alkali in alkali/surfactant/polymer flooding," *Journal of Industrial and Engineering Chemistry*, vol. 19, no. 2, pp. 450–457, 2013.

[18] W. Zhou, J. Zhang, M. Han et al., "Application of hydrophobically associating water-soluble polymer for polymer flooding in China offshore heavy oilfield," in *Proceedings of the International Petroleum Technology Conference (IPTC '07)*, pp. 1449–1453, Dubai, United Arab Emirates, December 2007.

[19] Z. Huang, H. Lu, and Y. He, "Amphoteric hydrophobic associative polymer: I synthesis, solution properties and effect on solution properties of surfactant," *Colloid and Polymer Science*, vol. 285, no. 3, pp. 365–370, 2006.

[20] A. Samanta, A. Bera, K. Ojha, and A. Mandal, "Effects of alkali, salts, and surfactant on rheological behavior of partially hydrolyzed polyacrylamide solutions," *Journal of Chemical and Engineering Data*, vol. 55, no. 10, pp. 4315–4322, 2010.

Hindawi Publishing Corporation
Journal of Chemistry
Volume 2013, Article ID 801570, 9 pages
http://dx.doi.org/10.1155/2013/801570

Research Article

Rheological Study on ATBS-AM Copolymer-Surfactant System in High-Temperature and High-Salinity Environment

Muhammad Shahzad Kamal,[1] Ibnelwaleed Ali Hussien,[1] Abdullah Saad Sultan,[2] and Ming Han[3]

[1] *Department of Chemical Engineering, King Fahd University of Petroleum and Minerals, Dhahran 31261, Saudi Arabia*
[2] *Department of Petroleum Engineering and Center of Petroleum and Minerals, King Fahd University of Petroleum and Minerals, Dhahran 31261, Saudi Arabia*
[3] *EXPEC Advanced Research Center, Saudi Aramco, Dhahran 31311, Saudi Arabia*

Correspondence should be addressed to Abdullah Saad Sultan; sultanas@kfupm.edu.sa

Received 7 May 2013; Accepted 21 June 2013

Academic Editor: Yujun Feng

Experimental studies were conducted to evaluate the rheological properties of surfactant-polymer (SP) system. This SP system consists of a copolymer of acrylamide (AM) and acrylamido tertiary butyl sulfonate (ATBS) and sodium dodecyl sulphate (SDS) surfactant. Effects of surfactant concentration, temperature, polymer concentration, and salinity on rheological properties of SP system were investigated by means of oscillation and shear measurements. Comparison with classical partially hydrolyzed polyacrylamide (HPAM) was made. For the same temperature range, the viscosity drop for HPAM was about four times higher than the viscosity drop for ATBS-AM copolymer. In deionized water, viscosity of both polymers and SP systems was very high as compared to viscosity in saline water. Viscosity reduction of ATBS-AM copolymer was higher for salts having divalent cations. The SP system showed precipitation in presence of divalent cations. It worked well with monovalent cations even at relatively high salinities. The addition of 0.1% surfactant to the polymer resulted in a 60% decrease in the viscosity. Some interfacial rheological experiments were also carried out to investigate the behaviors on the interface between SP solutions and oil. Addition of 0.1% surfactant showed a 65% decrease in G' at SP solution-oil interface. SP system consisting of ATBS-AM and SDS showed better performance at high temperature compared to HPAM-SDS system. Due to precipitation, the SP system should be restricted to environment having low divalent cations.

1. Introduction

In chemical enhanced oil recovery (cEOR), surfactants are used to reduce the interfacial tension between crude oil and water. Polymers are used to improve the mobility ratio by viscosifying displacing fluid. Enhanced viscosity of displacing fluids can increase macroscopic displacement efficiency by overcoming viscous fingering. Recently, some researchers have proved that these polymers not only improve macroscopic displacement efficiency but also microscopic efficiency due to elasticity [1–7].

HPAM which is widely used for cEOR applications [8] fails at high-temperature and high-salinity (HTHS) environment. Extensive hydrolysis of amide group at high temperatures may also cause precipitation of hydrolyzed product in the presence of divalent cations. Field applications of available polymers are limited to low-temperature and low-salinity reservoirs. HTHS reservoirs present a major challenge for implementation of cEOR techniques. Incorporation of some thermally stable and salt tolerant comonomers can enhance the performance of polyacrylamide in HTHS conditions. Recently, synthesized thermoviscosifying polymers [9–12]

showed some positive results in HTHS environment after some preliminary rheological tests.

Three major types of surfactant-polymer interactions may exist depending upon the nature and structure of polymer and surfactant head group. Firstly, attractive forces between surfactant and polymer may be stronger than mutual forces of surfactant molecule. Secondly, attractive forces among surfactant molecules may be greater than attractive forces between surfactant and polymer. Thirdly, repulsive forces between surfactant and polymer are very high as compared to attractive forces among surfactant molecules [13]. The system becomes more complex in the presence of oil, cosurfactant, alkali, and salts. Many approaches have been adopted to understand the interactions between surfactant-polymer systems. These include surface tension and interfacial tension measurement, rheology [14–17], fluorescence spectroscopy [18–20], potentiometry [21], light scattering [22, 23], and conductivity measurement [24–28].

There are some reports available in the literature on the rheology of classical HPAM/SDS [15] PAM/SDS [29] and hydrophobically modified PAM (HM-PAM)/SDS [14] system. Addition of the surfactant has no effect on the rheology of the polymer due to nonionic nature of PAM. Significant effect of surfactant addition has been reported for HPAM and HM-HPAM due to strong interactions between the surfactant and polymer. By addition of 30 mmol/L (0.86%) SDS, about 85% drop in the viscosity of HPAM is reported byBu et al. [17]. SP solution consisting of SDS and vinylpyridine-AM copolymer in 0.1 N NaCl solution has about 90% less viscosity than that of the viscosity of the SP solution in deionized water [16]. Temperature also plays an important role in surfactant-polymer interactions. For HM-HPAM/SDS system, Nystrom [29] found that the viscosity at 40°C is 80% less than that of viscosity at 10°C.

Rheology study can be used to screen many SP systems for cEOR applications. In addition, interfacial rheology can provide the insight on the interface between SP solution and oil. The objective of this work is to study the influence of salts, temperature, and surfactant concentration on rheological properties of SP system consisting of SDS and ATBS-AM copolymer. Some of the results were compared with HPAM.

2. Experimental

2.1. Materials. Copolymer of AM and ATBS (Flopaam An125SH) with a molecular weight of 8 million Dalton and 25% sulfonation degree was obtained from SNF FLOERGER in a powder form. Classical HPAM (Flopaam 3630S) with a molecular weight of 20 million Dalton and 30% hydrolysis degree was obtained from SNF FLOERGER. Sea water was prepared using laboratory grade sodium bicarbonate, sodium sulphate, sodium chloride, calcium chloride, and magnesium chloride with a total salinity of 57,638 mg/L (ppm). SDS with 99% purity was obtained from Sigma Aldrich. The oil used in interfacial rheology experiments has a density of 0.8767 g/cm^3.

2.2. Preparation of Polymer Solutions. A polymer solution was prepared by using magnetically driven stirrer. The polymer was added slowly on the shoulder of the vortex formed by deionized water, surfactant solution, or salt solution to avoid formation of slubs. As soon as the entire polymer was added the rotor speed was reduced from 300 to 80 rpm to avoid mechanical degradation. Stirring was turned off after 3 hours and the solution was kept at room temperature for the next 48 hours for complete hydration.

2.3. Rheological Measurements. Rheological measurements were carried out using discovery hybrid rheometer (DHR-3) from TA Instrument. Concentric cylinder geometry was used to measure both steady state and oscillation measurements. The range of shear rate for steady shear viscosity measurements was from 0.01 to 1000 s^{-1}. Frequency from 0.1 to 100 rad/s was applied for oscillatory measurements. All reported data points are within torque limits (±5 mN·m−2000 mN·m). Frequency sweep experiments were conducted in the linear viscoelastic region. Oscillation time experiment was performed to check the thermal stability of HPAM and ATBS-AM copolymer. Interfacial rheology experiments were performed using AR-G2 platinum double wall ring interfacial geometry. Frequency was kept at 1 rad/s in oscillation time and temperature ramp experiments unless it is stated otherwise.

3. Results and Discussion

3.1. Effect of Surfactant Concentration. Copolymer concentration was fixed to 0.25% for experiments with varying surfactant concentration. Unless otherwise specified, the term copolymer in this discussion refers to ATBS-AM copolymer. Figure 1 shows the viscosity versus shear rate plots of 0.25% copolymer in deionized water for different concentrations of surfactant. It is evident from Figure 1 that by increasing the surfactant concentration steady viscosity is decreasing. The viscosity of the SP system is low compared to the viscosity of copolymer. By adding 0.3% surfactant, the viscosity is 80% less than that of the viscosity of the copolymer. Similar degree of viscosity drop by adding SDS has been reported for HPAM [15, 17]. This decrease in viscosity by the addition of surfactant is due to charge shielding mechanism as reported by Mandal and Ojha [15] for HPAM. At very high shear rate, viscosity is almost the same for all surfactant concentrations due to the dominance of the effect of shear in comparison to charge interactions. Variation of complex viscosity at a frequency of 0.1 rad/s is also shown in Figure 2. Storage modulus, G', versus surfactant concentration is shown in Figure 3. G' decreases with the increase in surfactant concentration. As G' is a measure of elastic nature, it is obvious that addition of surfactant is causing loss in network structure of ATBS-AM copolymer. Interfacial rheological properties were also evaluated at oil/SP solution interface to examine the influence of surfactant concentration. Figure 4 shows the interfacial storage modulus (G_I') versus frequency curves at different surfactant concentrations. At all frequencies, G_I' decreases by increasing surfactant concentration. We can conclude that

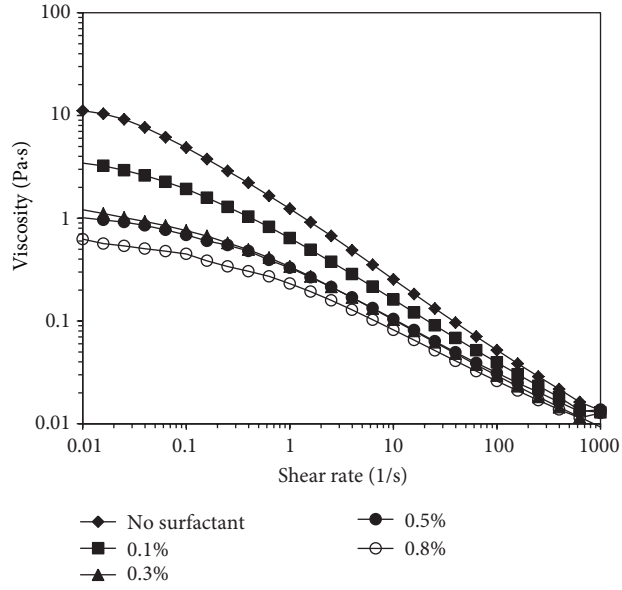

Figure 1: Effect of surfactant concentration on steady shear viscosity of copolymer at different shear rates in deionized water at 50°C.

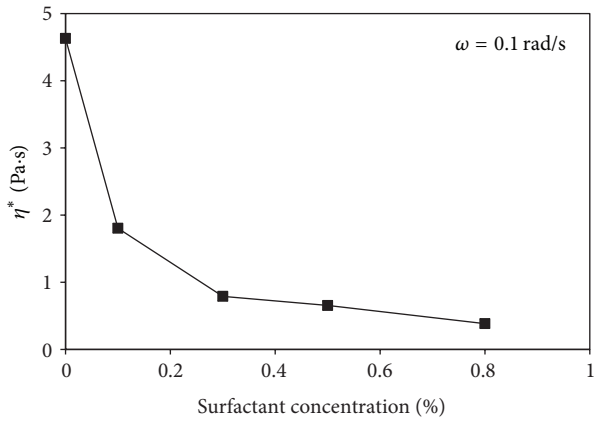

Figure 2: Effect of surfactant concentration on complex viscosity of copolymer in deionized water at 50°C.

addition of surfactant is weakening the interface between oil and SP solution. Time sweep measurements were also carried out to determine G_I'. These measurements were performed for 5 minutes and within experimental time no change in storage modulus was observed. Results of time sweep experiment are shown in Figure 5. A major drop in G_I' due to addition of 0.1% surfactant is observed, while, further addition of the surfactant has little effect.

3.2. Effect of Temperature. Viscosity versus shear rate plots for HPAM and ATBS-AM copolymer in the absence of surfactant is obtained at two different temperatures (Figure 6). It is evident that increasing temperature from 50°C to 90°C causes a major drop in steady shear viscosity of HPAM as compared to the copolymer. At low shear rate, the viscosity of HPAM at 90°C is about 60% less than its viscosity at 50°C. However,

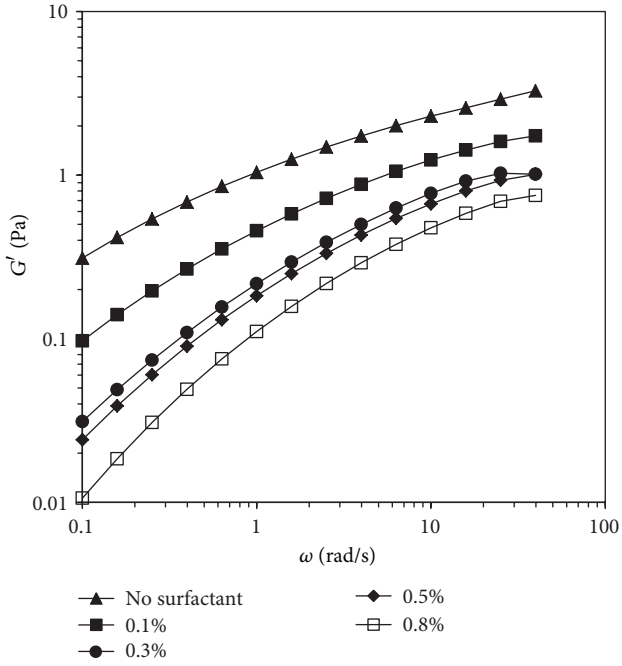

Figure 3: Effect of surfactant concentration on storage modulus of copolymer at different frequencies in deionized water at 50°C.

for ATBS-AM copolymer, small change in viscosity (15%) was observed in the same temperature range. This suggests that the viscosity of ATBS-AM copolymer is less sensitive to temperature in comparison with HPAM. Time sweep experiments were run for two hours for both polymers at 50°C and 90°C and results are shown in Figure 7. Both polymers were stable at 50°C within the experimental time. Within the experimental time, G' and viscosity (not shown) did not change for both polymers. At 90°C, completely different results were found. Unlike ATBS-AM copolymer a continuous decrease in storage modulus of HPAM was observed as experiment proceeds. From the above results it can be concluded that at 50°C both polymers show good stability and can be used at this temperature. However, at 90°C HPAM shows a continuous decrease in rheological properties while AM-ATBS copolymer is stable.

Figures 8 and 9 present results of temperature ramp experiments at 2°C/min for different surfactant concentrations. Viscosity versus temperature plots are shown in Figure 8. At all temperatures, the viscosity of the polymer and SP solutions is decreasing with increasing surfactant concentrations. However, the decrease in viscosity depends on the concentration of surfactant. With no surfactant added in the solution, 20% decrease in viscosity was observed in the temperature range 30°C to 85°C. With the addition of 0.1% surfactant, the viscosity decreases by 33% for the same temperature range. For 0.3% and higher surfactant concentrations about 58% drop in viscosity was observed. For HM-HPAM/SDS system 80% viscosity decrease was observed when temperature was increased from 10 to 40°C [29]. This shows that ATBS-AM/SDS system perform much better in high temperature compared to HM-HPAM/SDS system.

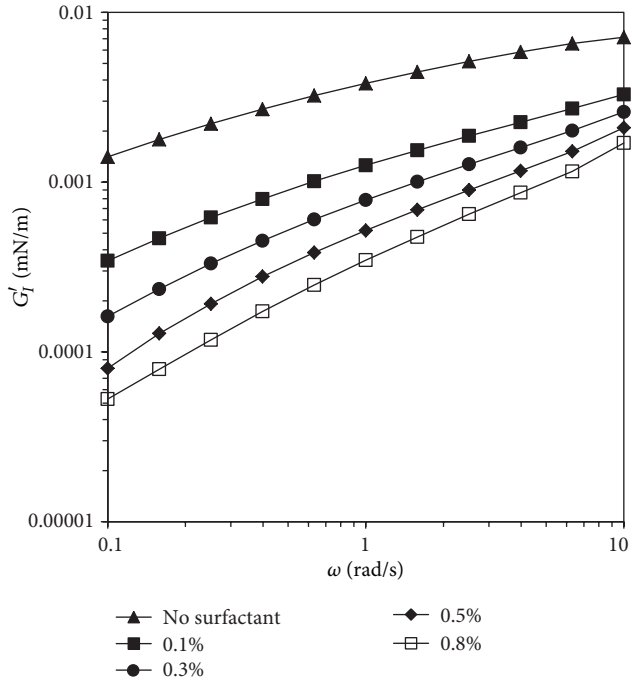

Figure 4: Effect of surfactant concentration on interfacial storage modulus of copolymer at different frequencies in deionized water at 25°C.

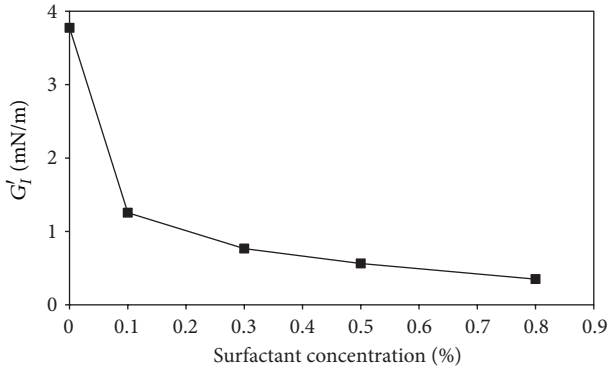

Figure 5: Effect of surfactant concentration on interfacial storage modulus of copolymer in deionized water at 25°C.

Arrhenius model was used to obtain activation energy of viscous flow and pre-exponential factor for solution of different surfactant concentrations. Activation energy of viscous flow increased while pre-exponential factor decreased with the addition of surfactant (Table 1). The percentage decrease in the pre-exponential factor is high as compared to the percentage increase in the activation energy. The above data indicate that in the presence of a surfactant, temperature has more effect on the viscosity of SP solutions as compared to copolymer solution having no surfactant. Similarly, for polymer solution without surfactant, a 26% drop in G' was noted. For 0.3% and higher surfactant concentrations about 70% decrease in storage modulus was observed in the same temperature range. Effect of temperature on G_I' is shown in Figure 10. With the increase in temperature G_I' also decreases. This shows that temperature is also weakening the interface, but its effect is not as much when we compare it to the effect of surfactant concentrations. The surfactant concentration is a major source of reduction in interfacial rheological properties between SP solution and oil interface.

Table 1: Activation energy and pre-exponential factors obtained from Arrhenius model for different surfactant concentrations.

Concentration (%)	E_a [a] (kJ/mole)	A [b] (mPa·s)
0	5.020	210.74
0.1	7.010	45.177
0.3	14.54	1.2797
0.5	15.38	0.8152
0.8	15.877	0.5497

[a] E_a is activation energy of viscous flow.
[b] A is pre-exponential factor.

Table 2: Activation energy and pre-exponential factors obtained from Arrhenius-type relation for different polymer concentrations.

Concentration (%)	E_a [a] (kJ/mole)	A [b] (mPa·s)
0.15	18.32	0.4266
0.20	16.94	1.1205
0.25	14.54	1.2797
0.30	14.90	5.0728
0.40	13.86	12.891

[a] E_a is activation energy of viscous flow.
[b] A is pre-exponential factor.

3.3. Effect of Polymer Concentration. Surfactant concentration was fixed to 0.3% for all experiments and polymer concentration was varied from 0.1 to 0.4%. Figures 11 and 12 summarize the effect of polymer concentration on SP system. No unusual results were observed by changing the polymer concentration. It is clear from Figures 11 and 12 that increasing the concentration of polymer will cause increase in steady shear viscosity. This increase is more prominent at low shear rate. Results of temperature ramp experiments at a rate of 2°C/min for different copolymer concentrations are shown in Figures 13 and 14. Both storage modulus and viscosity decrease with increasing in temperature at all polymer concentration. However, the decrease in the viscosity and storage modulus depends on the polymer concentration. Maximum drop in viscosity (58%) and storage modulus (70%) was found for SP solution having minimum polymer concentration (0.15%) and minimum drop in viscosity (49%) and storage modulus (57%) was found with SP solution of highest polymer concentration (0.4%). Activation energy of viscous flow and pre-exponent factors for SP solutions of different polymer concentrations were calculated and tabulated in Table 2. Pre-exponent factor and activation energy of viscous flow of the SP solutions do not change significantly by changing the polymer concentration. However, slight change in surfactant concentration significantly changes the pre-exponent factor and activation energy of the SP solutions.

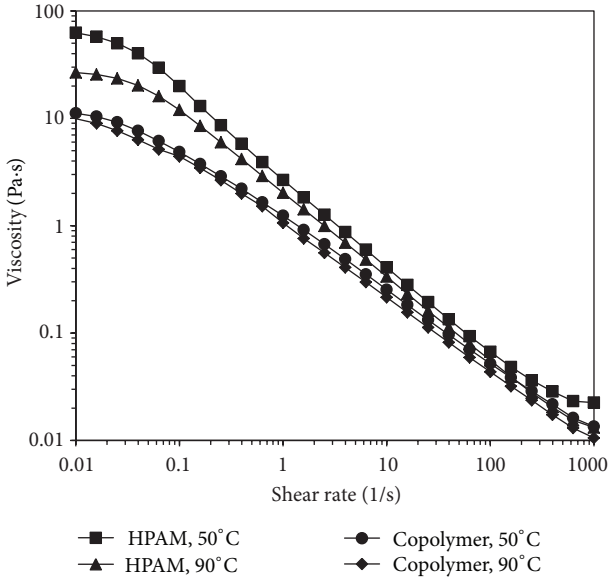

Figure 6: Steady shear viscosity profile of HPAM and ATBS-AM copolymer solutions in salt-free water without surfactant at 0.25% polymer concentration.

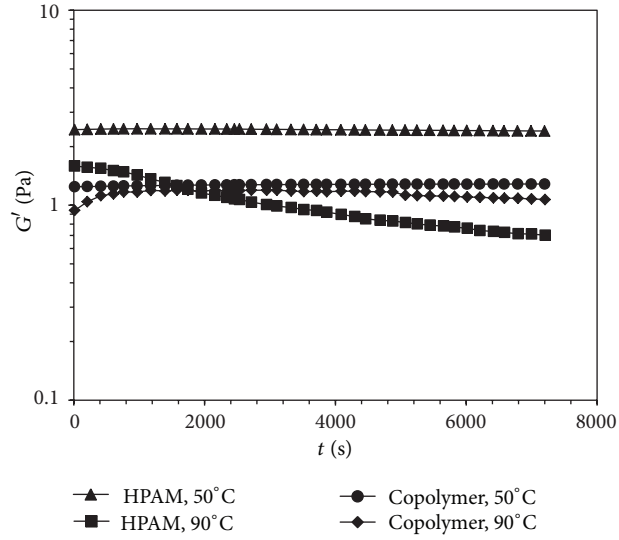

Figure 7: Comparison of G' of HPAM and ATBS-AM copolymer solutions in deionized water by time sweep measurements at 0.25% polymer concentration.

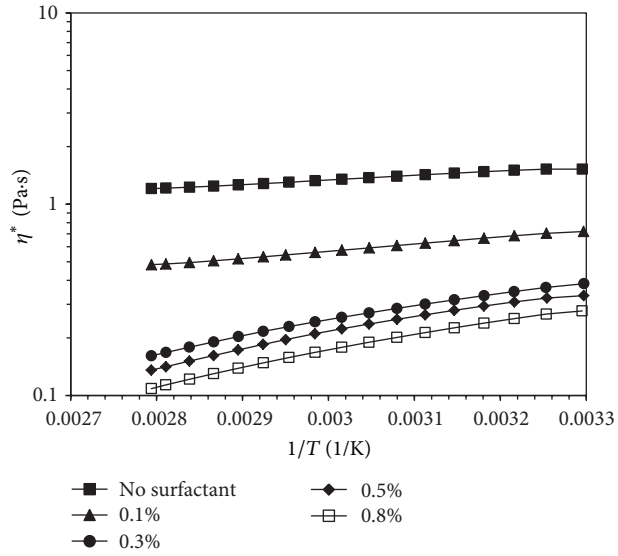

Figure 8: Effect of temperature on viscosity of 0.25% copolymer at different surfactant concentration.

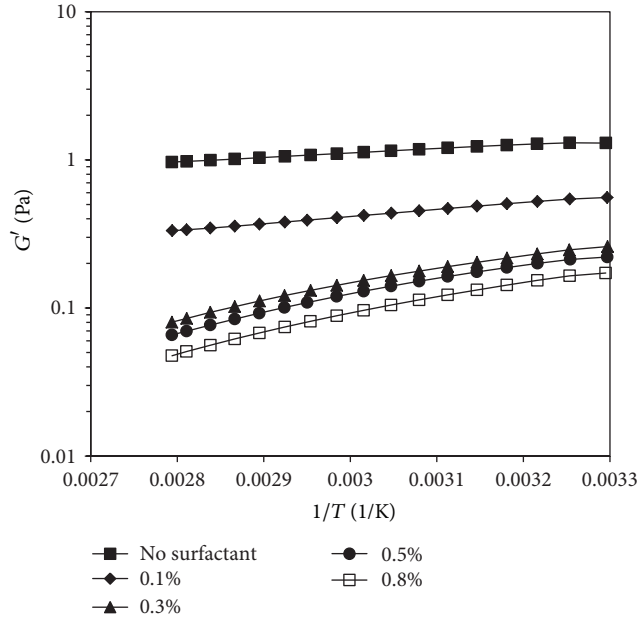

Figure 9: Effect of temperature on G' of 0.25% copolymer at different surfactant concentration.

Decrease in the viscosity with temperature depends mainly on surfactant concentration and polymer concentration has little effect.

3.4. Effect of Salts. High temperatures and high salinities are real challenges for polymer flooding for the Middle East carbonate reservoirs. In the presence of salts and higher temperatures, viscosity of HPAM decreases. Synthetic sea water with a total salinity of 57638 mg/L containing 2732 mg/L divalent cations was prepared in the lab. It is important to see the effect of each individual ion on the SP system used for chemical flooding. Besides sea water salt solutions of NaCl, Na_2SO_4, $MgCl_2$, and $CaCl_2$ were prepared with different molarities. SP solutions of 0.25% polymer and 0.3% surfactant concentration were used to evaluate the performance in different salts. Figure 15 shows the comparison of viscosity of both polymers in deionized water at 50°C without a surfactant. A major reduction in viscosity was observed for both polymers by adding synthetic sea water. Figures 16 and 17 show the effect of sodium chloride concentration on rheological properties of SP system. Steady shear viscosity reduces as the concentration of sodium chloride is increased.

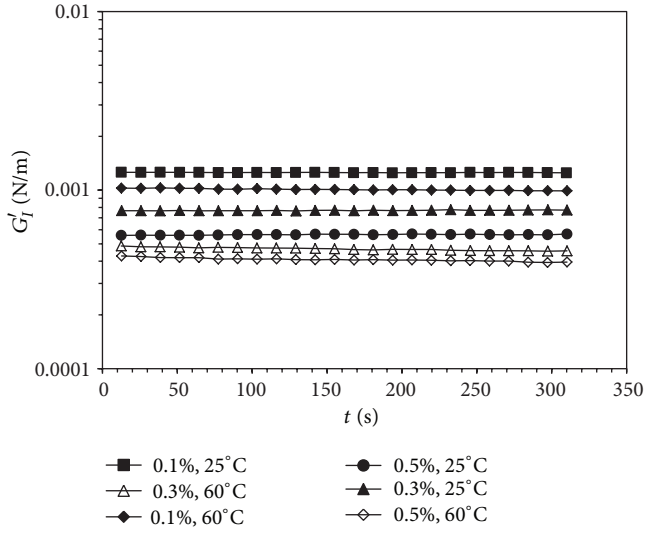

Figure 10: Effect of temperature on G_I' of 0.25% copolymer at different surfactant concentration.

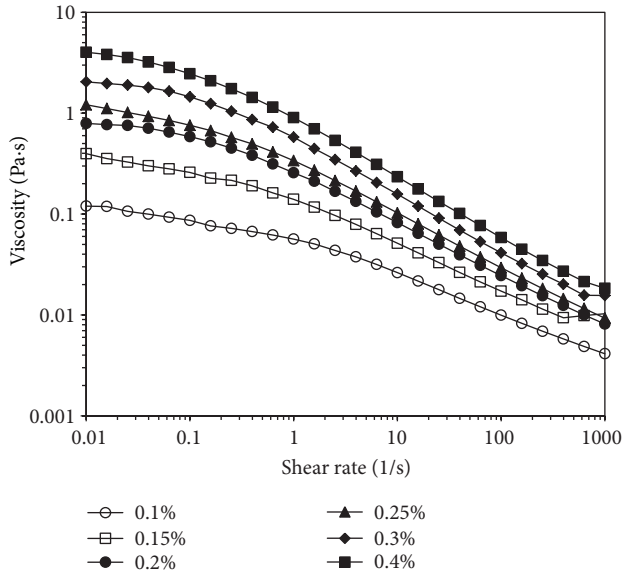

Figure 11: Steady state viscosity profile of SP solutions with varying concentration of copolymer at 50°C.

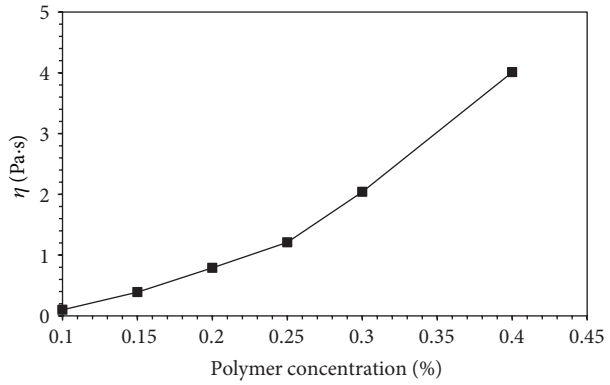

Figure 12: Effect of copolymer concentration on viscosity of SP solution at 50°C and shear rate of 0.01 s^{-1}.

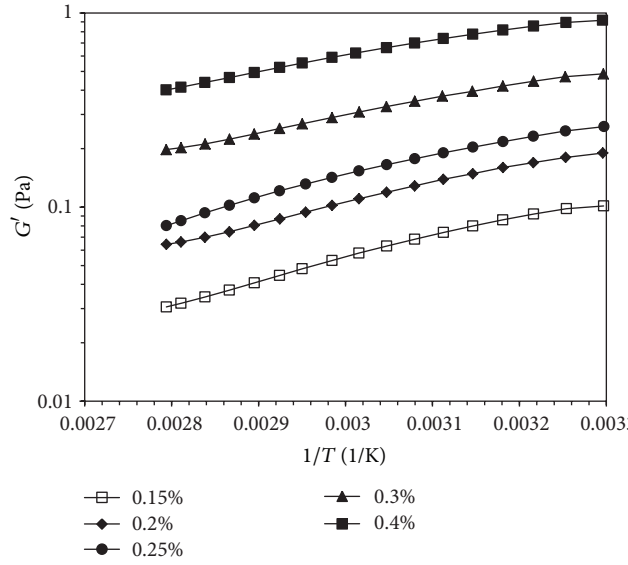

Figure 13: Effect of copolymer concentration on storage modulus of SP solution at different temperatures.

Viscosity at zero shear decreases with the increase in NaCl concentration. Similar trend was also observed for storage modulus. Addition of salts brings counterions in the system which reduces the stretching in polymer chains by charge screening and resulting in reduction in viscosity and storage modulus. A reduction in viscosity was also observed for sodium sulphate as shown in Figure 18. With calcium chloride and magnesium chloride precipitation of SP system was observed. With sea water there was also precipitation, but dilution of sea water to 25% sea water and 75% DW gives a clear solution. This observation shows that this SP system should be limited to environment having low divalent cations. In the absence of divalent cations this SP system can be used even at high salinities. Figure 19 presents a comparison of the impact of different counterions on the steady shear viscosity of copolymer. Compared to deionized water, viscosity of polymer is lower in 0.01 M NaCl solution. But this viscosity is still higher than that of SP solution in 0.01 M NaCl having a surfactant. Both surfactant and salts are bringing counterions. System having surfactant has more counterions and introducing additional chain collapse. It is also clear from Figure 19 that decrease in viscosity is higher for polymer solution having calcium ions as compared to monovalent sodium ions. Divalency is the major cause of reduction in viscosity.

4. Conclusions

About 60% reduction in viscosity for HPAM was observed by increasing temperature from 50°C to 90°C. However,

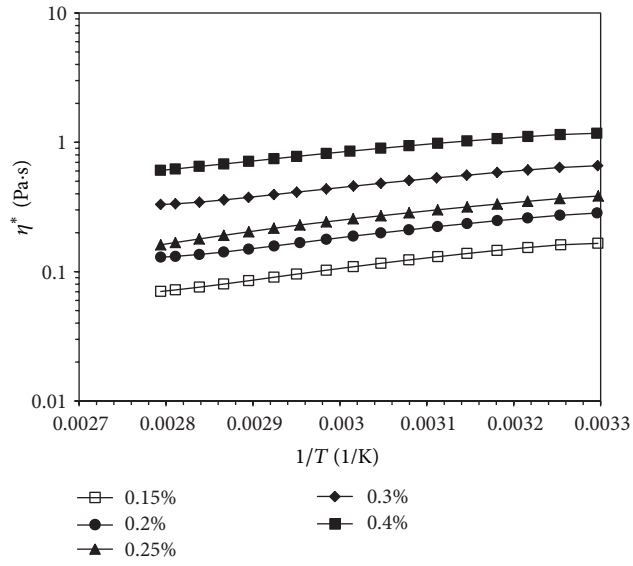

Figure 14: Effect of copolymer concentration on viscosity of SP solutions at different temperatures.

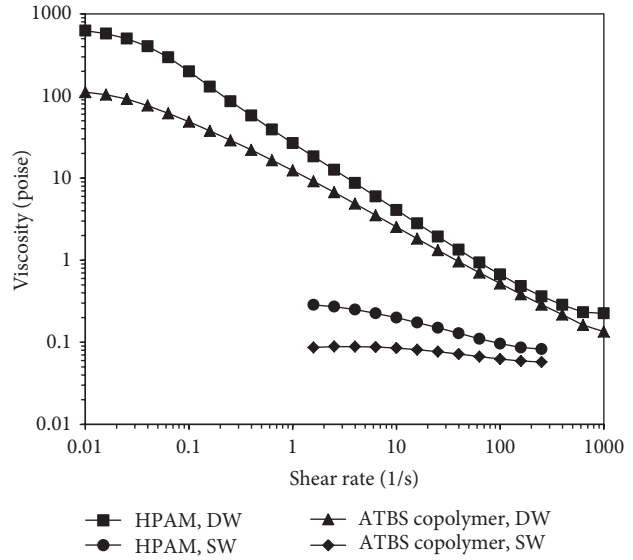

Figure 15: Effect of sea water on steady shear viscosity of HPAM and ATBS-AM copolymer without any surfactant at 50°C.

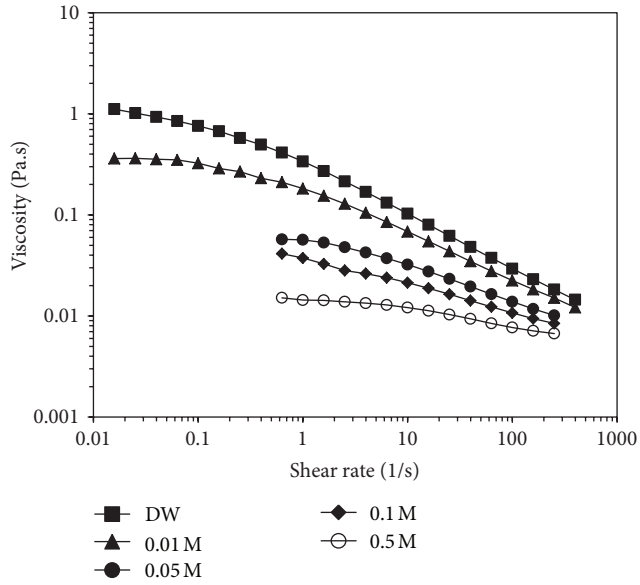

Figure 16: Effect of sodium chloride concentration on steady shear viscosity of copolymer at 50°C.

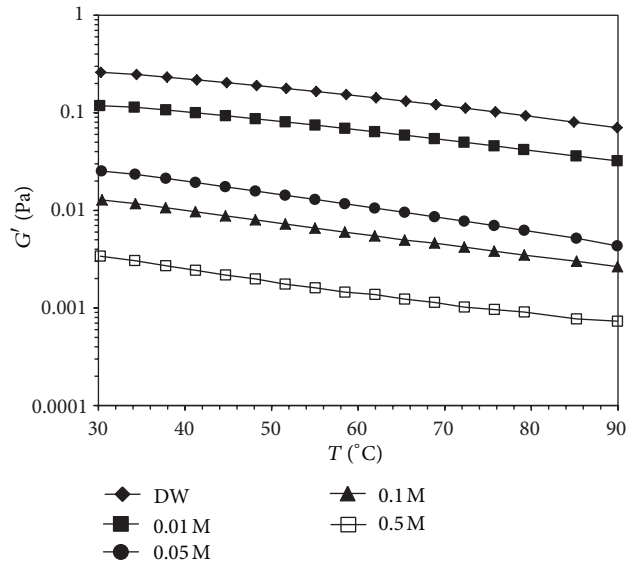

Figure 17: Effect of sodium chloride concentration on storage modulus of copolymer at different temperatures.

decrease in viscosity for ATBS-AM copolymer was 15% for the same temperature range. It can be seen from temperature sweep experiments that at 90°C there was a continuous decrease of storage modulus of HPAM. Copolymer did not show significant decrease in storage modulus and viscosity within the experimental time. Copolymer of acrylamide and acrylamido tertiary butyl sulfonate (ATBS) has better performance at higher temperatures as compared to partially hydrolyzed polyacrylamide. SP system consisting of AM-ATBS copolymer and SDS showed better performance from rheological point of view at high temperature compared to previously reported HPAM/SDS system. Presence of anionic surfactant SDS is also a source of reduction in the viscosity and storage modulus of polymer solution. Interfacial rheology experiments showed that this surfactant is significantly weakening the interface between SP solution and oil. Effect of each salt on the rheological properties of SP solution was investigated. There is a decrease in the viscosity in the presence of monovalent cations. In the presence of divalent cations precipitation was observed. There was precipitation with sea water. Dilution of this sea water by a ratio of 1 : 3 with DW yields a solution with no precipitation. Both polymers can be potential candidate for low temperature and low salinity reservoirs. HPAM is not suitable for high temperature

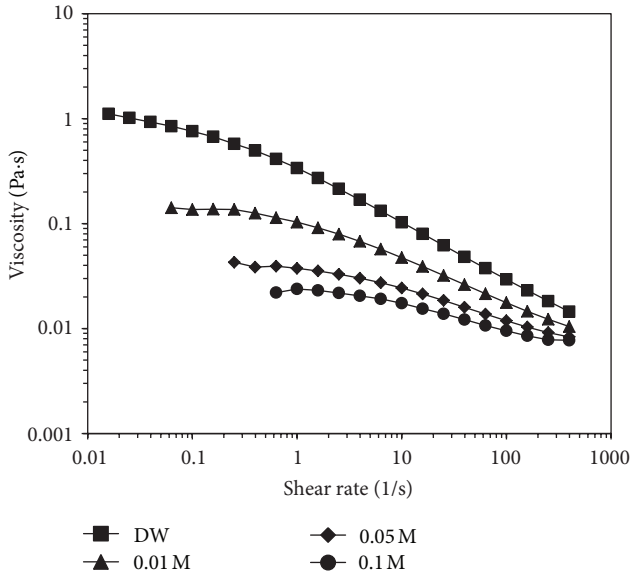

Figure 18: Effect of sodium sulphate concentration on steady shear viscosity of copolymer at 50°C.

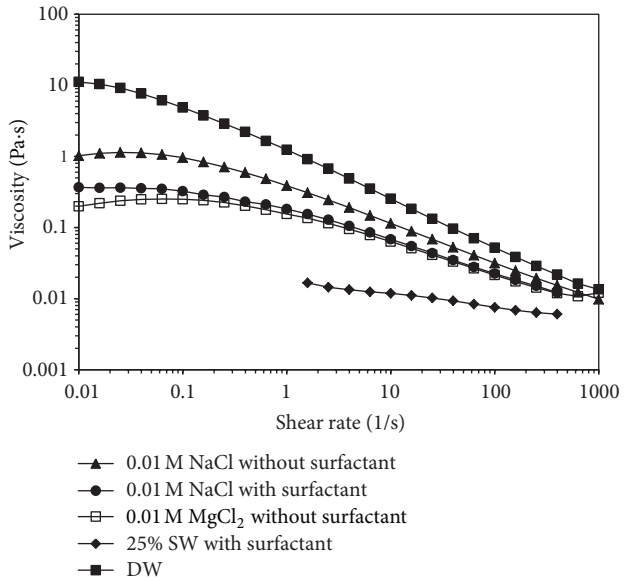

Figure 19: Effect of different salt on steady shear viscosity of copolymer at 50°C.

reservoirs while ATBS based copolymer can be a potential candidate for high temperature reservoirs.

Acknowledgments

This research is supported by Saudi Aramco through Project no. CPM 2297. The authors would like to thank King Fahd University of Petroleum & Minerals (KFUPM) for supporting this research. SNF is also acknowledged for providing polymer samples.

References

[1] D. Wang, J. Cheng, H. Xia, Q. Li, and J. Shi, "Viscous elastic fluids can mobilize oil remaining after water flood by force parallel to the oil water interface," in *SPE Asia Pacific Improved Oil Recovery Conference Proceedings*, Kuala Lumpur, Malaysia, 2001.

[2] T. S. Urbissinova, J. Trivedi, and E. Kuru, "Effect of elasticity during viscoelastic polymer flooding: a possible mechanism of increasing the sweep efficiency," in *SPE Western Regional Meeting Proceeding*, pp. 747–758, Anaheim, Calif, USA, May 2010.

[3] D. Wang, H. Xia, Z. Liu, A. Anda, and Q. Yang, "Study of the mechanism of polymer solution with visco-elastic behavior increasing microscopic oil displacement efficiency and the forming of steady "oil thread" flow channels," in *SPE Asia Pacific Oil and Gas Conference and Exhibition Proceedings*, Jakarta, Indonesia, April 2001.

[4] H. Xia, D. Wang, J. Wu, and F. Kong, "Elasticity of HPAM solutions increases displacement efficiency under mixed wettability conditions," in *SPE Asia Pacific Oil and Gas Conference and Exhibition Proceedings*, Perth, Australia, 2004.

[5] W. Wu, D. Wang, and H. Jiang, "Effect of the visco-elasticity of displacing fluids on the relationship of capillary number and displacement efficiency in weak oil-wet cores," in *SPE Asia Pacific oil & Gas Conference and Exhibition*, pp. 556–560, Jakarta, Indonesia, November 2007.

[6] H. Xia, Y. Ju, F. Kong, and J. Wu, "Effect of elastic behavior of HPAM solutions on displacement efficiency under mixed wettability conditions," in *Proceedings of the SPE International Petroleum Conference in Mexico*, pp. 171–178, Puebla, Mexico, November 2004.

[7] Z. Zhang, J. Li, and J. Zhou, "Microscopic Roles of "Viscoelasticity" in HPMA polymer flooding for EOR," *Transport in Porous Media*, vol. 86, no. 1, pp. 199–214, 2011.

[8] S. K. Veerabhadrappa, T. S. Urbissinova, J. J. Trivedi, and E. Kuru, "Polymer screening criteria for EOR application—a rheological characterization approach," in *Society of Petroleum Engineers Western North American Regional Meeting*, pp. 386–396, Anchorage, Alaska, USA, May 2011.

[9] Y. Wang, Z. Lu, Y. Han, Y. Feng, and C. Tang, "A novel thermoviscosifying water-soluble polymer for enhancing oil recovery from high-temperature and high-salinity oil reservoirs," *Advanced Materials Research*, vol. 306-307, pp. 654–657, 2011.

[10] X. Liu, Y. Wang, Z. Lu, Q. Chen, and Y. Feng, "Effect of inorganic salts on viscosifying behavior of a thermoassociative water-soluble terpolymer based on 2-acrylamido-methylpropane sulfonic acid," *Journal of Applied Polymer Science*, vol. 125, pp. 4041–4048, 2012.

[11] Q. Chen, Y. Wang, Z. Lu, and Y. Feng, "Thermoviscosifying polymer used for enhanced oil recovery: rheological behaviors and core flooding test," *Polymer Bulletin*, vol. 70, pp. 391–401, 2013.

[12] L. Petit, C. Karakasyan, N. Pantoustier, and D. Hourdet, "Synthesis of graft polyacrylamide with responsive self-assembling properties in aqueous media," *Polymer*, vol. 48, no. 24, pp. 7098–7112, 2007.

[13] C. Methemitis, M. Morcellet, J. Sabbadin, and J. Francois, "Interactions between partially hydrolyzed polyacrylamide and ionic surfactants," *European Polymer Journal*, vol. 22, no. 8, pp. 619–627, 1986.

[14] M.-R. Caputo, J. Selb, and F. Candau, "Effect of temperature on the viscoelastic behaviour of entangled solutions of multisticker associating polyacrylamides," *Polymer*, vol. 45, no. 1, pp. 231–240, 2004.

[15] A. Mandal and K. Ojha, "Optimum formulation of alkaline-surfactant-polymer systems for enhanced oil recovery," in *SPE Asia Pacific Oil & Gas Conference and Exhibition*, pp. 360–371, Perth, Australia, October 2008.

[16] L. Tennouga, K. Medjahed, A. Mansri, B. Bouras, and B. Grassl, "Interaction between weak neutralized polyelectrolyte complex polyacrylamide/poly(4-vinylpyridine) and sodium dodecyl sulfate in saline medium," *Der Pharma Chemica*, vol. 4, no. 3, pp. 1089–1092, 2012.

[17] H. T. Bu, Z. Z. Yang, and L. Huang, "Effect of thermal history on rheological properties of partially hydrolyzed polyacrylamide/anionic surfactant SDS complex systems," *Chinese Chemical Letters*, vol. 13, no. 5, pp. 456–459, 2002.

[18] H.-T. Bu, Z.-Z. Yang, and Y.-X. Zhang, "Experimental characterization of fluorocarbon-modified polyacrylamide/surfactant aqueous solutions," *Chinese Journal of Polymer Science*, vol. 21, no. 3, pp. 297–302, 2003.

[19] M. D. G. Miguel, H. D. Burrows, S. J. Formosinho, and B. Lindman, "Fluorescence studies of polymer-surfactant association," *Journal of Molecular Structure*, vol. 563-564, pp. 89–98, 2001.

[20] L. Tofani, A. Feis, R. E. Snoke, D. Berti, P. Baglioni, and G. Smulevich, "Spectroscopic and interfacial properties of myoglobin/surfactant complexes," *Biophysical Journal*, vol. 87, no. 2, pp. 1186–1195, 2004.

[21] J. Mata, J. Patel, N. Jain, G. Ghosh, and P. Bahadur, "Interaction of cationic surfactants with carboxymethylcellulose in aqueous media," *Journal of Colloid and Interface Science*, vol. 297, no. 2, pp. 797–804, 2006.

[22] K. Y. Mya, A. M. Jamieson, and A. Sirivat, "Interactions between the nonionic surfactant and polyacrylamide studied by light scattering and viscometry," *Polymer*, vol. 40, no. 21, pp. 5741–5749, 1999.

[23] R. López-Esparza, M.-A. Guedeau-Boudeville, Y. Gambin, C. Rodríguez-Beas, A. Maldonado, and W. Urbach, "Interaction between poly(ethylene glycol) and two surfactants investigated by diffusion coefficient measurements," *Journal of Colloid and Interface Science*, vol. 300, no. 1, pp. 105–110, 2006.

[24] M. Hai and B. Han, "Study of interaction between sodium dodecyl sulfate and polyacrylamide by rheological and conductivity measurements," *Journal of Chemical and Engineering Data*, vol. 51, no. 5, pp. 1498–1501, 2006.

[25] S.-C. Wang, T.-C. Wei, W.-B. Chen, and H.-K. Tsao, "Effects of surfactant micelles on viscosity and conductivity of poly(ethylene glycol) solutions," *Journal of Chemical Physics*, vol. 120, no. 10, pp. 4980–4988, 2004.

[26] A. Capalbi and C. La Mesa, "Polymer-surfactant interactions," *Journal of Thermal Analysis and Calorimetry*, vol. 66, no. 1, pp. 233–241, 2001.

[27] M. Y. Khan, A. Samanta, K. Ojha, and A. Mandal, "Interaction between aqueous solutions of polymer and surfactant and its effect on physicochemical properties," *Asia-Pacific Journal of Chemical Engineering*, vol. 3, no. 5, pp. 579–585, 2008.

[28] A. A. Mohsenipour, R. Pal, and K. Prajapati, "Effect of cationic surfactant addition on the drag reduction behaviour of anionic polymer solutions," *The Canadian Journal of Chemical Engineering*, vol. 91, pp. 181–189, 2013.

[29] H. M. Kopperud, F. K. Hansen, and B. Nyström, "Effect of surfactant and temperature on the rheological properties of aqueous solutions of unmodified and hydrophobically modified polyacrylamide," *Macromolecular Chemistry and Physics*, vol. 199, no. 11, pp. 2385–2394, 1998.

Hindawi Publishing Corporation
Journal of Chemistry
Volume 2013, Article ID 165970, 7 pages
http://dx.doi.org/10.1155/2013/165970

Research Article

An Experimental Method of Distribution Behavior of Hydrophobically Associated Polymer AP-P4 in Three-Phase Systems

Ruyin Li,[1,2] Guorong Tan,[1,2] and Jian Zhang[1,2]

[1] *State Key Laboratory of Offshore Oil Exploitation, Beijing 100027, China*
[2] *CNOOC Research Institute, Beijing 100027, China*

Correspondence should be addressed to Ruyin Li; liry3@cnooc.com.cn

Received 20 February 2013; Revised 8 April 2013; Accepted 8 April 2013

Academic Editor: Yujun Feng

A novel experimental method has been established for the first time to evaluate the distribution behavior of water soluble hydrophobically associated polymer AP-P4 in the oil-water-solid three-phase systems, based on the static adsorption principle. Suitable analysis method has been selected to measure the concentration of polymer in every phase. The enrichment of polymer has been observed between the oil-aqueous interlayer. The distribution coefficient of AP-P4 is obtained along with the variation of concentration and total salinity. The experimental method is helpful to reveal the property of polymer solution and has potential usage in predicting the adsorption and retention in polymer flooding and the wastewater dealing of polymer flooding.

1. Introduction

Polymer flooding has been widely used as one of the most important stimulation treatments in oil fields. Different from the ordinary polymers, the hydrophobically associated polymer has significantly exhibited the ability to enhance the viscosity, to modify the water/oil mobility ratio, to reduce the water permeability, and to enlarge the swept volume in the formation [1–3]. AP-P4 as one kind of hydrophobically associated polymer has been widely used in the oilfields and its driven process is assisted by several different environmental factors. The polymer molecules could be distributed in the formation, aqueous phase, oil phase, or emulsion phase after injection, and each of them could exhibit different adsorption and transfusion behavior. Plenty of works have been done on the static and dynamic adsorption principle of polymer AP-P4 under various concentrations [1, 4–14], and the properties of rheology, viscoelasticity, thermoendurance, salt tolerance, and shear degradation have been chartered. It has been revealed that the associated function group could be different from the linear polymer while adsorption [15]. The effective permeability could be lowered sharply after injection of polymer solutions, no matter the value of porosity of the formation [9, 15, 16]. However, the traditional adsorption experiments of AP-P4 were carried out on aqueous/solid phase, and the results of these experiments could only reflect the adsorption and retention behavior between two-phase systems. The model is too simple to find out the influence of concentration loss of polymer solutions. In polymer flooding process, most polymer molecules with hydrophobic function groups would exhibit the trend to get out of aqueous phase. Under the nonpolar interaction of oil phase, the polymer molecules would be likely to stay at the interlayer between aqueous and oil phases. The concentration of polymer in aqueous phase would be thus reduced. Although the composition of hydrophobic function group may be low, the effects of oil phase could not be neglected on AP-P4. However, there is no measurement method to estimate the polymer concentration in oil phase as far as we know and so does the polymer concentrations enriched at the oil/aqueous interlayer. So it is important to design an experiment method to analyze the distribution behavior of polymer among oil/aqueous/solid three-phase systems.

A novel experiment method of oil/aqueous/solid three-phase systems was designed in this work, in order to reveal

Table 1: The components of simulative water of SZ 36-1.

	NaCl/mg L^{-1}	$NaHCO_3$/mg L^{-1}	Na_2SO_4/mg L^{-1}	$CaCl_2$/mg L^{-1}	$MgCl_2 \cdot H_2O$/mg L^{-1}	Total salinity/mg L^{-1}
Simulative water, A	7461	430	304	192	352	8739
Simulative water, B	14922	860	608	384	704	17478

the trace, enrichment behavior, equilibrium state of polymer molecules after the solution was injected. Besides, a novel measurement method was designed to evaluate the polymer concentration in oil phase. The effect of oil phase could be estimated by this method, through the comparison of three-phase and two-phase experiment results.

2. Experiment

2.1. Materials and Instruments

Solid-Phase Sorbent. Pure quartz sand (100–160 mesh) was washed by deionized water and then dried.

AP-P4 Powder. $M_W = 1 \times 10^7$, degree of hydrolysis 25.3%.

Crude Oil. From SZ 36-1 oilfield, after electric dehydration.

Chemicals. NaCl, $CaCl_2$, $MgCl_2$, $NaHCO_3$, Na_2SO_4, solution of CH_3COOH, solution of NaClO, deionized water, and so forth.

Demulsifier and Electric Dehydration Performance Tester (DPY-2C, Jiangsu analytical instrument factory).

COD digestor and UV-Vis Spectrophotometer.

2.2. The Method to Measure the Concentration of AP-P4 Solution in the Oil Phase and Aqueous Phase. The distribution coefficient of AP-P4 could be determined by analyzing the concentration of AP-P4 in oil, water, and solid phases when the system reaches the equilibrium.

When crude oil, water, and quartz sand were coexisted and reached the phase equilibrium, the three layers were in the hierarchical mixture of state. Crude oil located in the upper layer; in the middle there were water and quartz sand soaked at the bottom of water phase. In order to measure the concentration of AP-P4 in each phase, we need to perform phase-separation operation. After we determined the polymer content in at least two phases, we were able to understand the partition law of the polymers among three phases. After phase separation, the polymer concentration in water phase can be directly measured while those in oil phase and quartz sand cannot.

Considering that polymers are easy to dissolve in water, and their solubility in crude oil is rather small, in this work, we select deionized water, a good solvent for AP-P4, as extractant, and mix it with the same amount of oil phase containing AP-P4, and heat them until the phase equilibrium is reached, then through liquid extraction, the aqueous phase can be obtained. Then the AP-P4 content can be qualitatively determined by total nitrogen nephelometry. Repeat the oil extraction operation until the polymer is completely transferred from the oil phase to water phase. Lastly, merge all water phases and measure the AP-P4 concentration so that the polymer concentration in crude oil can be known.

Selecting an exact and stable method to measure the AP-P4 concentration is an important step to obtain the accurate results. There are plenty of detailed studies on the method of measuring the concentration of polyacrylamide polymers [7, 17–25]. The starch-cadmium iodide working curve method was often employed both in the oilfield and lab. Such method has some disadvantages, such as instability of absorbance and large errors originated from working curve method, and thus it cannot assure good repeatability. The estimate of total nitrogen is a kind of high temperature oxidation/chemiluminescence method, which can measure the total nitrogen content of all chemicals in water, is suitable for the accurate determination for nitrogen-contained compounds in simple lab systems. Its mechanism includes adding oxidant to the solution, decomposing the liquid samples in high temperature to oxidize all nitrogen atoms to NO_3^-, reducing NO_3^- to NO_2^-, producing purple azo compounds by chromogenic agent, obtaining the accurate concentration by UV spectrophotometer, and calculating the nitrogen content. The result is very reliable since there is no clay or undissolved substances in the simple lab system and also UV spectrophotometer measurement is rather accurate.

2.3. The Distribution of AP-P4 in Oil/Aqueous/Sand Three-Phase Systems. (1) The formation water of offshore oilfield SZ 36-1 was taken as reference; two kinds of simulative water were prepared. In sample A, the salinity was 17478 mg L^{-1}. In sample B, the salinity was 8739 mg L^{-1}, a half of A. The compositions are listed in Table 1.

The formation circumstance of SZ 36-1 was taken as reference, the solid/aqueous ratio was 1 : 12, and aqueous/oil ratio was 6 : 4.

(2) Simulative water A and B were taken, and the AP-P4 solutions were prepared, and diluted into a series of target concentration, ranged from 750 ppm to 1750 ppm. The concentrations were calculated as the initial concentration C_{01}.

(3) 120.00 g AP-P4 solution was put along with 10.00 g sands into the 250 mL erlenmeyer flask, which was shaken until the mixture was uniformed. 80.00 g dehydrated crude oil was added into the erlenmeyer flask, which was shaken until the mixture was uniformed again. The three-phase system was oil/aqueous/sand from the top to the bottom. The erlenmeyer flask was sealed at the end.

(4) Put the 250 mL erlenmeyer flask in the oven at 65°C for 60 h.

(5) Take out the erlenmeyer flask. Use hypodermic syringe and take out the clear liquid by suction. The clear liquid was stayed still until the small size sands were deposited.The nitrogen content of liquid was measured, and

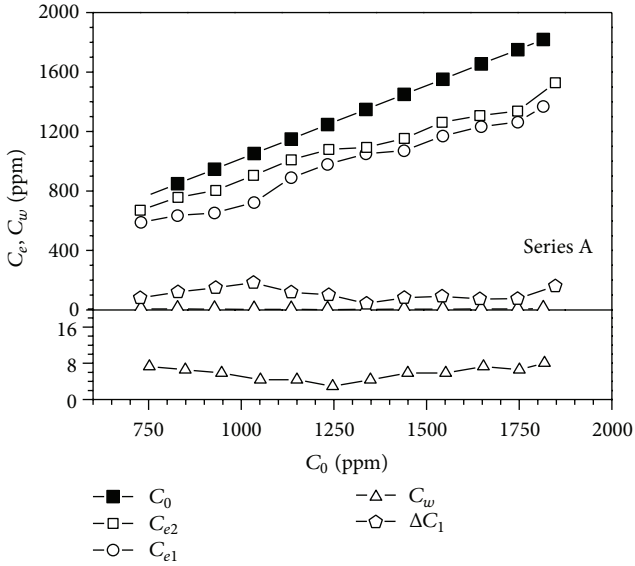

Figure 1: The adsorption experiment of two-phase and three-phase systems with the simulative water A.

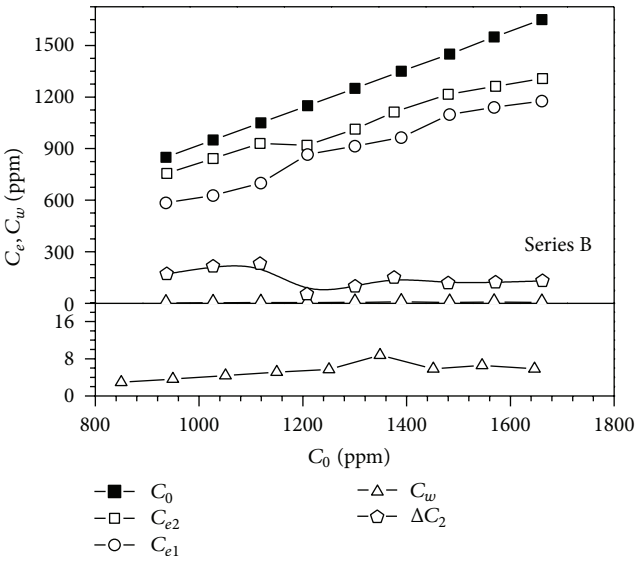

Figure 2: The adsorption experiment of two-phase and three-phase systems with the simulative water B.

the obtained data was the equilibrium concentration after adsorption, named as C_{e1}.

The process (6) to (11) is to extract the polymer from the oil phase and to estimate the concentration of it.

(6) The oil obtained from the erlenmeyer flask after adsorption was filled into the electric dehydrate bottle. After that, the oil phase was dehydrated.

(7) 40.00 g water and 40.00 g dehydrated oil were filled into a 150 mL erlenmeyer flask. Shake the erlenmeyer flask and mix them thoroughly.

(8) Put the 150 mL erlenmeyer flask in the oven under 65°C for 24 h. Shake them every 2 h to make the two-phase contact.

(9) Take out the 150 mL erlenmeyer flask. The clear aqueous phase at the bottom was taken out by the suction of hypodermic syringe.

(10) 10 mL aqueous phase was put in a beaker; the glacial acetic acid and sodium hypochlorite solution were added into it. The nephelometry was adopted to evaluate the existence of polymer [25].

(11) The oil phase was washed by water for the second time, and the nephelometry was carried out again until no turbid was observed.

(12) The aqueous phases that were extracted from the oil phase at two times were combined together. The total nitrogen estimates were carried out, and the obtained concentrations were C_w.

2.4. The Distribution of AP-P4 in Aqueous/Sand Two-Phase System. In the reported works, the adsorption of AP-P4 in queous/sand two-phase systems had been frequently studied to evaluate the adsorption and retention properties [15, 26]. In this work, similar experiments had been done as a blank test in order to make comparison with three-phase systems for full research.

(1) Simulative water A and B are prepared, the compositions are same as Table 1.

(2) AP-P4 polymer solutions were made same as in the three-phase experiments, with the concentrations from 750 ppm to 1750 ppm. The concentration was calculated and named with C_{02}, and herein the C_{02} was prepared to be nearly C_{01}.

(3) Put 120.00 g AP-P4 solution along with 10.00 g sands into the 250 mL erlenmeyer flask.

(4) Put the 250 mL erlenmeyer flask in the oven and stay still under 65°C for 60 h.

(5) Take out the erlenmeyer flask. Use hypodermic syringe and take out the clear liquid by suction. The clear liquid was standing until the small sized sands were deposited. The nitrogen content of liquid is measured, and the obtained data was the equilibrium concentration after adsorption, named as C_{e2}.

3. Results and Discussions

3.1. The Equilibrium Concentration Curve. By using two kinds of simulative waters (A and B), three-phase static adsorption experiments and two-phase static adsorption experiments were carried out with oil, water, and sand.

As shown in Figures 1 and 2, the curve C_0 represents the initial concentration of the AP-P4 polymer solution in simulative water A and B, respectively. As the proceeding of static adsorption, the concentrations of the AP-P4 are gradually reduced. The curve C_{e1} represents the equilibrium concentration of AP-P4 in the three-phase systems that remained in aqueous phase after static adsorption and the curve C_{e2} represents the ones in two-phase systems. C_w is the AP-P4 concentration extracted from the oil phase after static adsorption, which is only a few ppm and is three orders

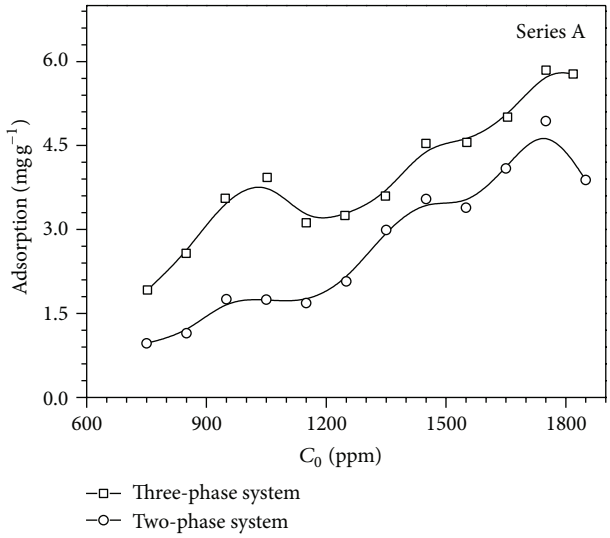

Figure 3: The isothermal adsorption of AP-P4 on the solid phase of two-phase and three-phase systems in the simulative water A.

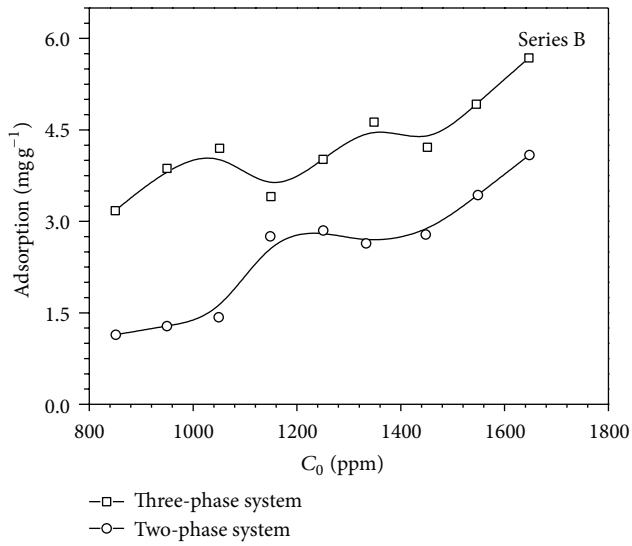

Figure 4: The isothermal adsorption of AP-P4 on the solid phase of two-phase and three-phase systems in the simulative water B.

of magnitude lower than C_{e1} and C_{e2}. The fluctuation of the curve C_w is very small and does not represent the trend of the distribution process. ΔC is the difference between the equilibrium concentration of C_{e1} and C_{e2}, which is caused by the added crude oil. As been confirmed that there is no solubility of AP-P4 in the oil phase, and the adsorption ability of quartz is stable, there is no transfer of AP-P4 from aqueous phase to the oil phase or the solid phase. In this way, the shift of ΔC has two possible paths: one is the interface between the water phase and the oil phase and the other is emulsion phase formed by the mixture of water and the oil. Although the polymer has little dissolution in the crude oil, the introduction of the crude oil induced a distinct transfer and enrichment of AP-P4 around the interlayer region. In the AP-P4 flooding oilfield, there are large number of oil-water interfaces in the produced fluid, which are usually composed of polymer AP-P4, oil, and aqueous phase. These intermediate phases are always exhibiting relatively stable properties within a certain period of time. Compared to the water/solid two-phase systems that are normally studied in laboratory, the novel experimental method in this work is a more accurate way to reflect the true situation in oilfield.

3.2. Isothermal Adsorption Curve. After analysis of the experimental data in two salinity environments, the three-phase systems and two-phase systems isothermal adsorption curves on the solid phase were calculated, as shown in Figures 3 and 4.

During the static adsorption process, the polymer molecules transferred from the aqueous phase to the surface of sands. For the two kinds of simulative water, the polymer adsorption behaviors under different concentrations are shown in Figures 3 and 4. The amount of the AP-P4 adsorption at the surface of the quartz sands appears stepped growth process along with the increment of initial concentration. It could be observed from the comparison of Figures 3 and 4 that the increment of the salinity could cause a significant increase in the amount of polymer adsorption on sands.

3.3. The Distribution Coefficient of Polymer AP-P4 in Water-Sands System. For the two kinds of simulative water, the distribution coefficient of the AP-P4 in water-sands phases could be calculated, as shown in Figures 5 and 6. The distribution coefficient is between 0.12 and 0.46 for simulative water A and between 0.12 and 0.52 for the simulative water B. The distribution coefficients of AP-P4 in water- sands phases are fully consistent in trends in two salinity systems.

The variation of salinity affects the performance of AP-P4 from the comparison of Figures 5 and 6. The distribution coefficient in water-sands system becomes higher in simulative water A and lower in simulative water B, which implies that AP-P4 exhibits excellent salt resistance behavior. These properties are consistent with the results that have been reported [5, 12–14, 27].

It could be easily observed from the isothermal adsorption curve that the adsorption of AP-P4 on the sands exhibits a step shaped increment rather than Langmuir curve, which implies the variation of energy. The adsorption of polymer was caused by the fragment adsorption. When the polymer concentration is low, single layer adsorption occurred, the surface of sand was occupied by the polymer molecules, and the surface energy gets decreased. The repulsive interaction was emerged between adsorbed molecules and the surrounding molecules along with the increase of polymer concentration. As a result of repulsion, the surface energy gets raised and the step of adsorption curve occurs. The further increase of polymer concentration could facilitate the association between the adsorbed molecules and the molecules in aqueous, which results the second layer adsorption of

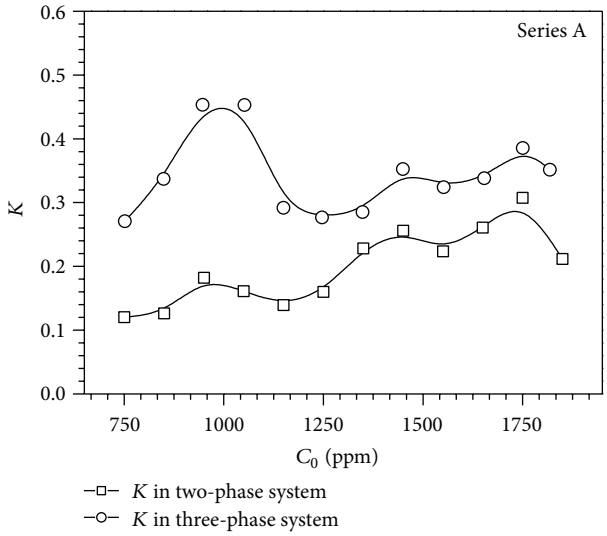

Figure 5: The distribution coefficient in water-sands system in the two-phase and three-phase systems in the simulative water A.

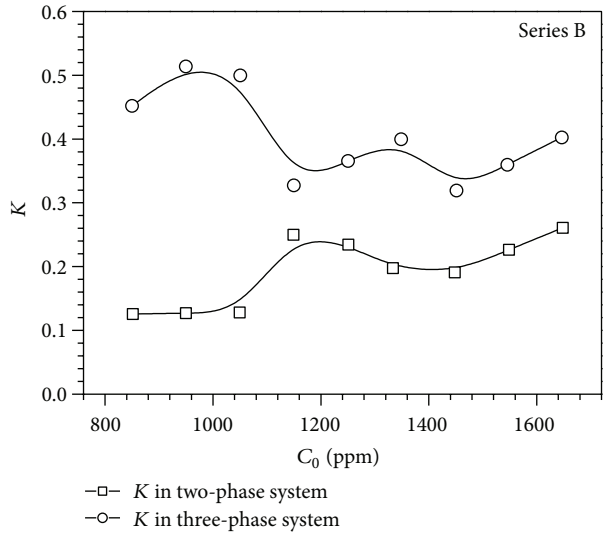

Figure 6: The distribution coefficient in water- sands system in the two-phase and three-phase systems in the simulative water B.

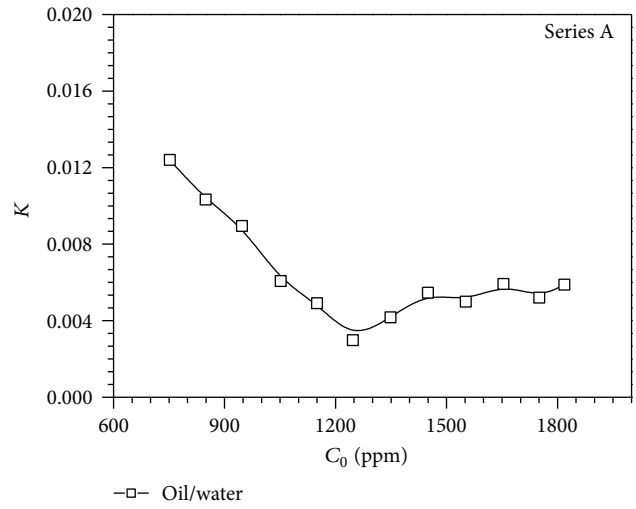

Figure 7: The distribution coefficient in water-oil system in the simulative water A.

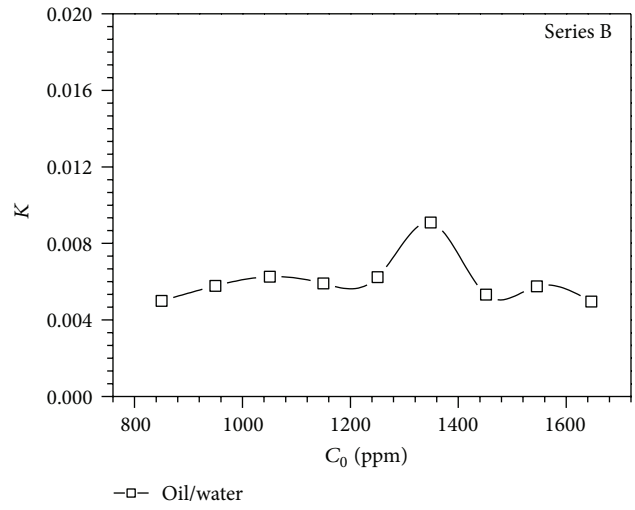

Figure 8: The distribution coefficient in water-oil system in the simulative water B.

polymer molecules. The surface energy gets raised again and the step of adsorption curve occurs.

3.4. The Distribution Coefficient of Polymer AP-P4 in the Water-Oil System. The distribution coefficient K of the AP-P4 in water-oil system is defined as the proportion of AP-P4 concentration in the oil phase and water phase ($K = C_w/C_{e1}$), and can be calculated from the experiment results, as shown in Figures 7 and 8.

The distribution coefficients of AP-P4 in water-oil system range from 0.003 to 0.0124 for simulative water A and from 0.005 to 0.009 for simulative water B. The C_w is much lower than the C_e, so the calculated distribution relationship has confirmed that polymer does not dissolve in the oil phase.

The enrichment of AP-P4 between aqueous and oil phase obeys the laws of polymer adsorption and hydrophobic adsorption. The molecular structure of AP-P4 is consisted with the HPAM skeleton and a little hydrophobic function groups (1–5%). The polarity of hydrophobic function groups is weak, which make it impossible to form the hydrogen bonds with water molecules. So the chemical potential of these hydrophobic function groups is very high, and the solubility in aqueous phase is low. The hydrophobic microdomains are easily formed in aqueous phase, and the reorientation of molecules is easily occurred when the oil phase is added. The AP-P4 molecules stay in the aqueous phase while the hydrophobic function groups are pointed to the oil phase. In this way, the molecules are enriched between oil/aqueous interface.

3.5. The Potential Utilities of the Experiment Methods. The solubility of polymer in oil phase is very low, so the former experiments on polymer static adsorption focus on the competing enrichment regulations between aqueous and solid phases. By using the experiment method in this work, the obtained distribution of AP-P4 among three-phase systems indicates the function of oil phase, which influence the orientation and distribution of polymer molecules. Values of ΔC were observed by the comparison of the obtained aqueous polymer concentration in three-phase systems C_{e1} and C_{e2} in two-phase systems. The value of ΔC is around 200 ppm and has no responds on the variation of aqueous concentration. The experiment method is a more comprehensive and precise way to descript the reorientation and distribution of polymer molecules under the interactions of multiphase after injecting into the formation.

The obtained data could be helpful to simulate the regulation of the concentration loss during the polymer flooding. The viscosity of solution and displacement efficiency are high when the polymer solution was injected into the formation. However, after the adsorption and retention process, the adsorption of polymer would be nearly saturated around the injection point, the RF and RRF would be raised, and the following water driven efficiency would be raised. During the migration of polymer solution, the concentration gets lowered in the deep side of formation, so does the saturated adsorption amount. The modification of RF and RRF decreased too. By using the data obtained in this work, the decrement regulation of polymer concentration and the ability of the formation modification could be simulative by numerical modeling. Besides, the variation of oil displacement and swept ability could also be predicted.

Plenty of emulsion phases existed in the oilfield produced water, for the enrichment trend of AP-P4, to control the water cut of crude oil and the oil content of sewage is one of the most important issues. In the process of produced water treatment, the pertinence methods would be adopted in order to enhance the dehydration efficiency and to prevent the failure of electric dehydration. In this work, the effect of oil phase on polymer distribution was taken into consideration. The comparison of the results from three-phase system and two-phase system could help to understand the polymer content in emulsion phase and the enrichment status of polymer molecules, which would provide the basis of the usage and dosage of demulsifier.

4. Conclusions

(1) A novel experiment method was designed to estimate the distribution of hydrophobic associated polymer AP-P4 among three-phase systems. The adsorption experiments were carried out in oil/aqueous/solid system, and the comparison experiments with aqueous/solid two phases were carried out too. By using the experiment method, the distribution behavior of AP-P4 among oil/aqueous/solid system was obtained, and the influence of mineralization polymer concentration was revealed.

(2) The experiment method is different from the former adsorption experiments in two-phase systems, which could reveal a more comprehensive character of the system. Although there is no solubility of polymer in oil phase, significant affection had been done on the distribution of polymer molecules by the existence of oil phase.

(3) A distinct decrease of polymer concentration was observed in aqueous phase by the experiment method, which could be induced by the enrichment of polymer molecules on the oil/aqueous interface under the appearance of oil phase. The enrichment of polymer could be estimated by evaluating the emulsion phase, which could help to understand the enrichment and the concentration of polymer molecules in the emulsion phase.

Acknowledgment

The authors gratefully acknowledge the financial support from subject 4 "Chemical Flooding Technology for Offshore Heavy Oil" (2011ZX05024-004) that belongs to project 24 "New and High Effective Development Technique for Offshore Heavy Oil" of Natural Science and Technology Major Project "Development of Large Field and Coal Bed Methane" in 12th five-year plan.

References

[1] N.-J. Lai, Y. E. Zhongbin, Y. Zhou, and T. Jia, "Study on solution properties of new hydrophobic associated polymer and enhanced oil recovery," *Petroleum Geology and Recovery Efficiency*, vol. 12, no. 2, pp. 63–65, 2005.

[2] Y.-F. Wang, H.-Y. Yu, J. Zhang, W. H. Chen, and S. L. Wang, "Study on decompression and augmented injection by surfactants during hydrophobically associating polymer flooding in Bohai Oilfield," *Zhongguo Shiyou Daxue Xuebao*, vol. 34, no. 6, pp. 151–156, 2010.

[3] H. Ren, Z. Luan, Z. Li, and Z. Yang, "Enrichment of polycyclic aromatic hydrocarbons by hydrophobically associated polymers," *Environmental Chemistry*, vol. 30, no. 2, pp. 471–475, 2011.

[4] L. Yang and J. Zhang, "The effect of inorganic salts on the adsorption of amphoteric ion polymer on clay surface," *Journal of Southwest Petroleum Institute*, vol. 19, pp. 49–52, 1997.

[5] X. Song, G.-Y. Yang, and J. Ke, "Enthalpy of adsorption and adsorption isotherms of polyacrylamide on oil sand," *Chinese Chemical Society*, no. 1, pp. 39–41, 1998.

[6] G. Liu, "The adsorption property of polymers on the solids of clay and drilling fluid," *Environmental Protection of Oil & Gas Fields*, vol. 9, pp. 38–41, 1999.

[7] B.-Z. Mu and P.-Y. Luo, "Experimental methods and techniques for determining adsorrtion behavior parameters of polymers at solid/liquid interfaces," *Oilfield Chemistry*, vol. 16, no. 1, pp. 97–98, 1999.

[8] Y.-J. Guo, F.-S. Li, and L.-H. Li, "Adsorption behavior of water-soluble hydrophobic associated polymer at water/kaolin interface," *Chinese Journal of Applied Chemistry*, vol. 19, pp. 26–28, 2002.

[9] J.-S. Miao, F.-L. Zhao, S. Li, Y.-H. Yu, and M. Chen, "Presence and distribution of residual polymer in formation," *Special Oil & Gas Reservoirs*, vol. 12, pp. 88–90, 2005.

[10] K. Ren, G. Jiang, M. Lin, and C. Xu, "Influence of salt concentration on the properties of the hydrophobically associated polymer solution," *Journal of Functional Polymers*, vol. 2, pp. 321–324, 2005.

[11] J.-P. Shi, Q.-Y. Yang, and C.-F. Liu, "The experiment of influence of polymer absorbance in the properties of formation," *Journal of Oil and Gas TEchnolory*, vol. S1, pp. 224–227, 2005.

[12] C.-J. Zhou, H.-B. Li, and C.-Q. Shu, "Measuring the static state adasorption isotherm of the hydrophobically associated polymer on oil sand in suizhong oilfield," *Offshore Oil*, vol. 25, pp. 27–30, 2005.

[13] J.-Z. Zhou, Y.-Z. Zhao, and C.-Y. Zhang, "Study of the adsorption of surfactant,polymer and alkali on the surface of solid particle by XPS," *Applied Chemical Industry*, vol. 37, pp. 713–716, 2008.

[14] D.-S. Li, J.-R. Hou, and J.-R. Hou, "Adsorption of components from ASP flooding solution onto reservoir rock of Daqing," *Oilfield Chemistry*, vol. 18, no. 4, pp. 358–382, 2001.

[15] J.-F. Zhang, *The behavior of adsorption and retention and characteristic of flowing through the porous media of hydrophobically associated polymers [M.S. thesis]*, 2004.

[16] H.-J. Zhu, J.-H. Luo, and J.-B. Yang, "Three key factors influencing oil-displacement capacity in hydrophobically associating polymer flooding," *Acta Petrolei Sinica*, vol. 26, no. 3, pp. 52–55, 2005.

[17] S.-X. Guan, H.-F. Fan, and J.-G. Duan, "Starch-cadmium iodide, the estimate method of concentration of HPAM," *Journal of Daoqing Petroleum Institute*, vol. 31, no. 12, pp. 110–112, 2007.

[18] C.-Q. Hong, Z.-B. Ye, L.-T. Shi, C. Zhang, and Z.-C. Yang, "Research on solution property and evaluation method of polymer gels and hydrophobic associated polymer," *Oil Drilling & Production Technology*, vol. 29, pp. 61–64, 2007.

[19] B.-L. Kong, "A review on methods for determing hpam concentration of aqueous solutions," *Oilfield Chenmistry*, vol. 13, no. 3, pp. 284–288, 1996.

[20] B.-L. Kong and H.-C. Zhang, "Determination of hydrolysis degree of polyacrylamide by starch-trhodide method," *Oilfield Chemistry*, vol. 14, no. 1, pp. 73–76, 1997.

[21] X.-B. Nie, J. Liu, and Q. Qiao, "An improved method for quantitative analysis of hpam in asp-flooding," *Oilfield Chemistry*, vol. 14, no. 4, pp. 369–371, 1997.

[22] C. Yang, R. K. Wu, P.-D. Zhu, and X. R. Yang, "Determination of total nitrogen in water using high temperature oxidation & chemiluminescence method," *Chinese Journal of Analytical Chemistry*, vol. 35, no. 4, pp. 529–531, 2007.

[23] Z.-G. Ye and Z.-G. Cui, "Preparation properties and characterization of inorganic nano-scale materials," *China Surfactant Detergent & Cosmetics*, vol. 34, no. 1, pp. 52–54, 2004.

[24] Q. You, F.-L. Zhao, L.-N. Mu, L. He, and Y. P. Jia, "A new method for the accurate determination of polyacylamide concentration in produced fluids of ploymer flooding oil well- a film drying method after ultrafiltration and condensation," *Acta Petrolei Sinica*, vol. 23, no. 1, pp. 109–113, 2007.

[25] B.-C. Zhao and G.-X. Zhang, "Determination of hydrolysis degree and concentration of HPAM by nitrogen determination method," *Oilfield Chemistry*, vol. 2, no. 3, pp. 233–235, 1985.

[26] X.-N. Li, Z.-B. Ye, H. Chen et al., "Effect of polymer on crude oil demulsification," *Advances in Fine Petrochemicals*, vol. 7, pp. 15–17, 2006.

[27] J.-F. Zhang, Z.-B. Ye, and Z.-J. Li, "Adsorption behavior of hydrophobic associated polymer (Hap) in quartz sands," *Natural Gas Eaploration & Developmaent*, vol. 27, pp. 48–51, 2004.